The route from formamide to RNA and metabolism. Part II

Ernesto Di Mauro
Università di Roma “Sapienza”

Trieste 15 September 2015

Alexander I. Oparin

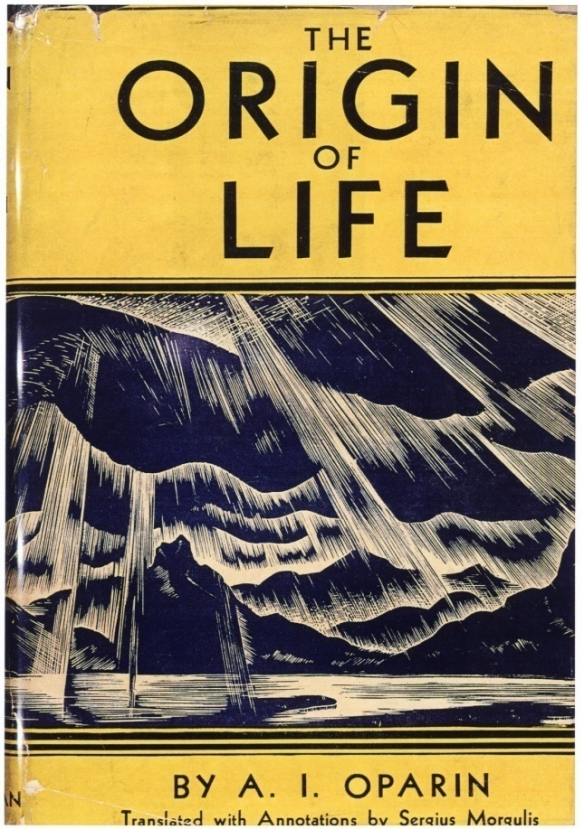

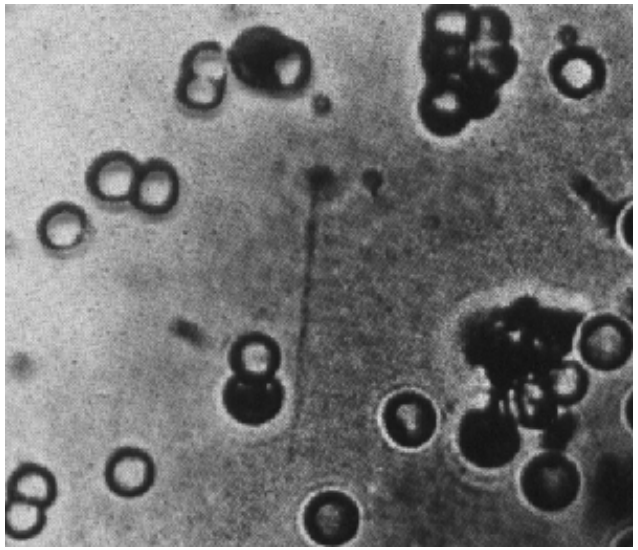

Proiskhozhdenie zhizny (The Origin of Life) 1924

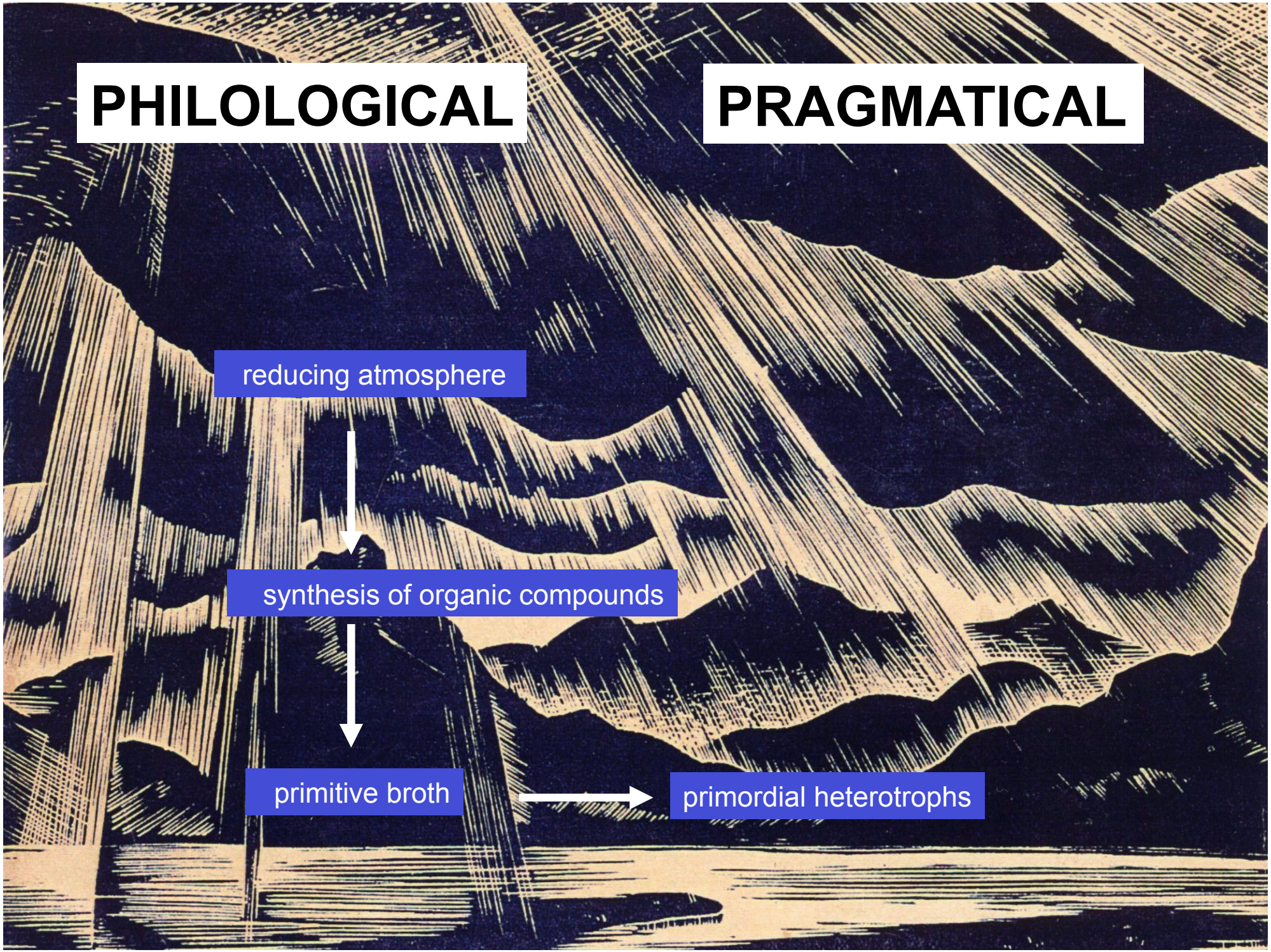
PHILOLOGICAL
PRAGMATICAL
reducing atmosphere
synthesis of organic compounds
primitive broth
primordial heterotrophs

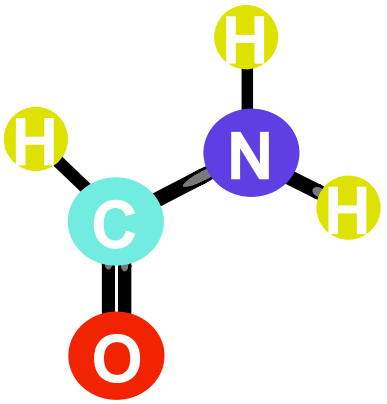

liquid between 4 and 210°C

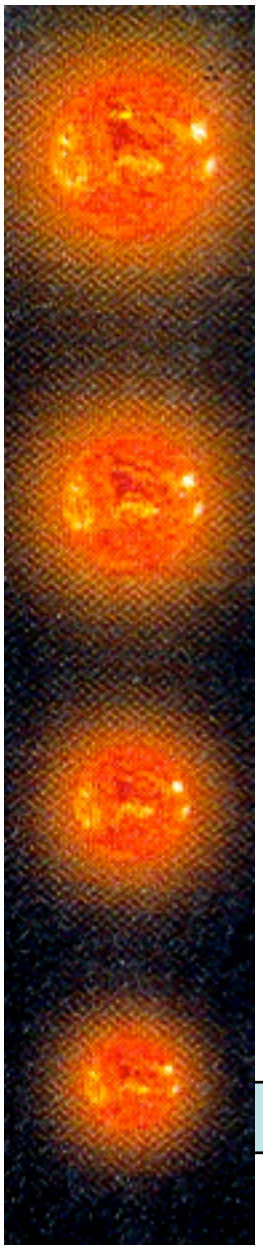

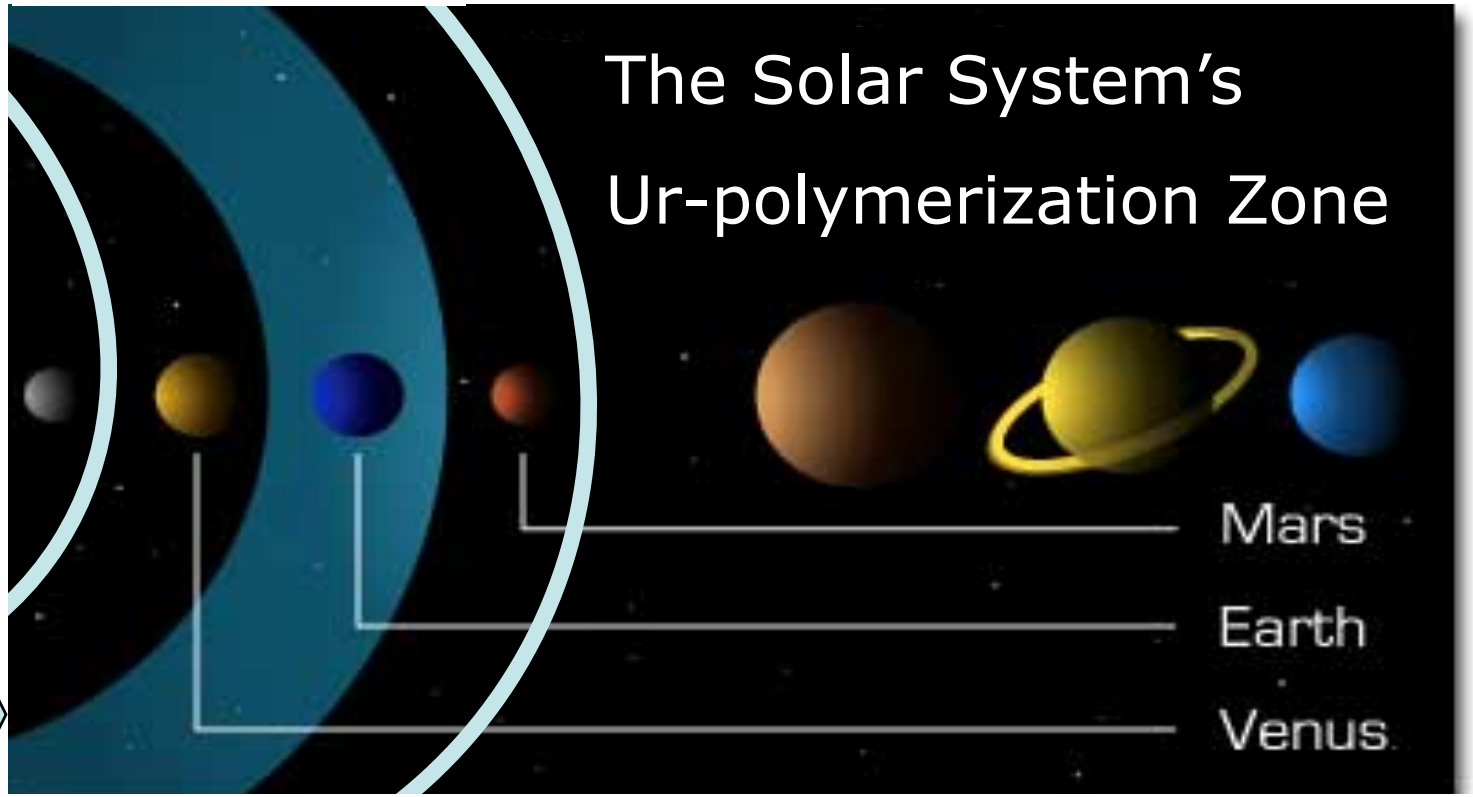

ANYTHING CAN HAPPEN
and probably will
RIGHT HERE ON EARTH

You don't have to rent a spaceship or sign up for a singles cruise to Saturn or spend your weekends star-hopping along the Milky Way because

EARTH IS ROOM ENOUGH.

Earth is where the action is and each tomorrow unleashes new discoveries.

Here are brilliant, witty, frightening, and fascinating stories of the future by the greatest science fiction master of them all. Just hitch your mind to these weird and wonderful tales for a spin around the world of tomorrow that will take you right to the center of your wildest dreams.

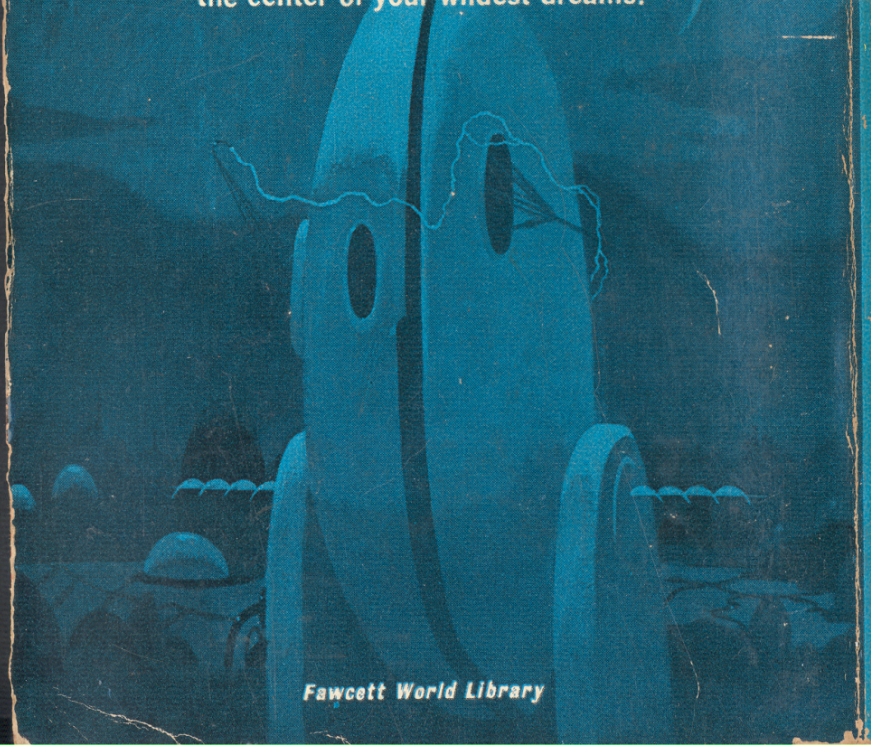

Fawcett World Library

A Fawcett

EARTH IS ROOM ENOUGH Isaac Asimov

T1401
75¢

A Fawcett Crest Book

Mind-Tingling Tales of Tomorrow
By the Master of Science Fiction

isaac asimov

Earth Is Room Enough

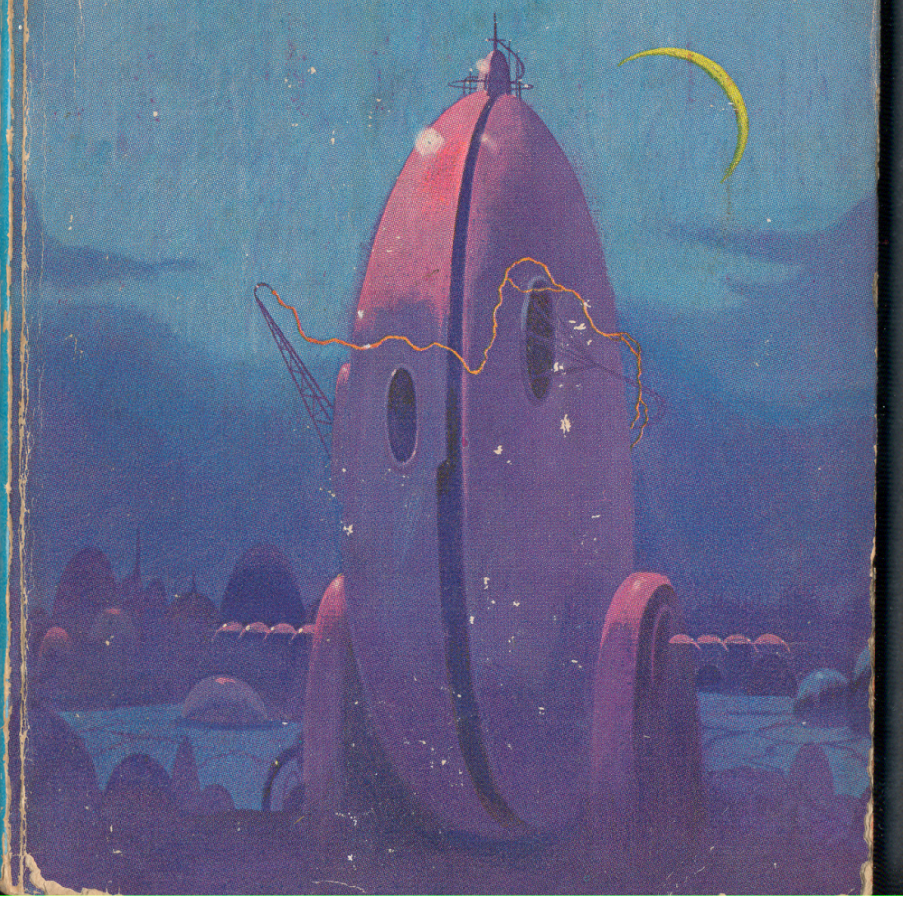

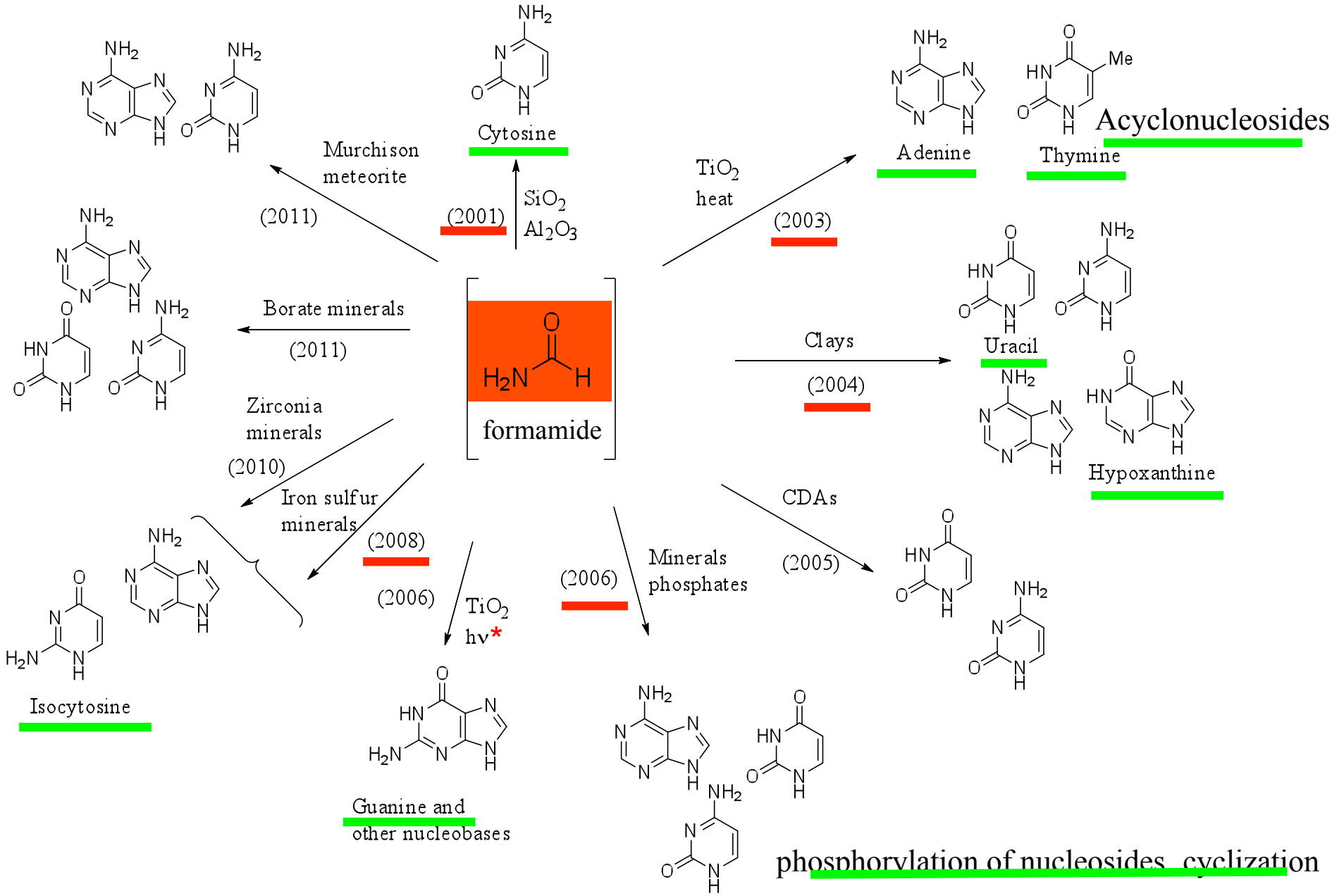

Yamada & Okamoto, 1972; * Idriss & Senanayake, 2006

Synthesis of nucleobases from formamide metal oxides and minerals

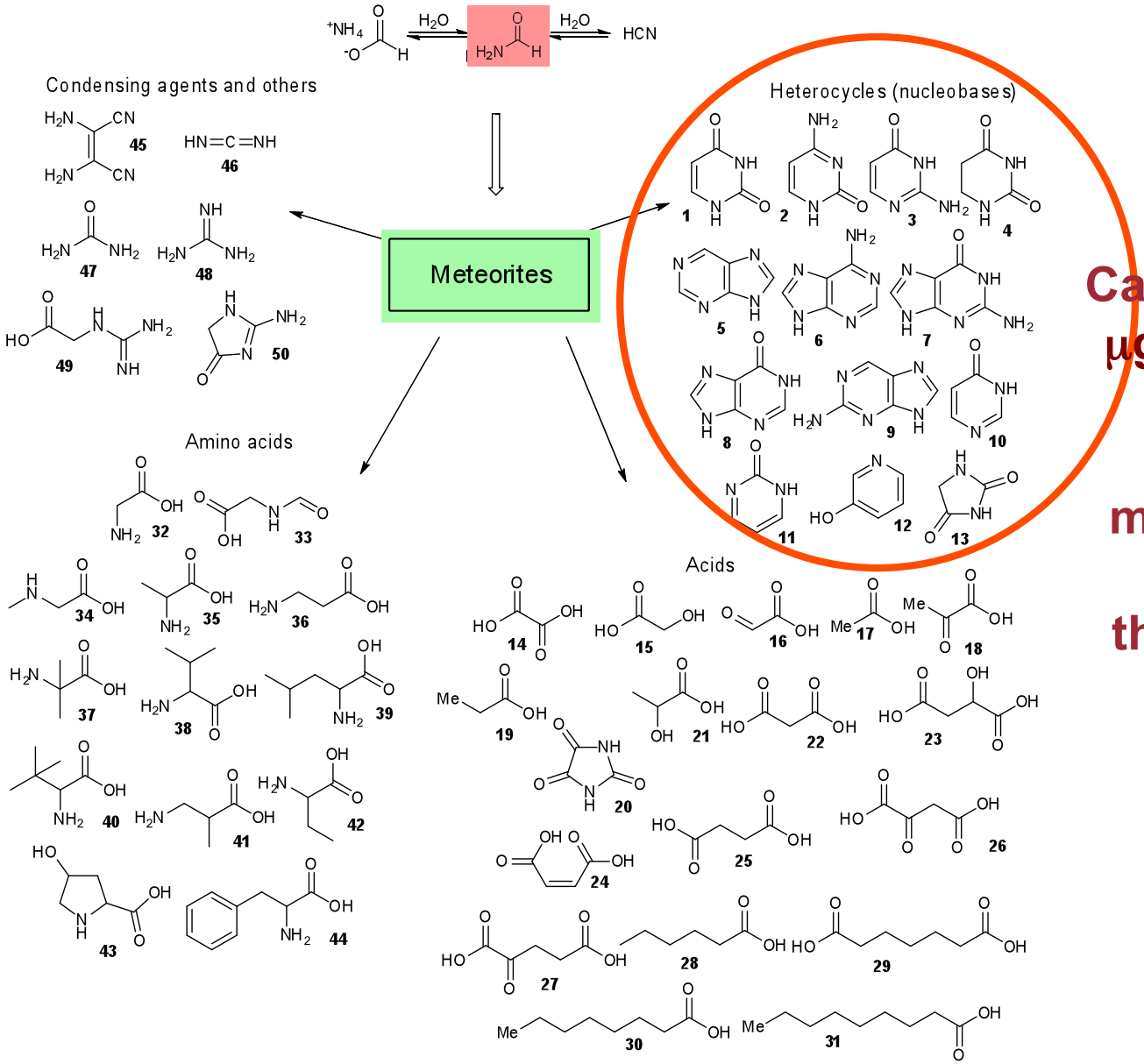

The 50 most abundant products of the syntheses catalyzed by meteorites in the presence of NH_2COH Formamide. The compounds are numbered according to their mention in the text. Nucleobases: uracil (**1**), cytosine (**2**), isocytosine (**3**), dihydrouracil (**4**), purine (**5**), adenine (**6**), guanine (**7**), hypoxanthine (**8**), 2-aminopurine (**9**), 4(3H)-pyrimidinone (**10**), 2(1H)-pyrimidinone (**11**), 3-hydroxypyrimidine (**12**) and hydantoine (**13**). Acids: oxalic (**14**), glycolic (**15**), glyoxylic (**16**), acetic (**17**), pyruvic (**18**), propanoic (**19**), parabanic (**20**), lactic (**21**), malonic (**22**), malic (**23**), maleic (**24**), succinic (**25**), oxalacetic (**26**), ketoglutaric (**27**), hexanoic (**28**), pimelic (**29**), octanoic (**30**) and nonanoic (**31**). Amino acids: glycine (**32**), *N*-formylglycine (**33**), *N*-methylglycine (**34**), alanine (**35**), β-alanine (**36**), 2-methylalanine (**37**), valine (**38**), leucine (**39**), tert-leucine (**40**), β-amino isobutyric acid (β−AIBA) (**41**), 2-aminobutanoic acid (2-ABA) (**42**), hydroxyproline (**43**) and phenylalanine (**44**). Condensing agents and others: diaminomalonitrile (DAMN) (**45**), carbodiimide (**46**), urea (**47**), guanidine (**48**), guanidine acetic acid (**49**), glycocyanidine (**50**).

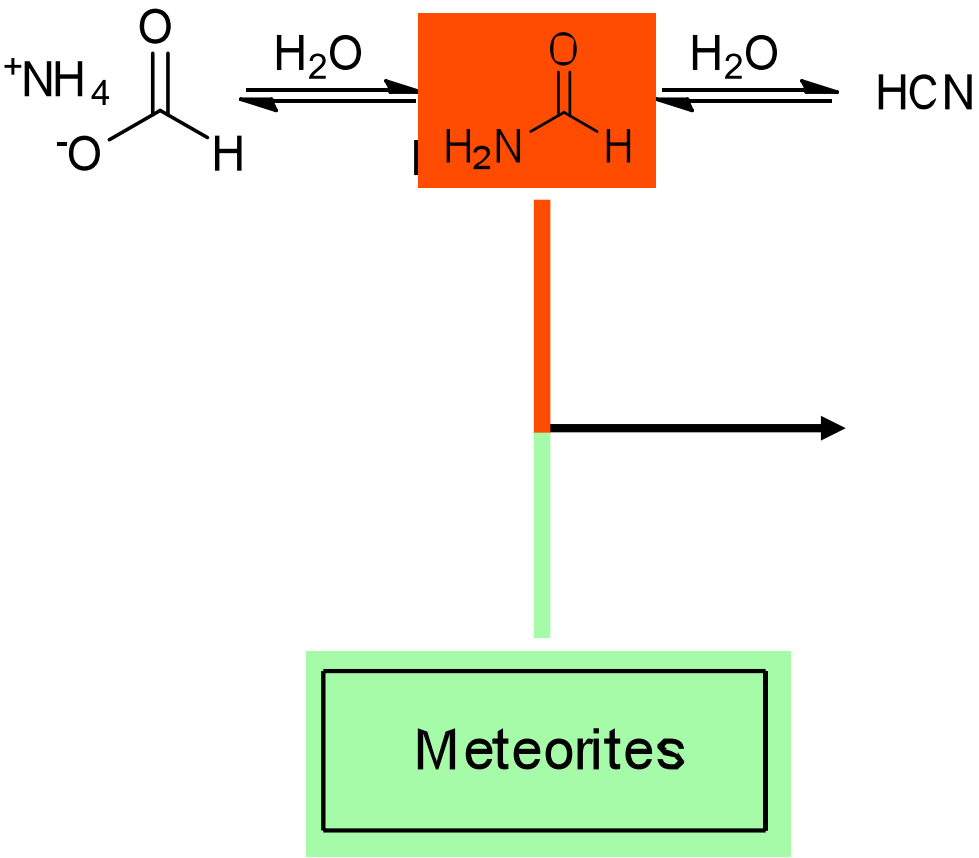

Heterocycles (nucleobases)

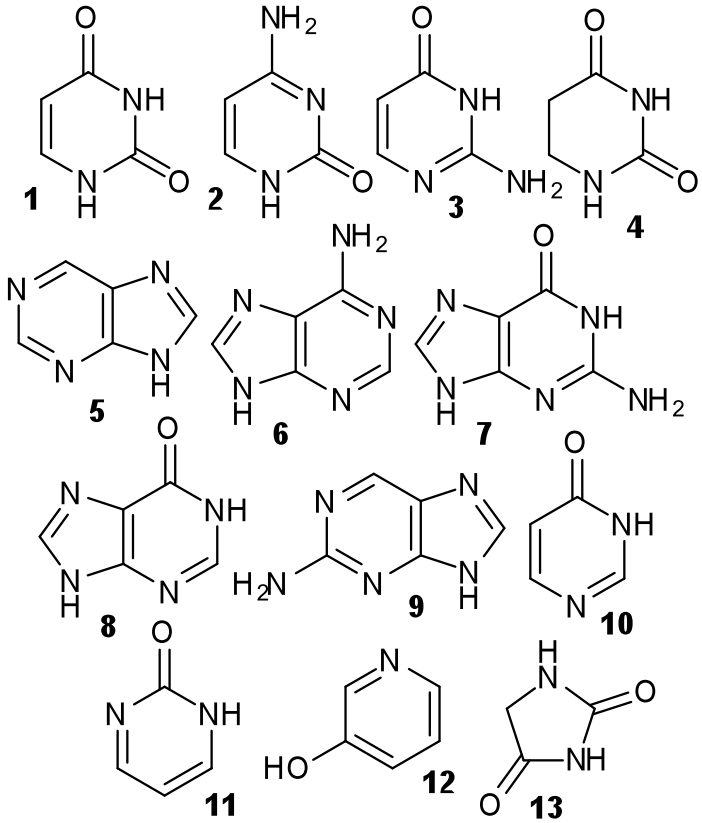

Nucleobases: uracil (**1**), cytosine (**2**), isocytosine (**3**), dihydrouracil (**4**), purine (**5**), adenine (**6**), guanine (**7**), hypoxanthine (**8**), 2-aminopurine (**9**), 4(3H)-pyrimidinone (**10**), 2(1H)-pyrimidinone (**11**), 3-hydroxypyrimidine (**12**) and hydantoine (**13**).

Nucleobases

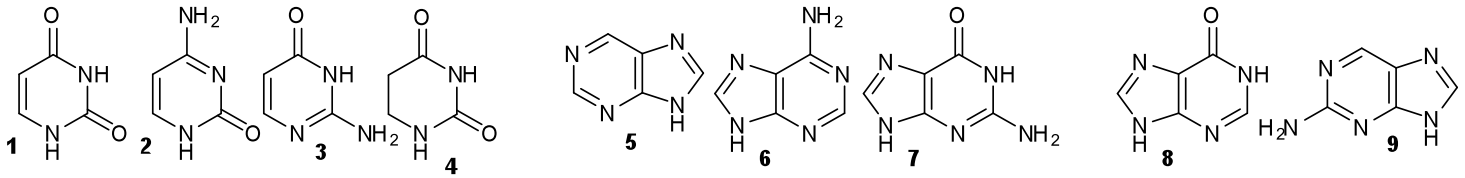

Table II. Heterocycles: products (μg) grouped into meteorite's families

	Iron meteorites			Stony iron meteorites		Chondrites				Achondrite		
	Canyon Diablo	Campo del Cielo	Sikhote Alin	Seymchan	NWA 4482	Gold Basin	Dhofar 959	NWA 1465	Murchison	NWA 2828	NWA 5357	Al Haggounia
Uracil	250	238	278	345	300	34	61	33.3	50		481.5	470
• Cytosine	122	51	120	30	32	23	32	13	29		30	44
• Isocytosine	395.7	790	811	1836	689	270	323	337	249		700	613
Dihydrouracil	0	0	0	0	0	0	0	0	0		62	70
Purine	41318	19056	1400	5257.4	1863	2372	1376.8	705	2663		890.8	770
Adenine	250	211	400	107.5	103	499	510	50	41		800	810.5
• Guanine	0	0	0	0	0	0	0	0	0		50	60
• Hypoxanthine	380	489	500	0	0	0	0	0	0		0	0
• 2-NH_2 purine	0	0	0	10.8	128	0	0	0	0		0	0
4(3H)-pyr	1296	4221	2470	5545.4	2546.8	344.46	350	6053.2	362		821	297,1
2(1H)-pyr	0	0	0	20	16.7	50	41.8	1687	1400		649	668
3-(OH)Pyr	0	0	0	15	12	23.96	25	31	26		12.62	10
Hydantoin	0	0	0	0	0	0	0	264,64	100		0	0

Nucleobases and their analogues were obtained in the range of 0.43-2.32 mg per 1-0 mL of NH_2COH
These amounts are 10^5, 10^6-fold higher than that recovered in the original meteorites

R. Saladino, E. Di Mauro Chemistry-A European Journal 2013

Saladino et al. ChemBioChem 2006
Saladino et al. J Am Chem Soc 2008
Saladino et al. J Mol Evol 2010

condensing agents

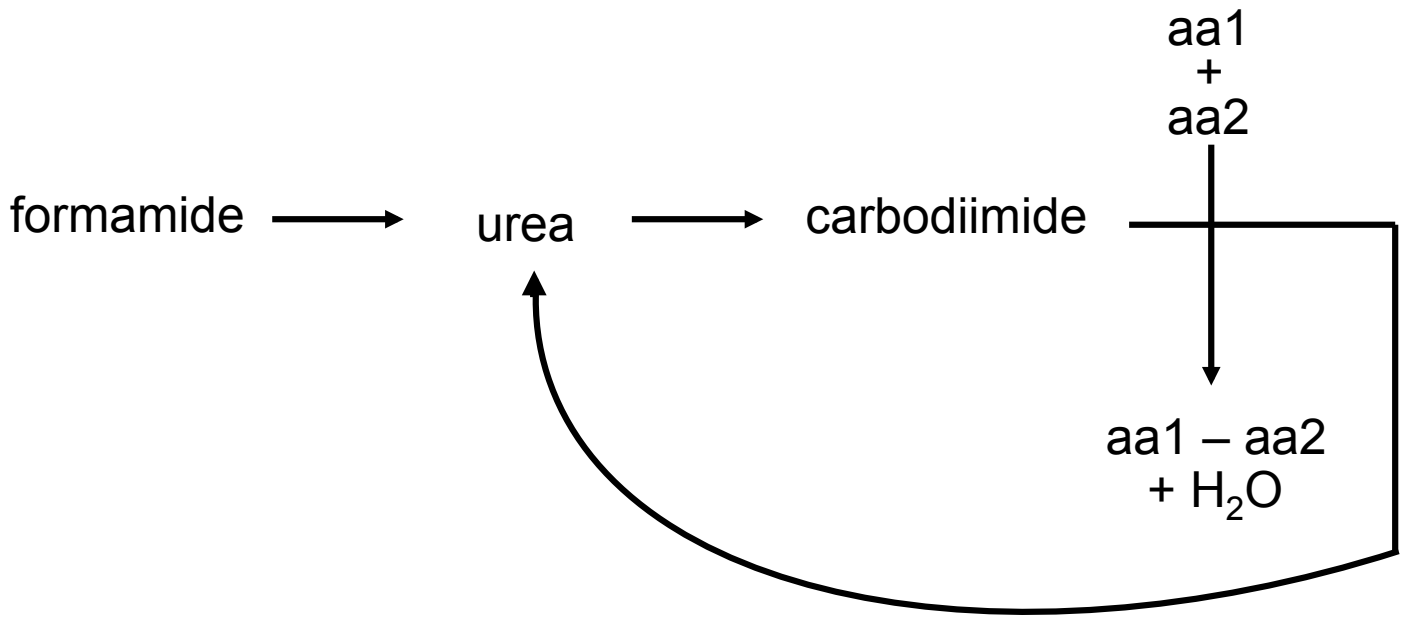
formamide
urea
carbodiimide
aa1
+
aa2
aa1 – aa2
+ H2O

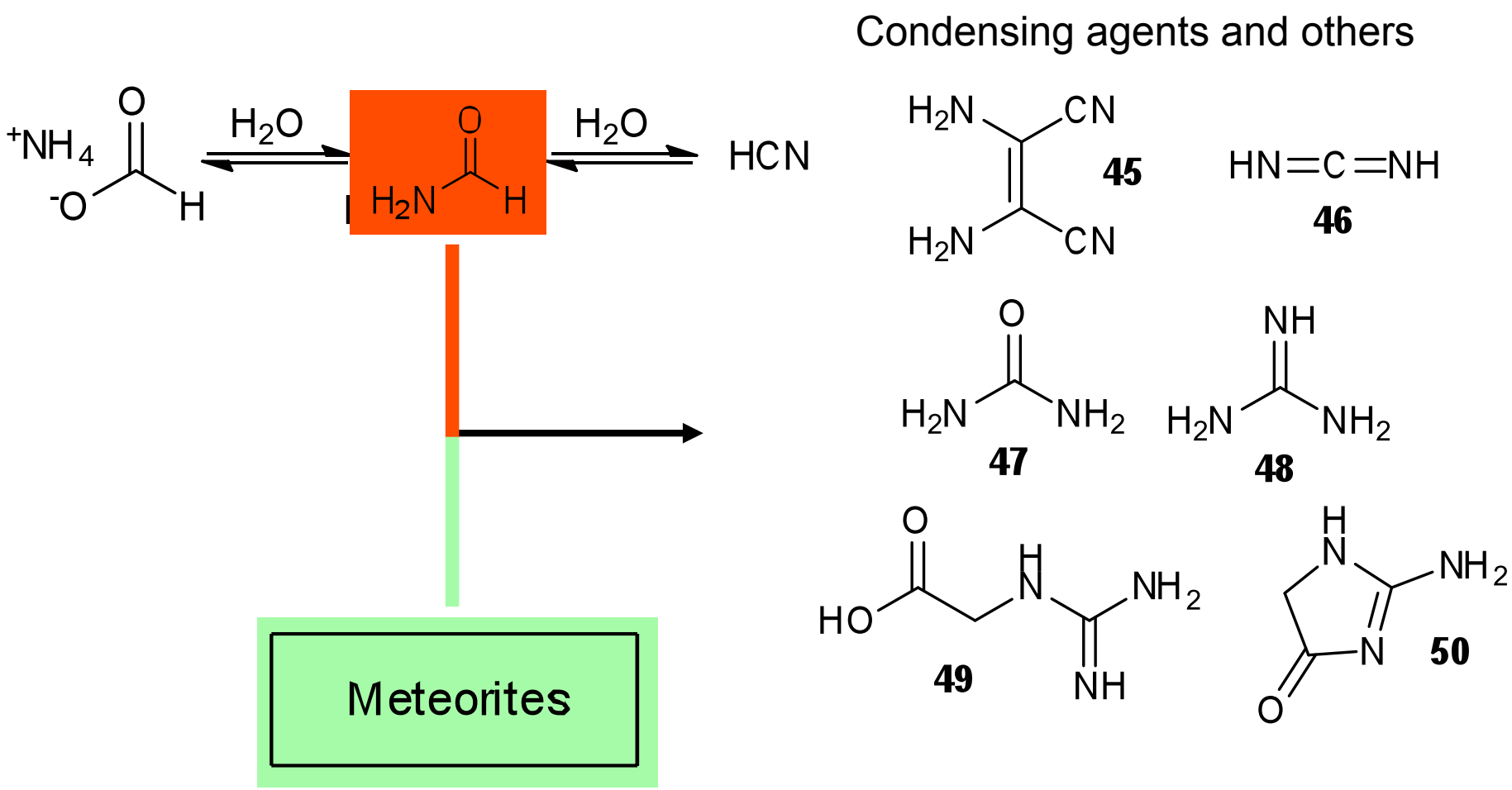

Condensing agents and others: diaminomalonitrile (DAMN) (**45**), carbodiimide (**46**), urea (**47**), guanidine (**48**), guanidine acetic acid (**49**), glycocyanidine (**50**).

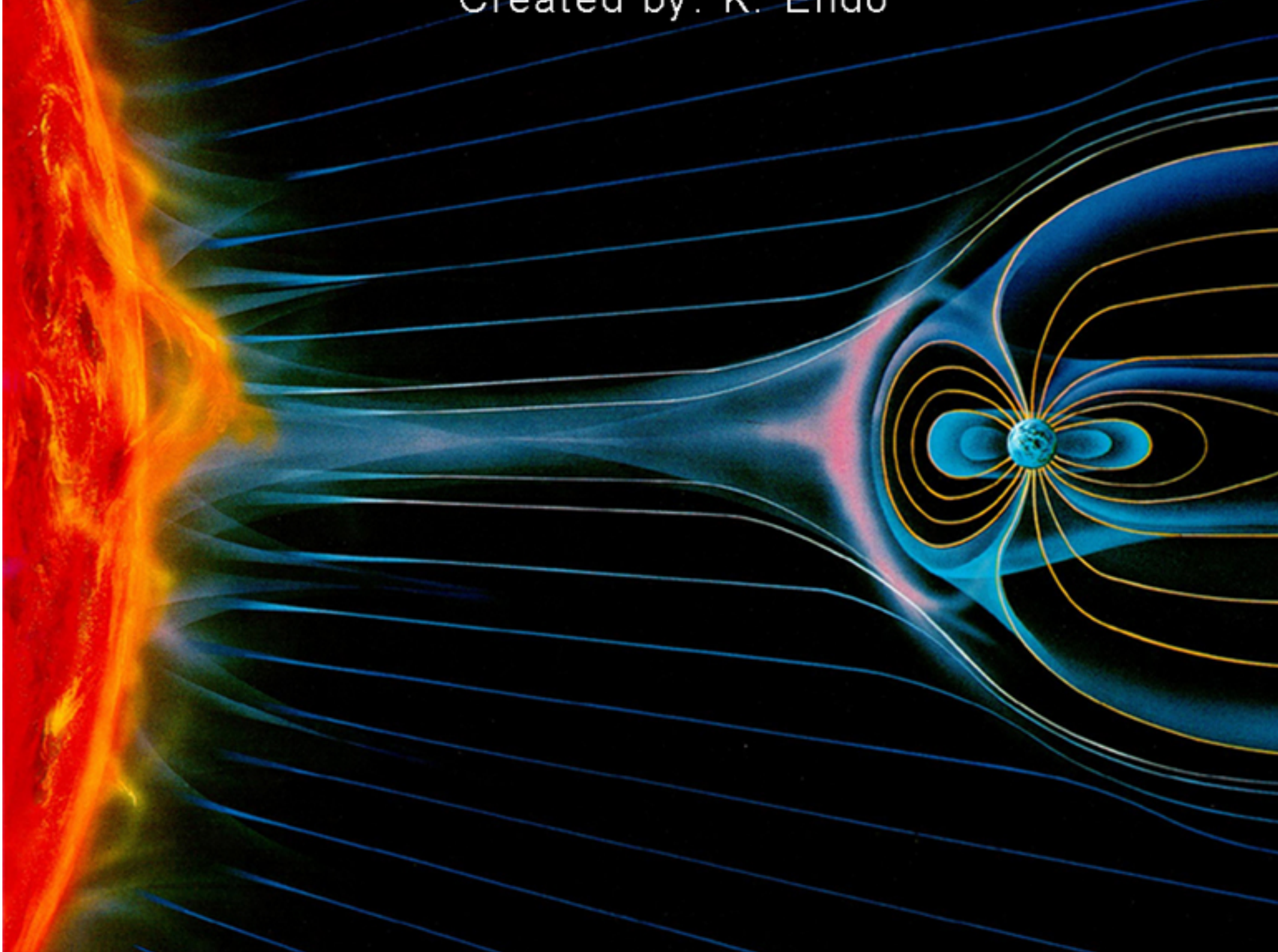
Created by: K. Endo

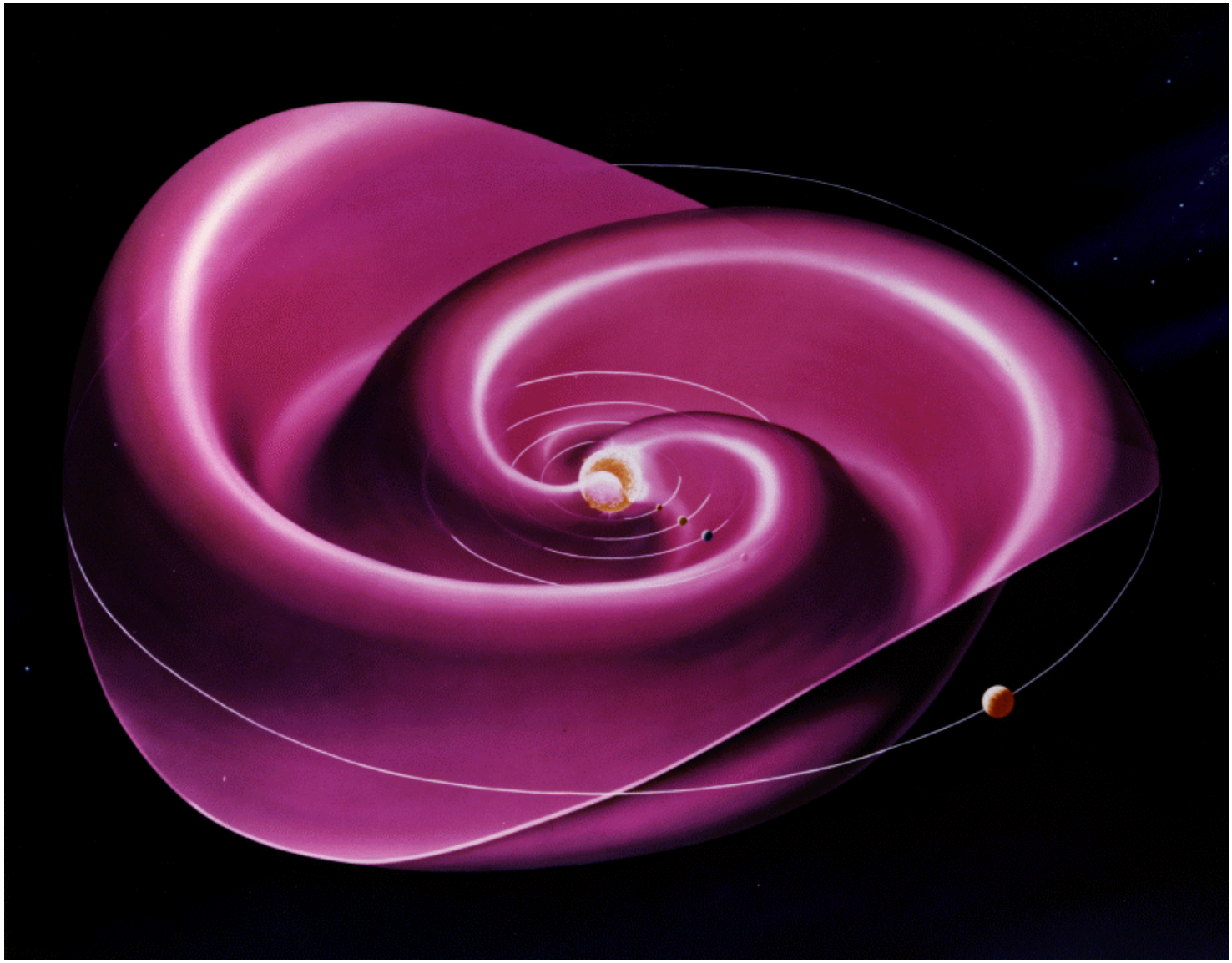

The solar wind is a stream of plasma released from the upper atmosphere of the Sun.
It consists of mostly electrons and protons with energies usually between 1.5 and 10 keV.

Mechta

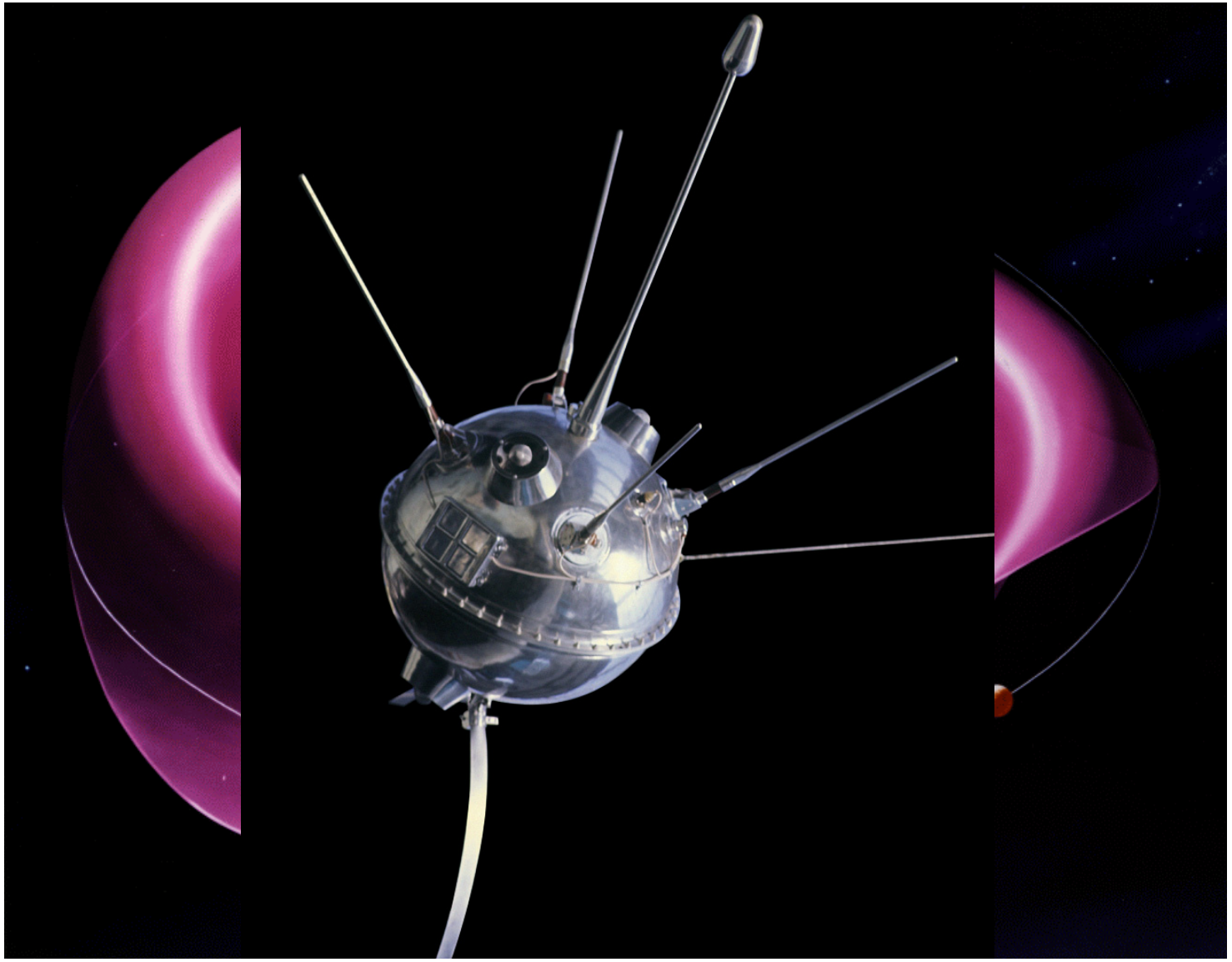

Luna 1 January 1959 first detected and measured the solar wind, strong flow of ionized plasma emanating from the sun

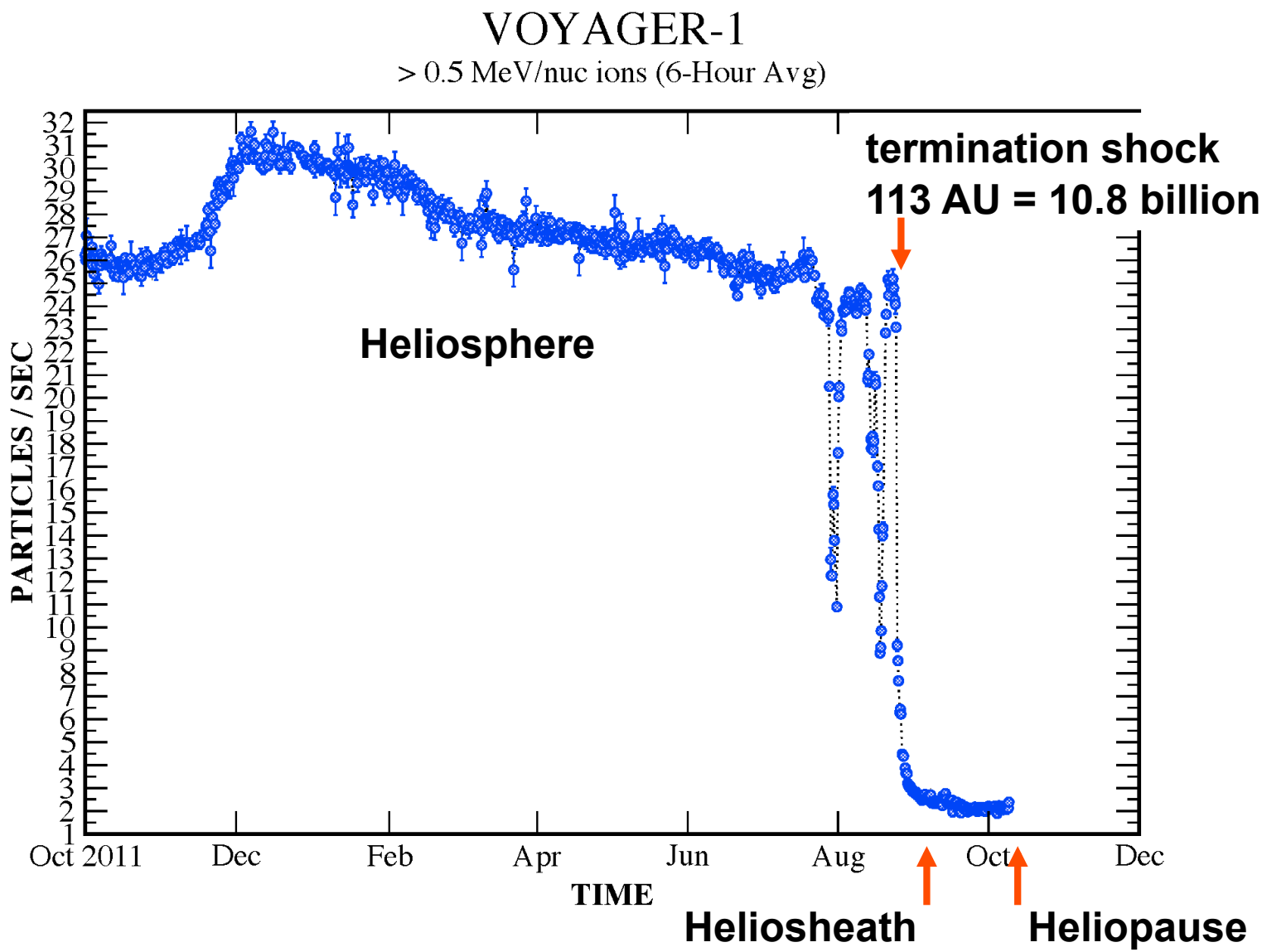

at heliosheath

Plot showing the decreased detection of solar wind particles by Voyager 1 starting in August 2012.

- solar wind particles
- magnetic field intensity doubled
- 100-fold high-energy electrons from galaxy

PNAS
Proceedings of the National Academy of Sciences of the United States of America www.pnas.org

PNAS Celebrating 100 Years 1915-2015

vol. 112 no. 21, E2746–E2755

Meteorite-catalyzed syntheses of nucleosides and of other prebiotic compounds from formamide under proton irradiation

[a]Raffaele Saladino, [a]Eleonora Carota, [a]Giorgia Botta,[b]Michail Kapralov, [b]Gennady N. Timoshenko, [b]Alexei Rozanov, [b]Eugene Krasavin, [c,1] Ernesto Di Mauro.

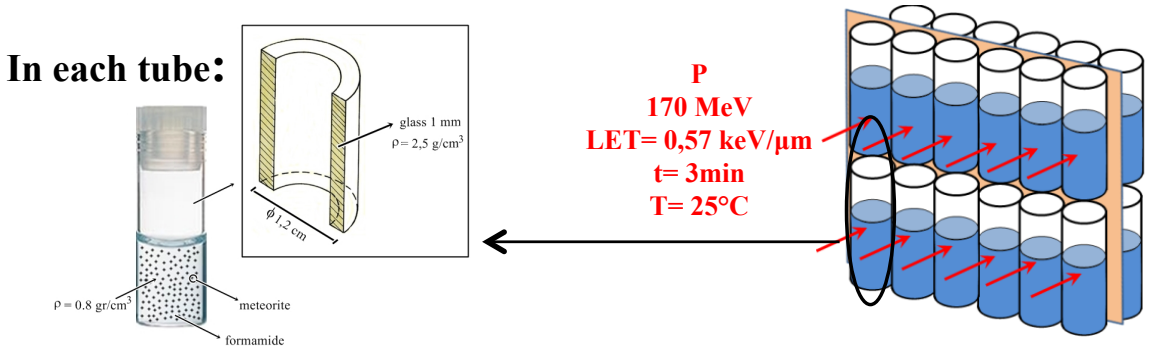

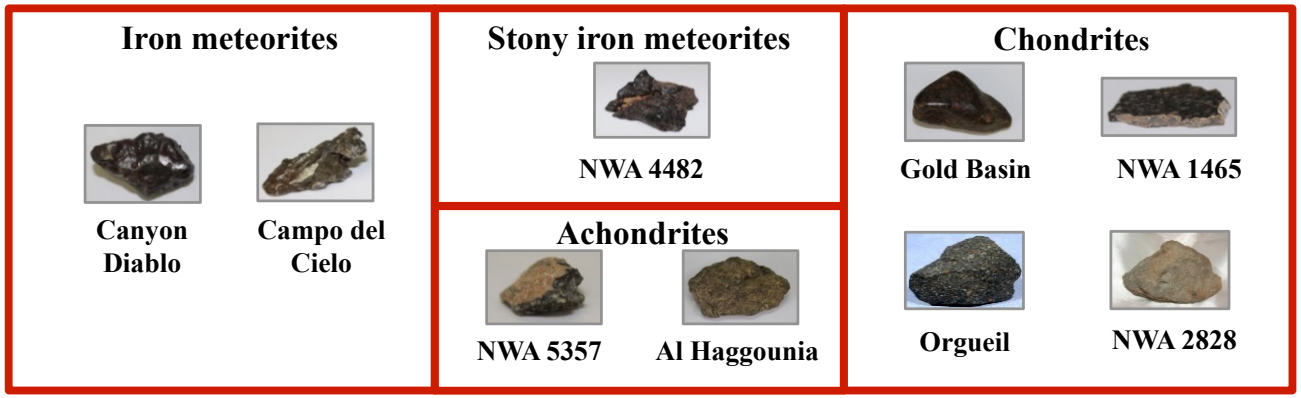

	Name[a]	Class	Type
1 2	**Canyon Diablo** **Campo del Cielo**	Iron Iron	IA Hexaoctahedrite normal IAB Hexaoctahedrite coarse
3	**NWA4482**	Stony iron	Pallasite Anomalous
4 5 6 7	**NWA2828** **Gold basin** **Orgueil** **NWA1465**	Chondrite Chondrite Chondrite Chondrite	Enstatite Ordinary Carbonaceoous LV3 Anomalous
8 9	**NWA5357** **Al Haggounia**	Achondrites Achondrites	Diogenite Aubrite

Table 2. Synthesis of nucleosides, nucleobases (and their analogues), and sugars: products (µg) grouped by meteorite type.

Product[a]	Canyon Diablo	Campo del Cielo	NWA 4482	NWA 2828	Gold Basin	Dhofar 959	NWA 1465	Chelyabinsk	Orgueil	NWA 5357	Al Haggounia
3(OH)pyridine (**13**)	-	-	0.25	-	-	-	-	-	0.26	-	-
AHMN (**14**)	-	-	-	-	0.06	-	-	-	0.22		0.13
DAMN (**15**)	-	-	0.05	-	0.12	0.35	-	-	0.93	0.47	0.03
4-AMI (**16**)	-	-	0.19	0.15	0.2	0.05	-	-	-	-	0.52
Ribose (**17**)	-	-	1.01	0.16	-	-	0.30	-	-	-	0.10
2'-Deoxy-ribose (**18**)	-	-	2.30	0.98	0.10	1.28	0.44	0.05	0.43	-	0.80
Glucose (**19**)	-	-	-	0.12	-	-	-	-	0.31	-	-
2'-Deoxy-glucose (**20**)	-	-	0.05	0.66	0.08	0.27	1.06	-	1.68	-	-
Galactose (**21**)	-	-		0.70	-	-	0.80	-	0.42		-
Mannose (**22**)	-	-	-	-	0.03	-	0.44	-	-	-	-
Inositol (**23**)	-	-	2.88	-	-	-	-	-	-	-	-
Arabitol (**24**)	-	-	-	0.67	-	0.39	-	-	-	-	-
Uridine (**25**)	-	-	0.54	-	0.03	-	0.96	0.01	1.0	-	0.45
cytidine (**26**)	-	-	-	-	-	-	2.2	-	0.03	-	-
Adenosine (**27**)	-	-	-	-	-	0.58	-	0.76	-	-	0.49
Thymidine (**28**)	-	-	-	-	-	-	-	-	-	-	0.77

[a] The data are the mean values of three experiments with standard deviation less than 0.1 %. Products are given in µg (per 1 mL formamide reactions). See Text.

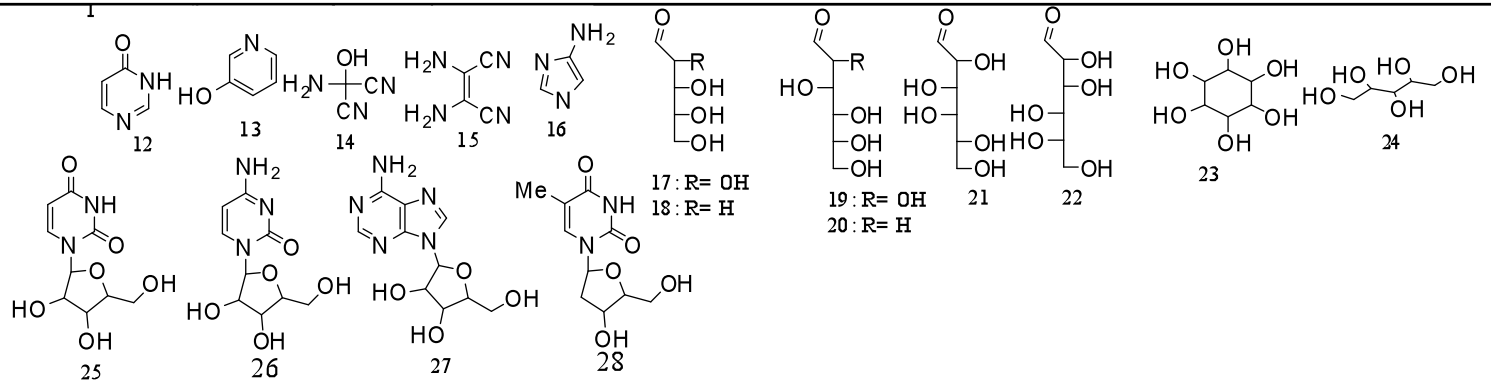

(170 MeV)

Uridine (**25**)
cytidine (**26**)
Adenosine (**27**)
Thymidine (**28**)

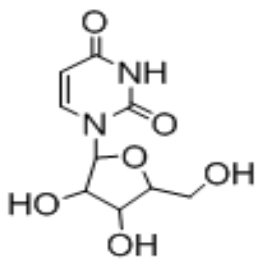

25

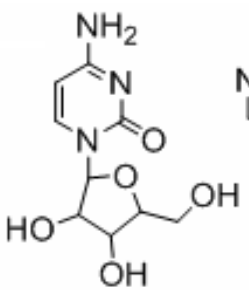

26

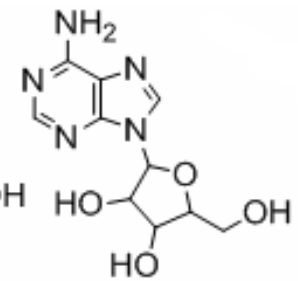

27

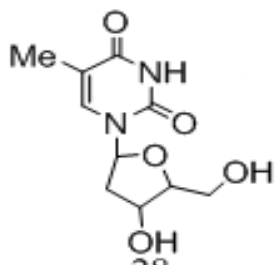

28

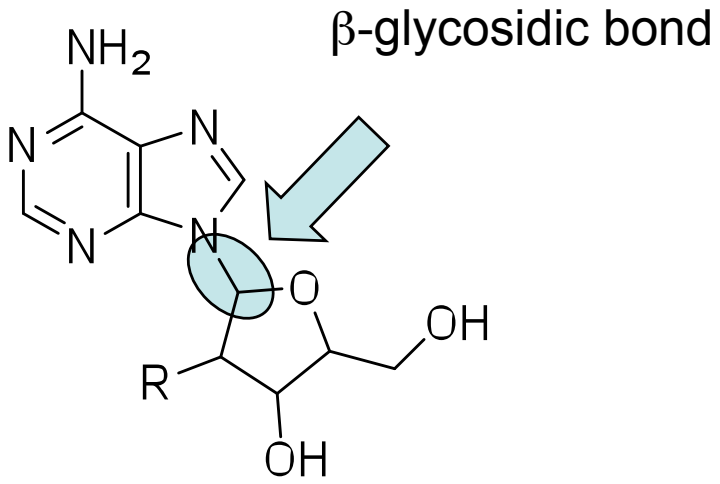
β-glycosidic bond
NH2
N
N
N
N
O
OH
R
OH

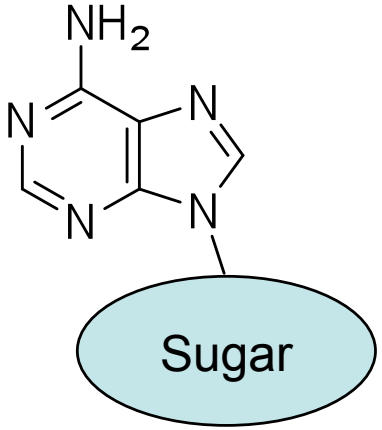
NH2
N
N
N
N
Sugar

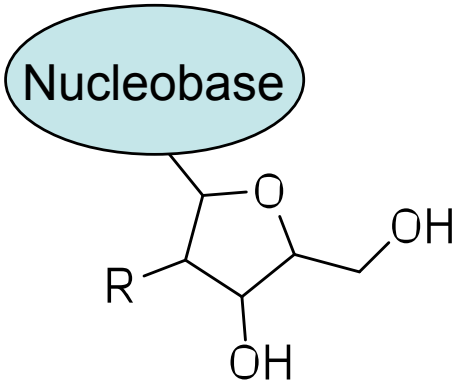
Nucleobase
O
OH
R
OH

NWA 4482-Comparison between ^{11}B and proton irradiation

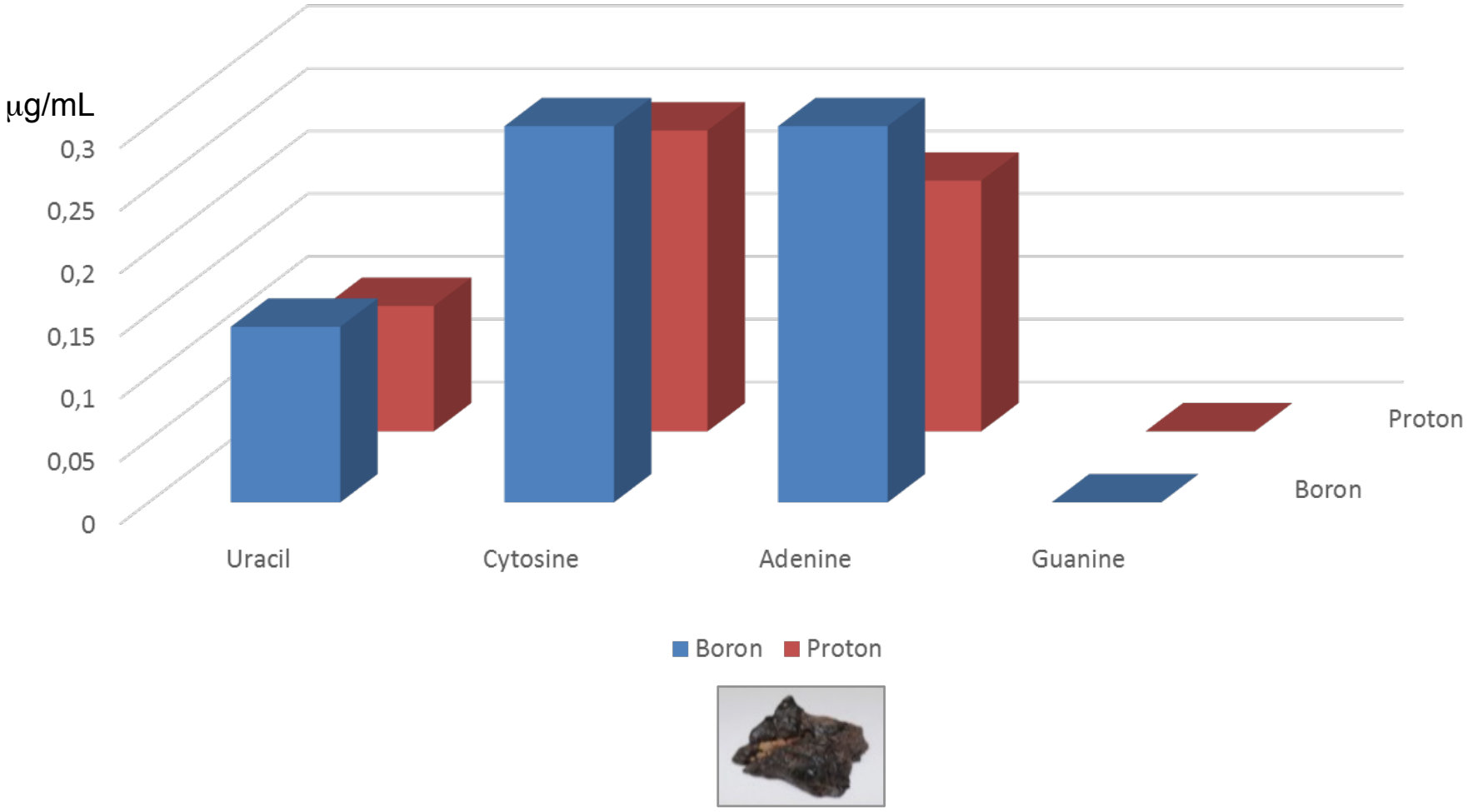


Italian Astrobiology Society - Societa' Italiana di Astrobiologia


UNIVERSITAS STUDIORUM TUSCIAE
VITERBIUM MCMLXXIX

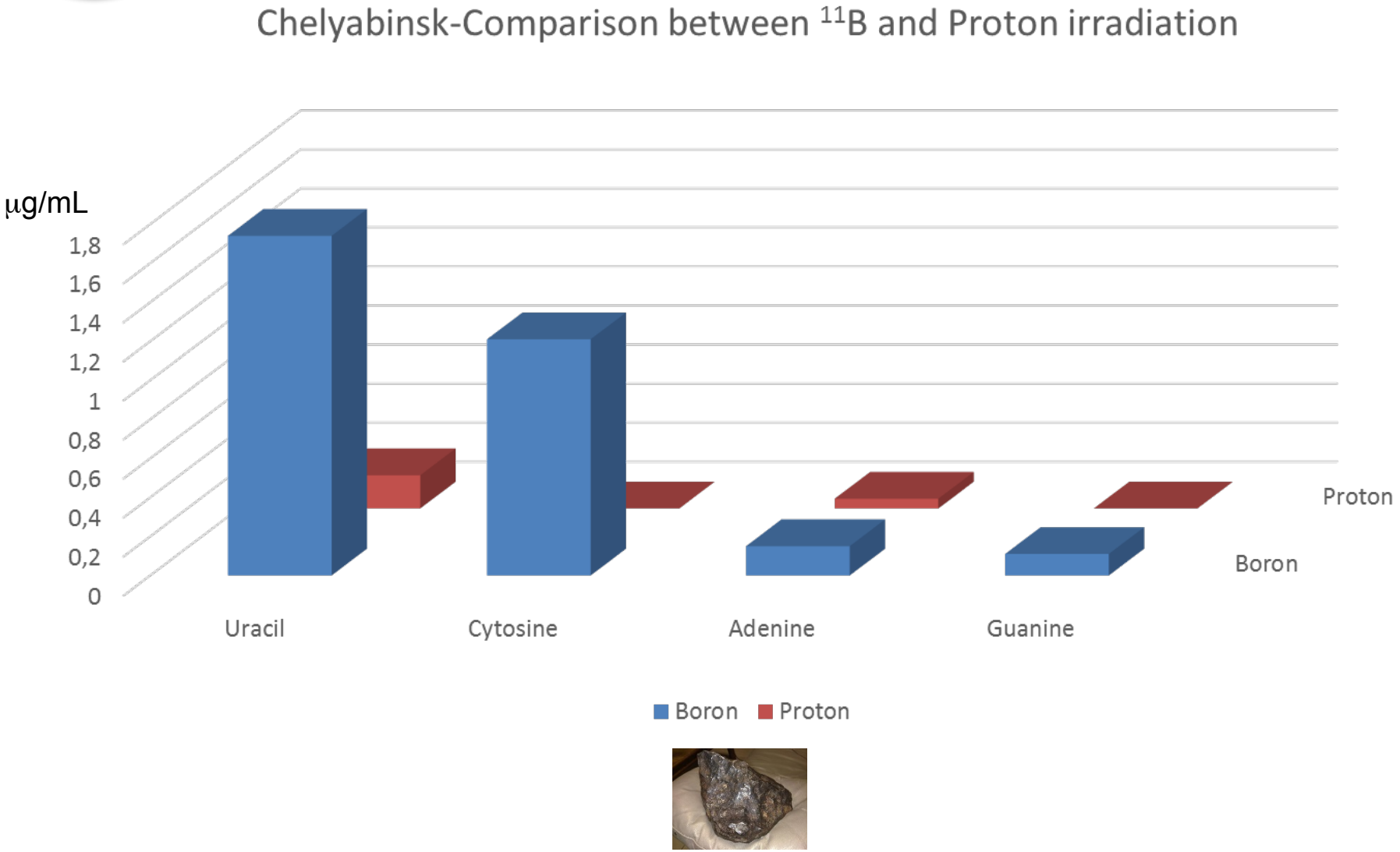
Chelyabinsk-Comparison between 11B and Proton irradiation
μg/mL
1,8
1,6
1,4
1,2
1
0,8
0,6
0,4
0,2
0
Uracil
Cytosine
Adenine
Guanine
Proton
Boron
Boron
Proton

NWA 1465-Comparison between ^{11}B and Proton irradiation

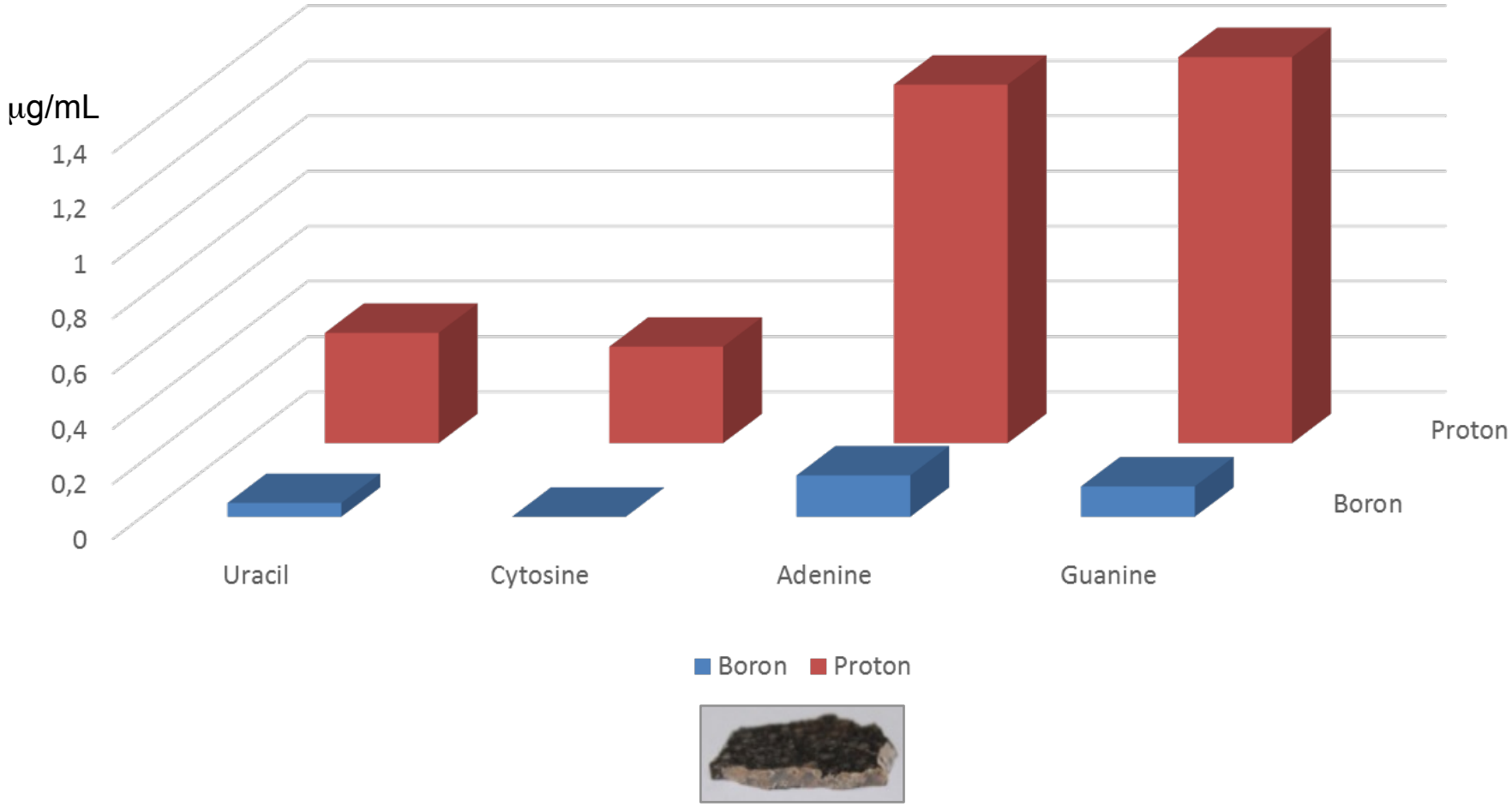

the formamide connection

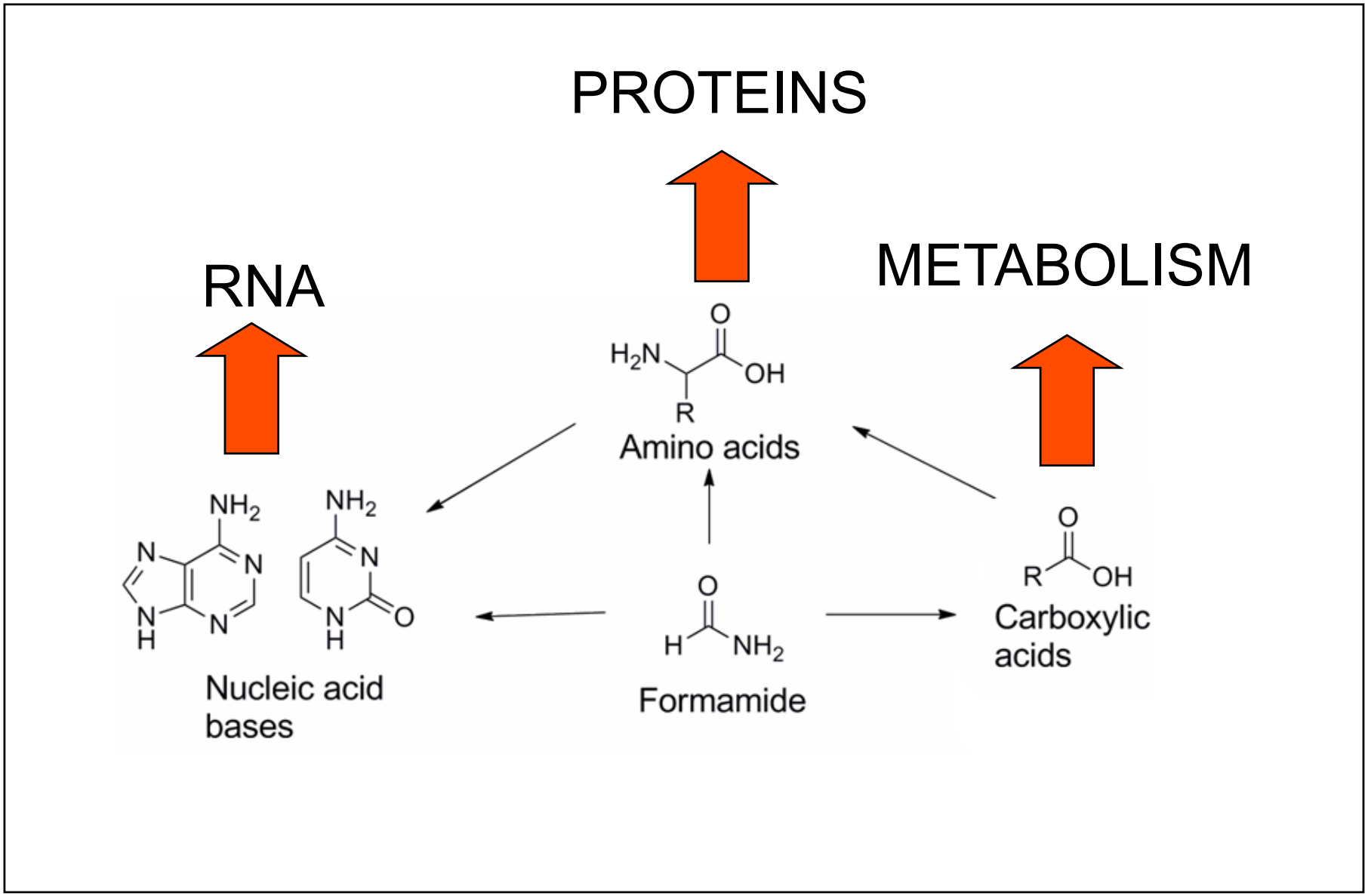

the egg and the chicken

R. SALADINO , G. BOTTA , S. PINO , G. COSTANZO,E. DI MAURO
Genetics first or metabolism first? The formamide clue
CHEMICAL SOCIETY REVIEW (2012) 41, 5526–5565

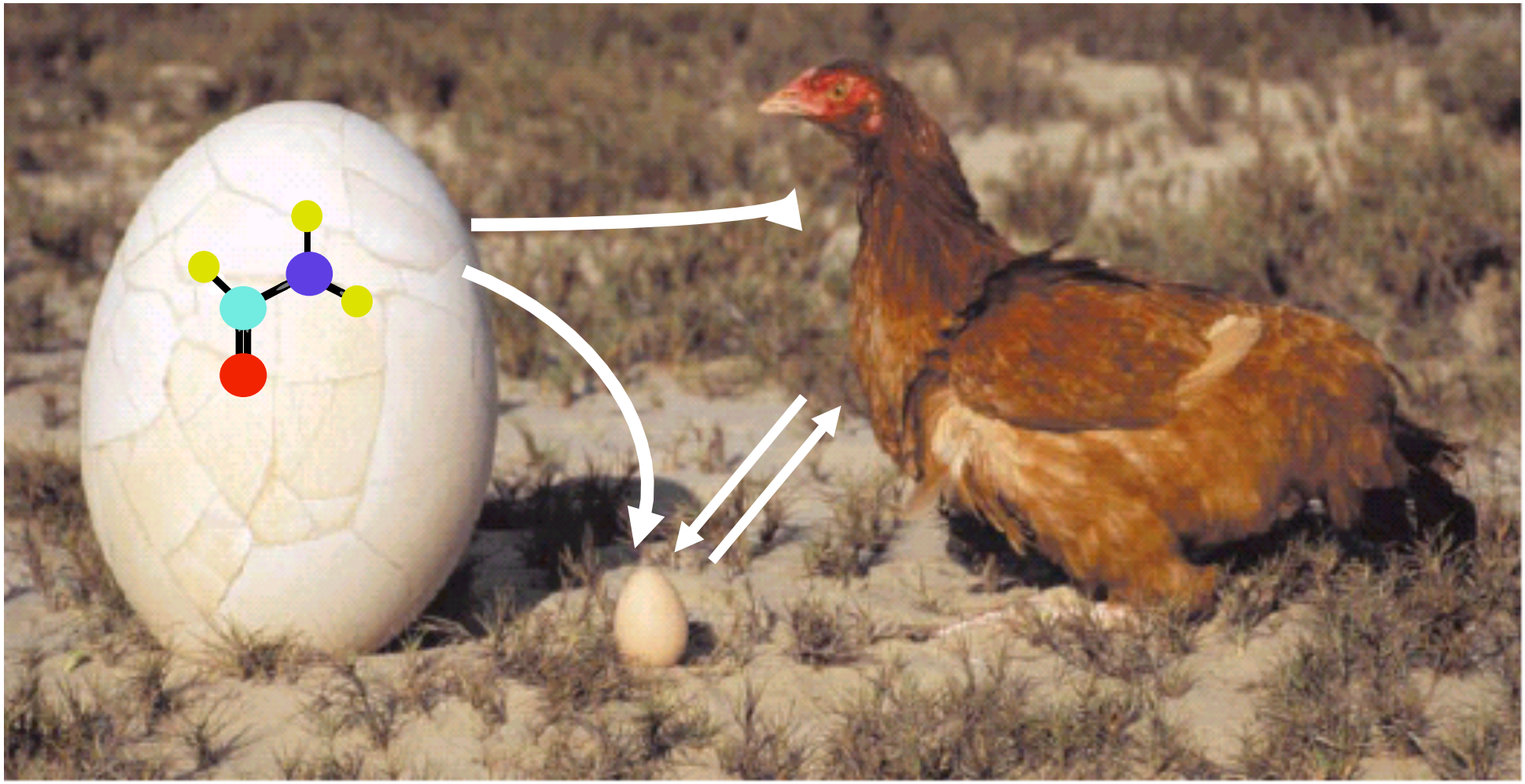



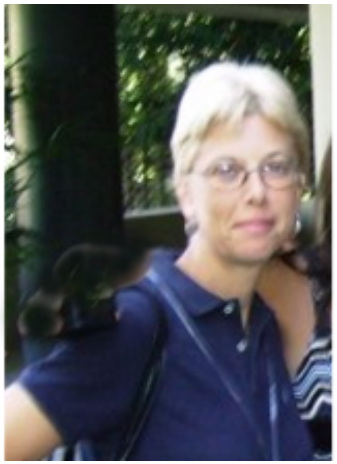

E. Di Mauro, R. Saladino, G. Costanzo, S. Pino, J. & J. Šponer

the organic cycle on Titan

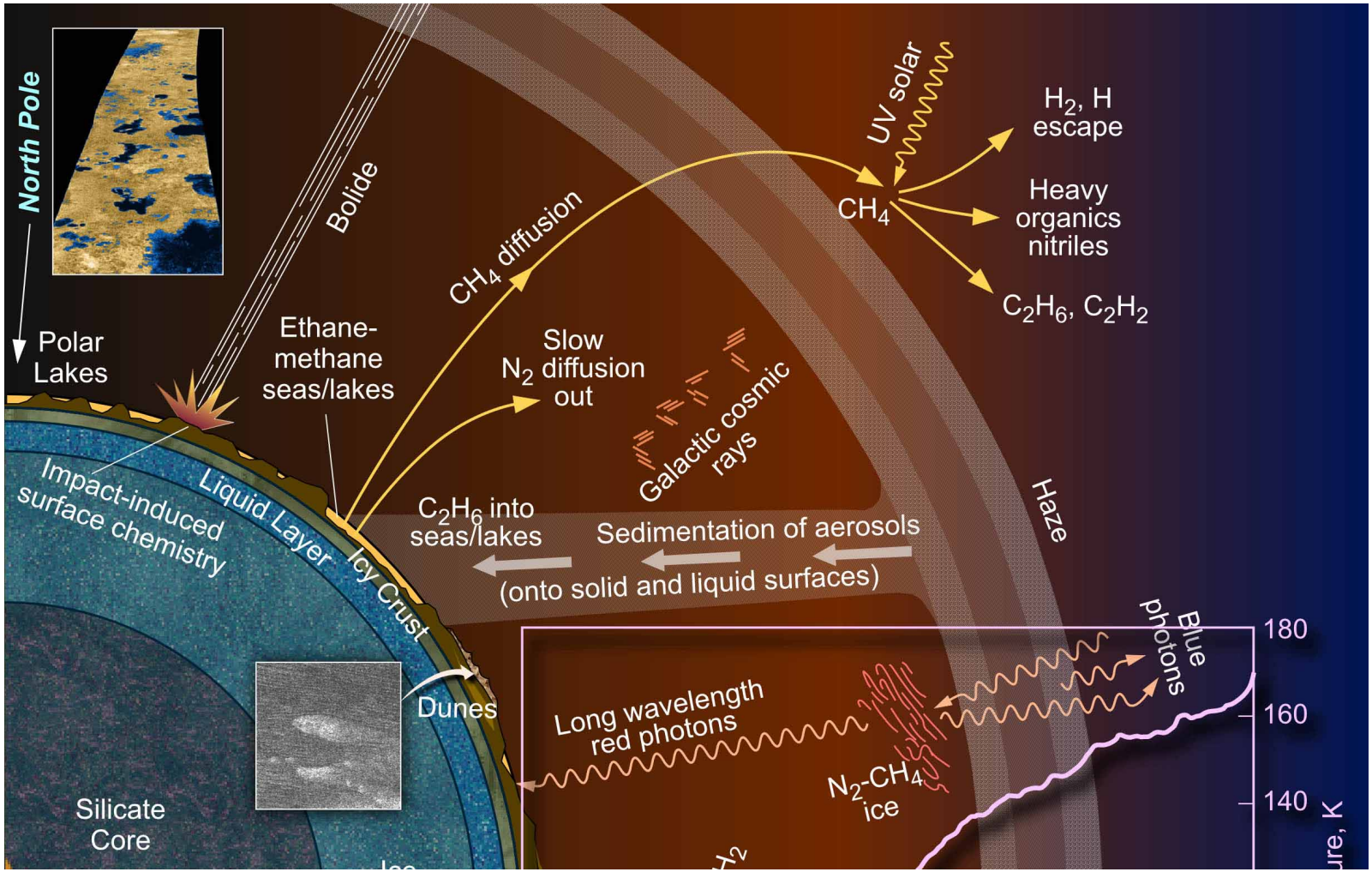


the water planet

CONTENTS

THE DEAD PAST 7
THE FOUNDATION OF S.F. SUCCESS 55
FRANCHISE 57
GIMMICKS THREE 75

THE WATERY PLACE

THE MESSAGE 119
SATISFACTION GUARANTEED 121
HELL-FIRE 137
THE LAST TRUMP 139
THE FUN THEY HAD 157
JOKESTER 161
THE IMMORTAL BARD 175
SOMEDAY 179
THE AUTHOR'S ORDEAL 189
DREAMING IS A PRIVATE THING 193

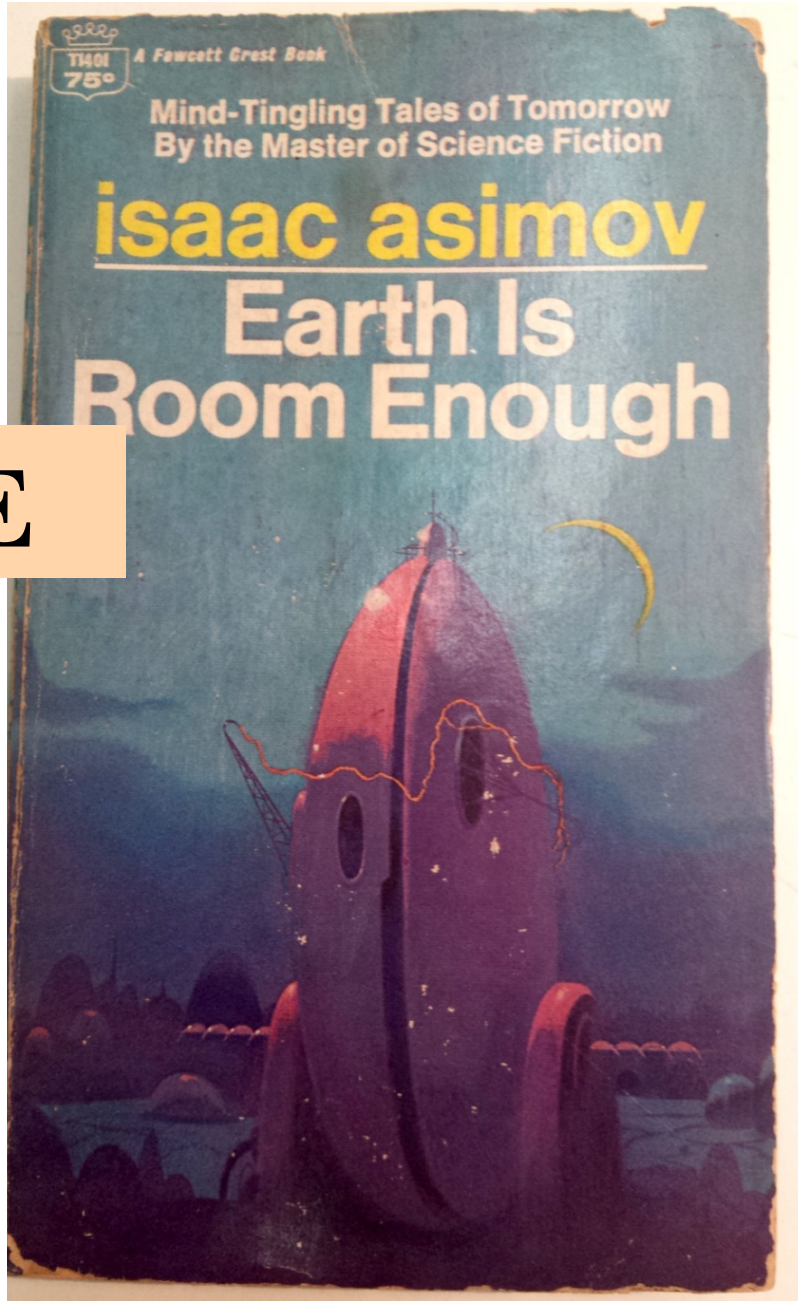

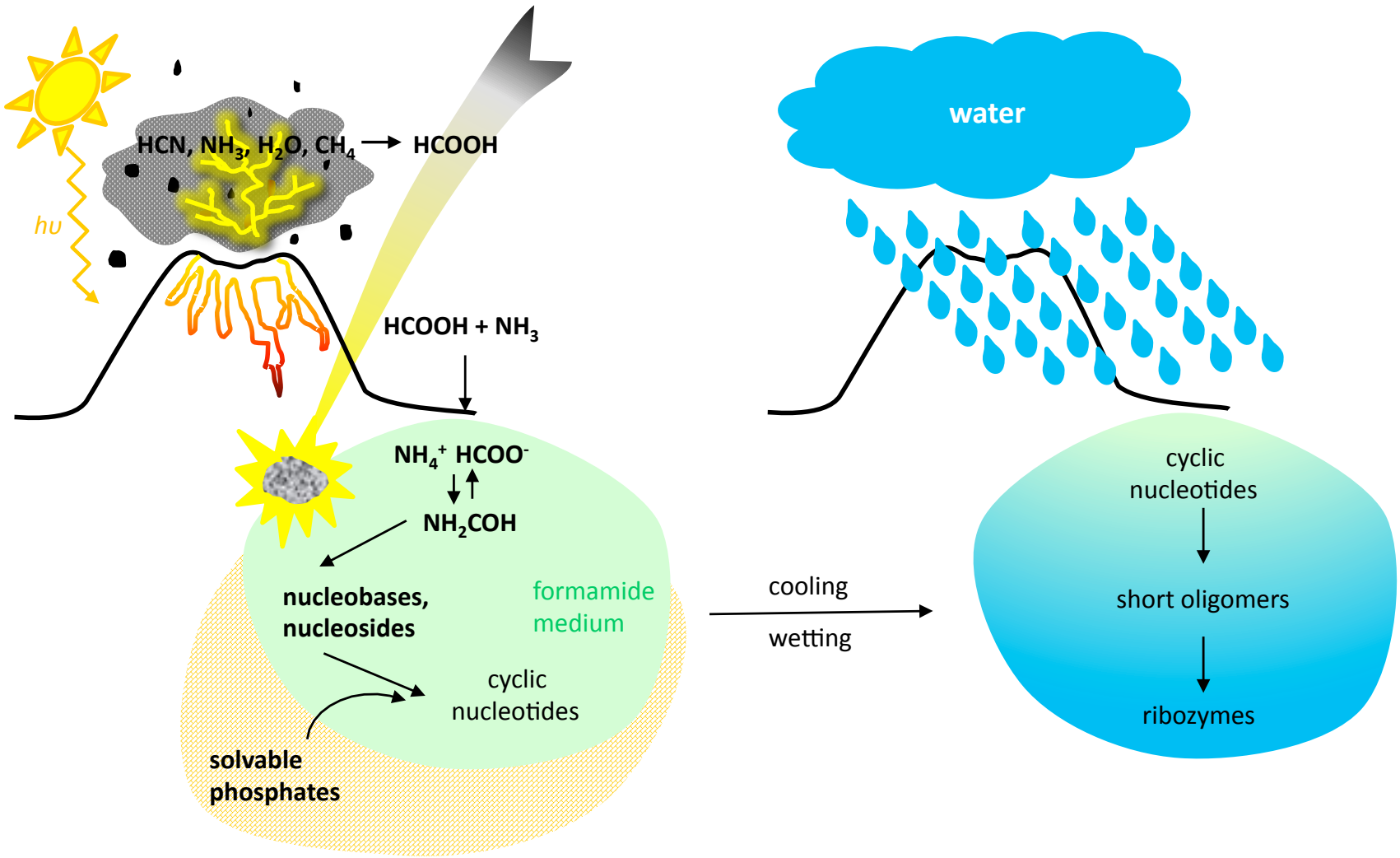
HCN, NH3, H2O, CH4
HCOOH
hu
HCOOH + NH3
NH4+ HCOO-
NH2COH
nucleobases,
nucleosides
formamide
medium
cyclic
nucleotides
solvable
phosphates
water
cooling
wetting
cyclic
nucleotides
short oligomers
ribozymes

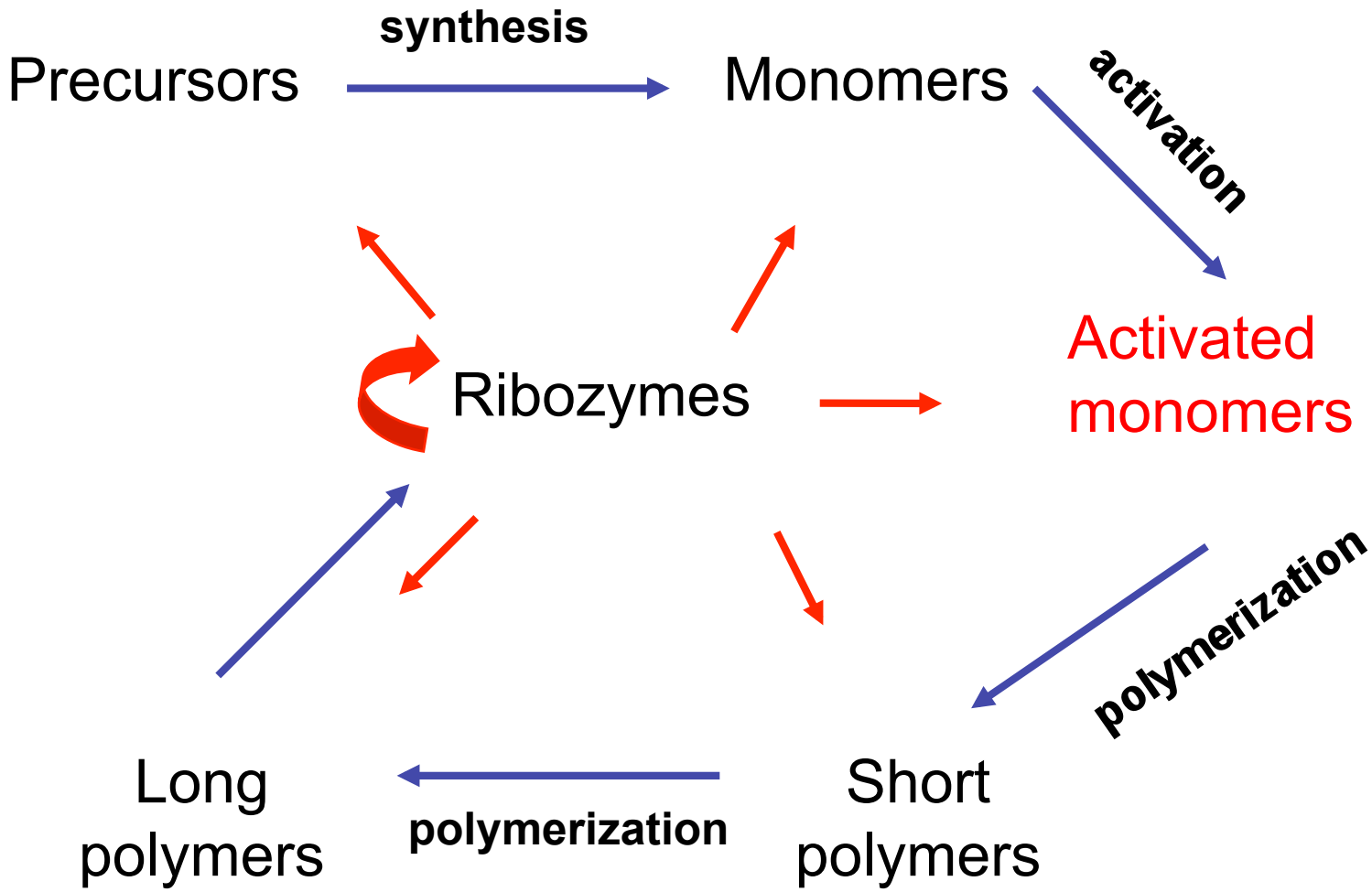
Precursors
synthesis
Monomers
activation
Activated monomers
Ribozymes
polymerization
Short polymers
polymerization
Long polymers

phosphate minerals

- Variscite $Al(PO_4)(H_2O)_2$
- Augelite $Al_2\ PO_4(H_2O)_3$
- Wavellite $Al_3(OH)_3(PO_4)_2(H_2O)_5$
- Hydroxylapatite $Ca_5(PO_4)_3OH$
- Hureaulite $Mn^{2+}{}_5(PO_3(OH)_2(PO_4)(H_2O)_4$
- Reddingite $Mn^{2+}{}_3(PO_4)_2(H_2O)_3$
- Purpurite $Mn^{3+}(PO_4)$
- Ludlamite $Fe^{2+}{}_3\ (PO_4)_2(H_2O)_4$
- Vivianite $Fe^{2+}{}_3(PO_4)_2(H_2O)_8$
- Strengite $Fe^{3+}(PO_4)(H_2O)_2$
- Cacoxenite $Fe^{3+}{}_{25}(PO_4)_{17}O_6(OH)_{12}(H_2O)_{75}$
- Libethenite $Cu^{2+}{}_2(PO_4)(OH)$
- Cornetite $Cu^{2+}{}_3(PO_4)(OH)_3$
- Tarbuttite $Zn_2(PO_4)(OH)$
- Monazite $Ce(PO4)$
- Montebrasite $Li[Al(PO_4)(OH)]$
- Beryllonite $Na[BePO_4]$
- Brasilianite $NaAl_3(PO_4)_2(OH)_4$
- Wardite $NaAl_3(OH)_4(PO_4)_2(H_2O)_2$
- Hydroxylapatite $Ca_5(PO_4)_3OH$
- Lazulite $Mg[Al(PO_4)(OH)]_2$
- Childrenite $Mn^{2+}[Al(PO_4)(OH)_2(H_2O)]$
- Triphylite $LiFe^{2+}(PO_4)$
- Eosphorite $Fe^{2+}[Al(PO_4)(OH)_2(H_2O)]$
- Vauxite $Fe^{2+}Al_2(PO_4)(OH)_2(H_2O)_6$
- Fairfieldite $Ca_2\ [Mn^{2+}(PO_4)(H_2O)\ _2]$
- Laueite $Mn^{2+}[Fe^{3+}{}_2(PO_4)_2(OH)_2(H_2O)_2](H_2O)_4(H_2O)_2$
- Rockbridgeite $Fe^{2+}Fe^{3+}{}_4(PO_4)_3(OH)_5$
- Fluorapatite $Ca_5(PO_4)_3F$
- Crandallite $CaAl_3(PO_4)_2(OH)_5{+}H_2O$
- Anapaite $Ca_2[Fe^{2+}(PO_4)_2(H_2O)_4]$
- Scholzite $CaZn_2(PO_4)_2(H_2O)_2$
- Turquoise $Cu^{2+}Al_6(PO_4)_4(OH)_8(H_2O)_4$
- Pyromorphite $Pb_5(PO_4)_3Cl$
- Autunite $Ca[(UO_2)\ (PO_4)]_2(H_2O)_{10\text{-}12}$
- Torbenite $Cu^{2+}[(UO_2\ (PO_4)]_2\ (H_2O)_8$
- Herderite $Ca[BePO_4F]$
- Pseudomalachite $Cu^{2+}{}_5\ (PO_4)_2(OH)_4$
- Calcioferrite $Ca_4MgFe_4(PO_4)_6(OH)_4(H_2O)_{13}$

phosphate minerals

Class 1 **NO release of (P)**	herderite $Ca[BePO_4F]$ pyromorphite $Pb_5(PO_4)_3Cl$ **turquoise** $Cu^{2+}Al_6(PO_4)_4(OH)_8(H_2O)_4$ fluorapatite $Ca_5(PO_4)_3F$
Class 2 **release of (P)** **proportional phosphorylation in solution**	hureaulite $Mn^{2+}_5(PO_3(OH)_2(PO_4)(H_2O)_4$ hydroxylapatite $Ca_5(PO_4)_3OH$ vivianite $Fe^{2+}_3(PO_4)_2(H_2O)_8$ **cornetite** $Cu^{2+}_3(PO_4)(OH)_3$ **pseudomalachite** $Cu^{2+}_5(PO_4)_2(OH)_4$
Class 3 **surface reaction**	**libethenite** $Cu^{2+}_2(PO_4)(OH)$ retention YES **reichenbachite** $Cu^{2+}_5(PO_4)_2(OH)_4$ retention NO **ludjibaite** $Cu^{2+}_5(PO_4)_2(OH)_4$ retention NO
Class 4 **phosphorylation enhancers**	**malachite** $Cu_2^{2+}(CO_3)(OH)_2$

spontaneous phosphorylation of nucleosides

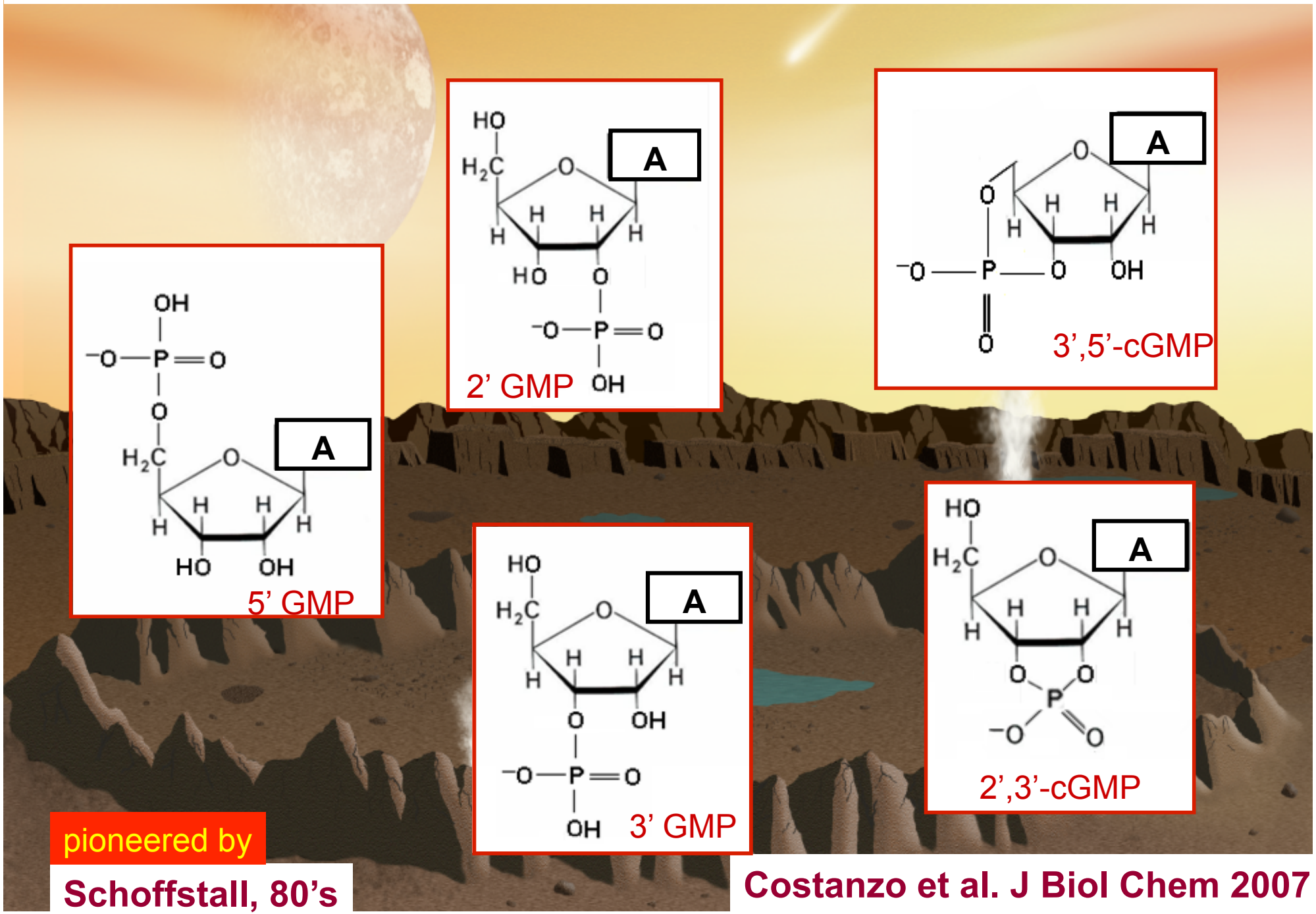

pioneered by

Schoffstall, 80’s

Costanzo et al. J Biol Chem 2007

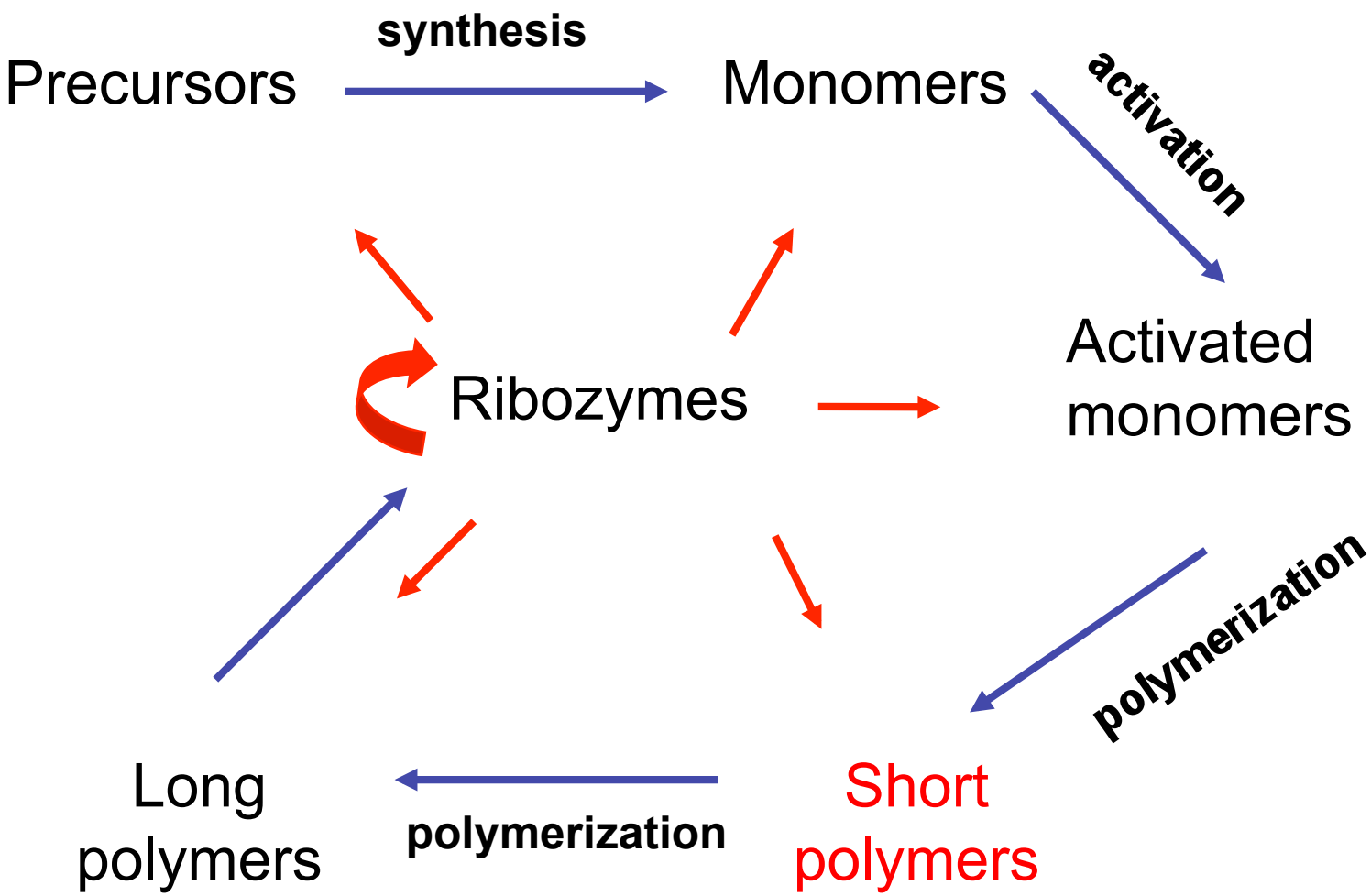
Precursors
synthesis
Monomers
activation
Activated monomers
Ribozymes
polymerization
Short polymers
polymerization
Long polymers

Costanzo et al. J Biol Chem 2009
Pino et al. Biochemistry 2011
Costanzo et al. ChemBioChem 2012
Stadlbauer et al. Chemistry Eur J 2015

RNA polymerization in water and in dry

pioneered by

J. molec. Evolution 2, 303—316 (1973)

Catalysts for the Self-Polymerization of Adenosine Cyclic 2′,3′-Phosphate

M. S. Verlander*, R. Lohrmann, and L. E. Orgel

The Salk Institute for Biological Studies, San Diego, California 92112

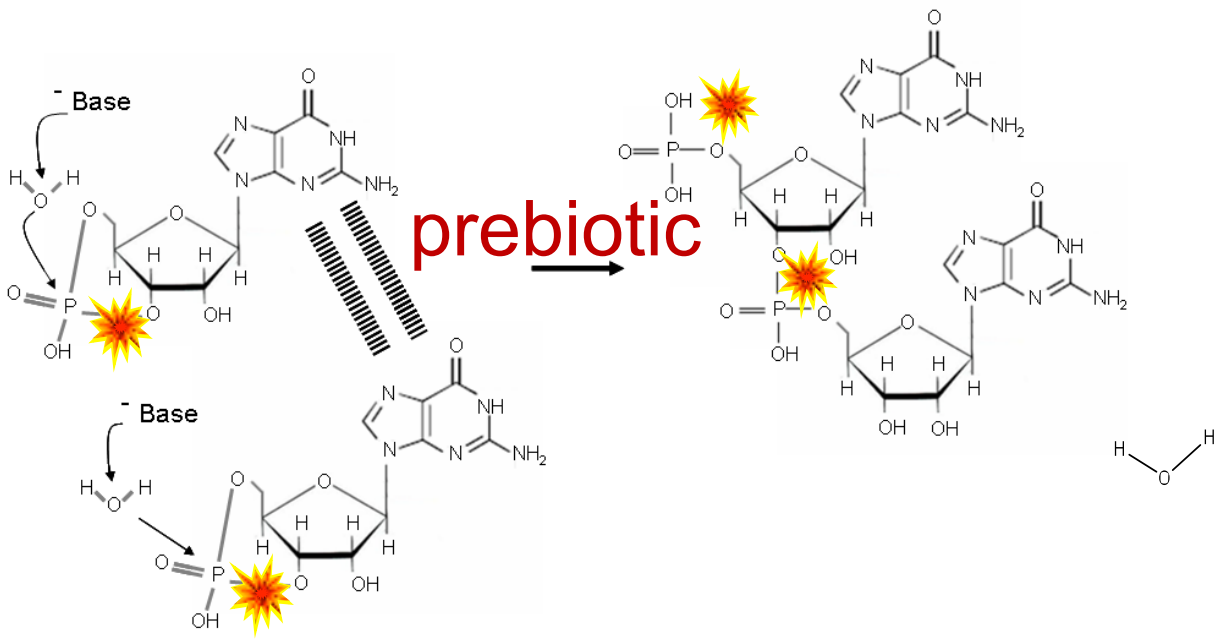

why cyclics?

GMP vs. cGMP

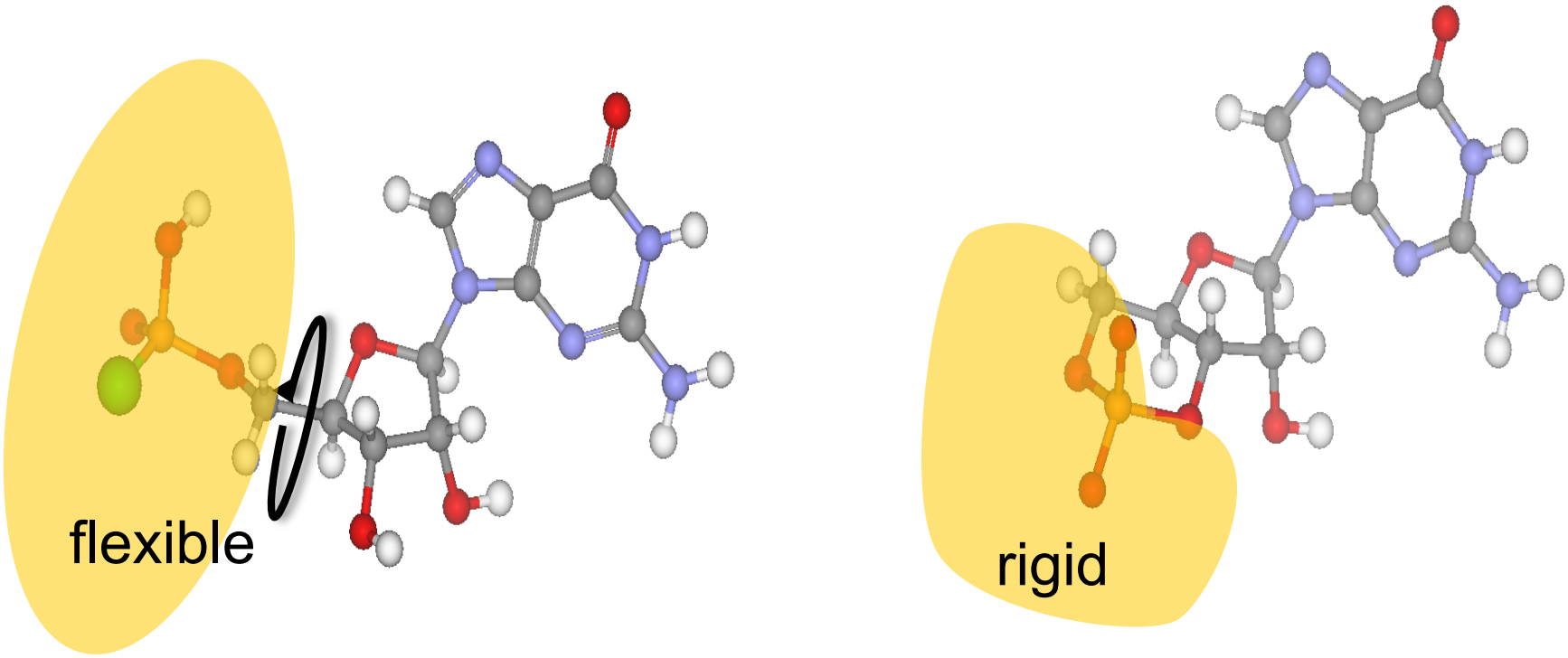

Polymerization model

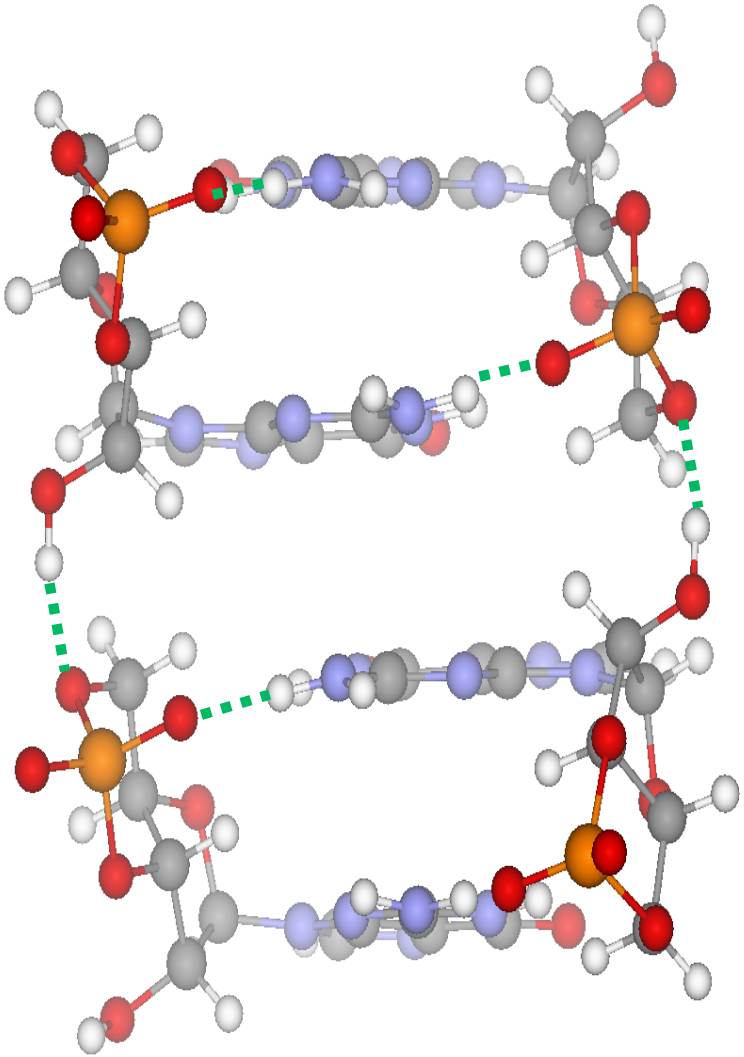

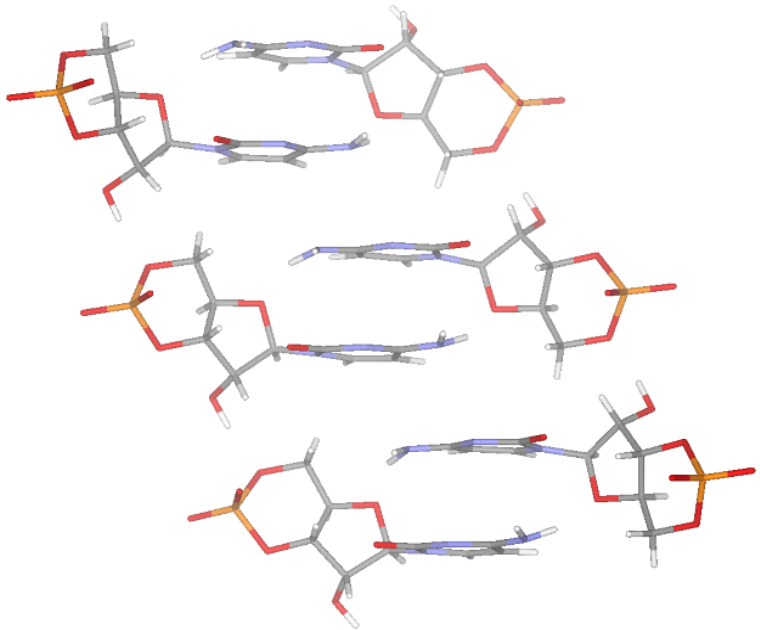

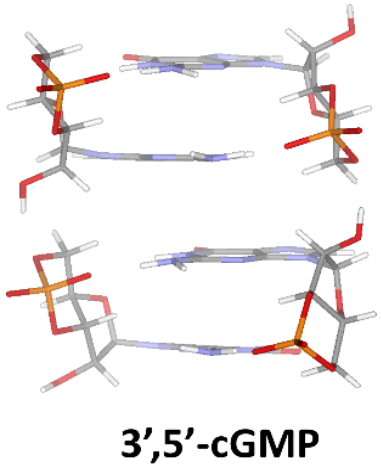

Figure S3. Comparison of the stacked architectures compatible with the polymerization mechanism described in Ref. 26 for 3',5'-cGMP. Geometry optimizations were performed at TPSS-D2 level of theory using the TZVP basis set. For details of the calculations see the *Quantum chemical calculations* part of the Supporting information.

Polymerization of 3',5'-cGMP

the (hypothetical) mechanism

Costanzo et al. J.Biol. Chem. 2009
Costanzo et al. ChemBioChem 2012
Stadlbauer et al.Chemistry Eur J 2015

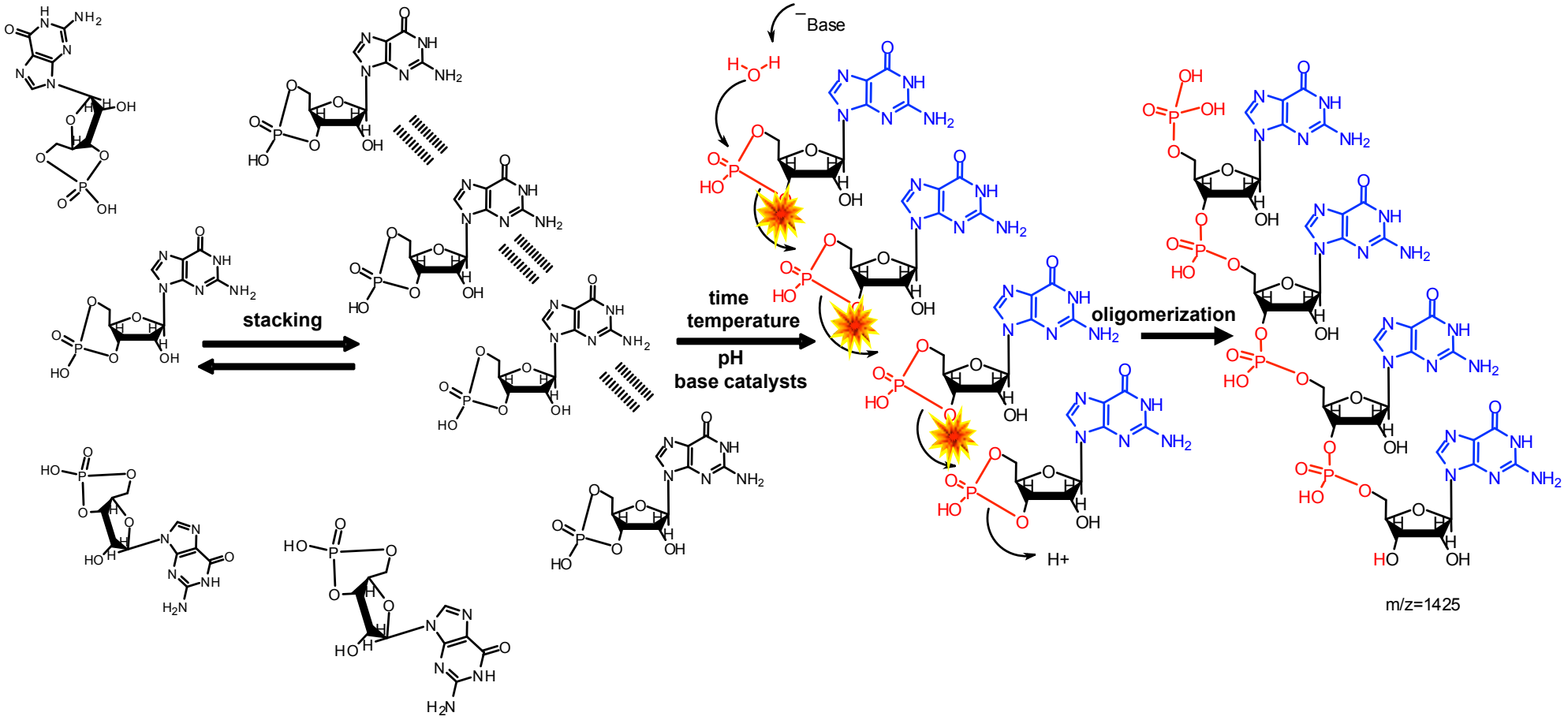

Stacking

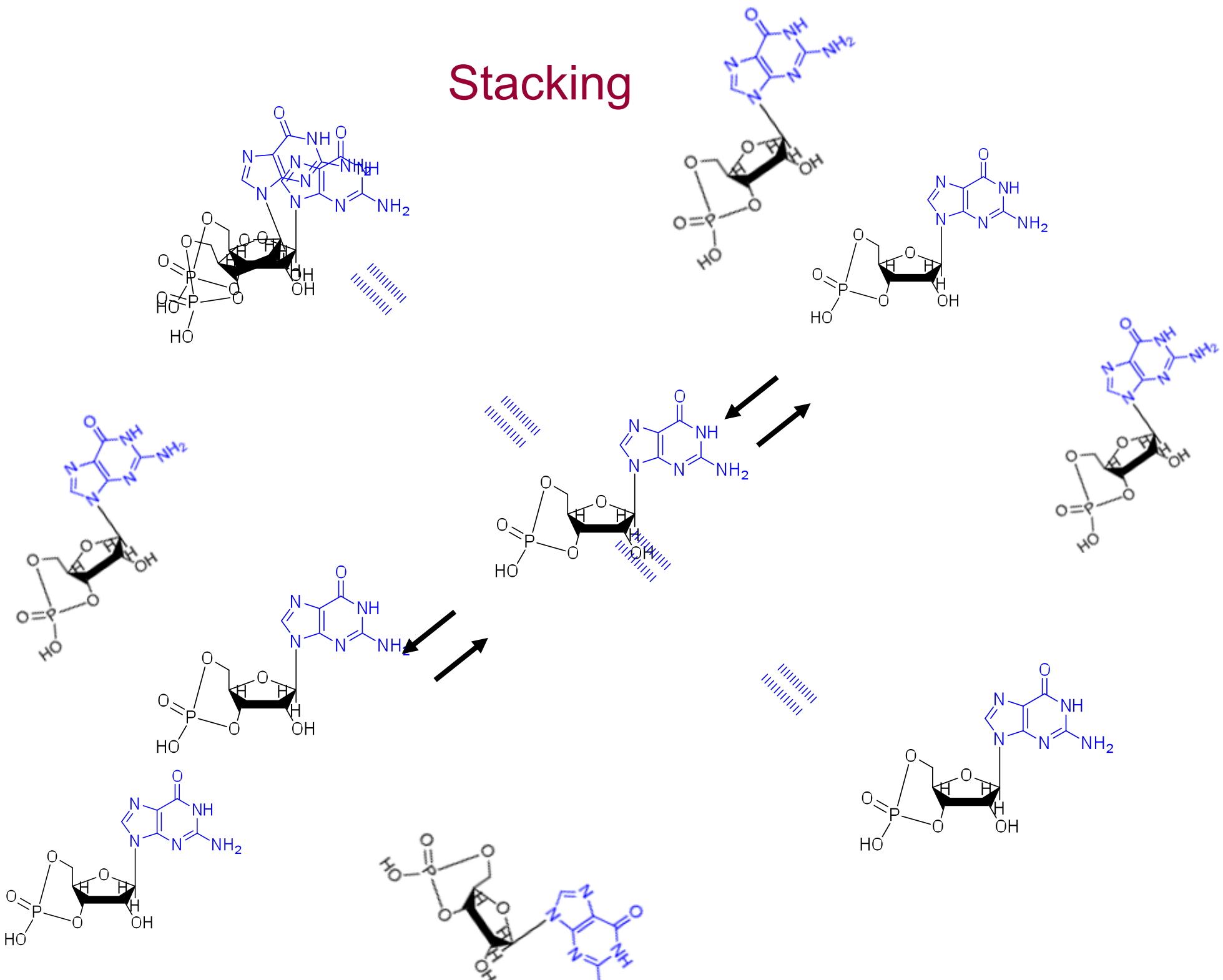

Stacking

Lambert-Beer Law $A = \varepsilon \cdot c \cdot l$

absorbance, extinction

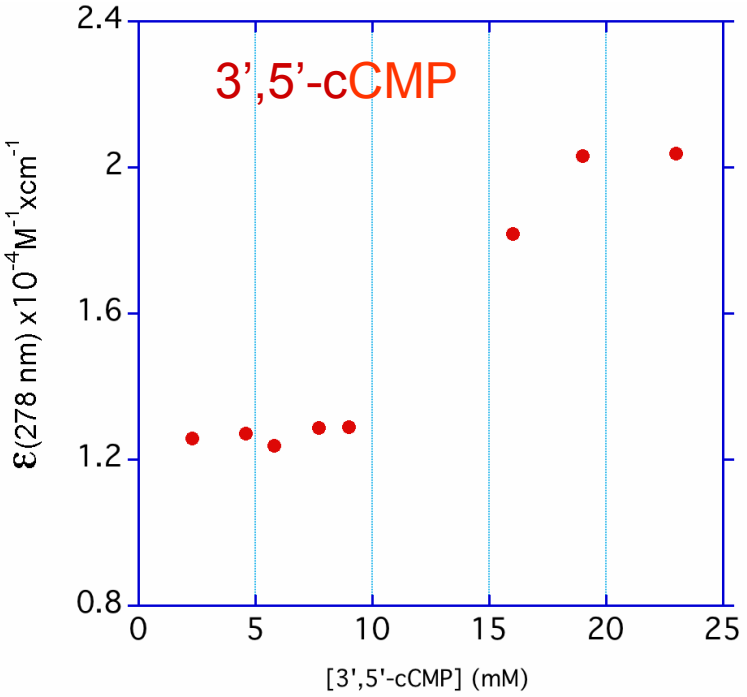

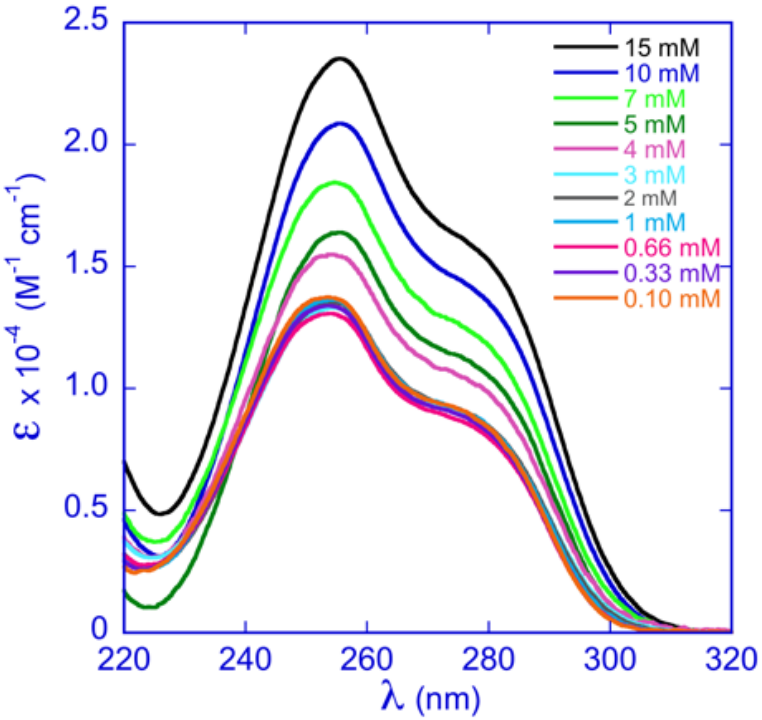

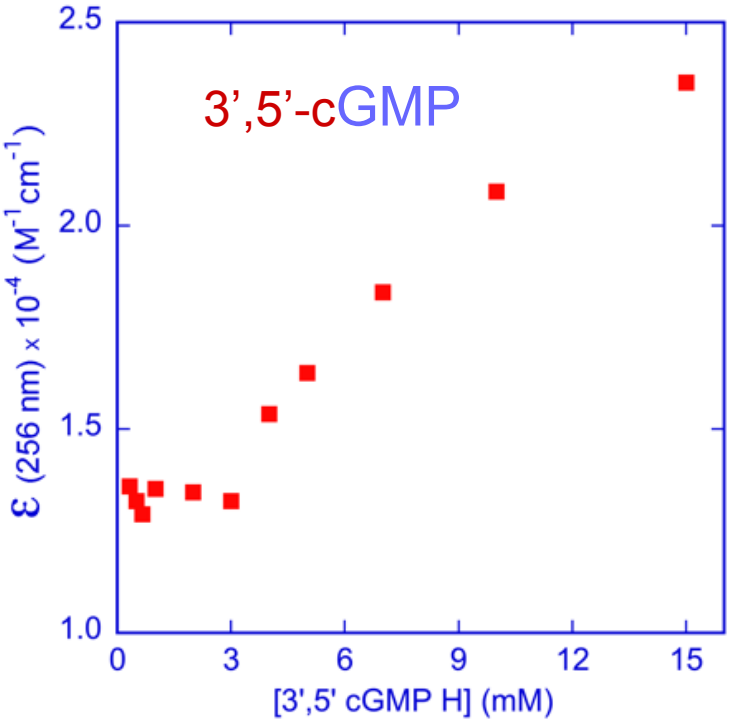

Heat-driven molecular accumulation in hydrothermal pores.

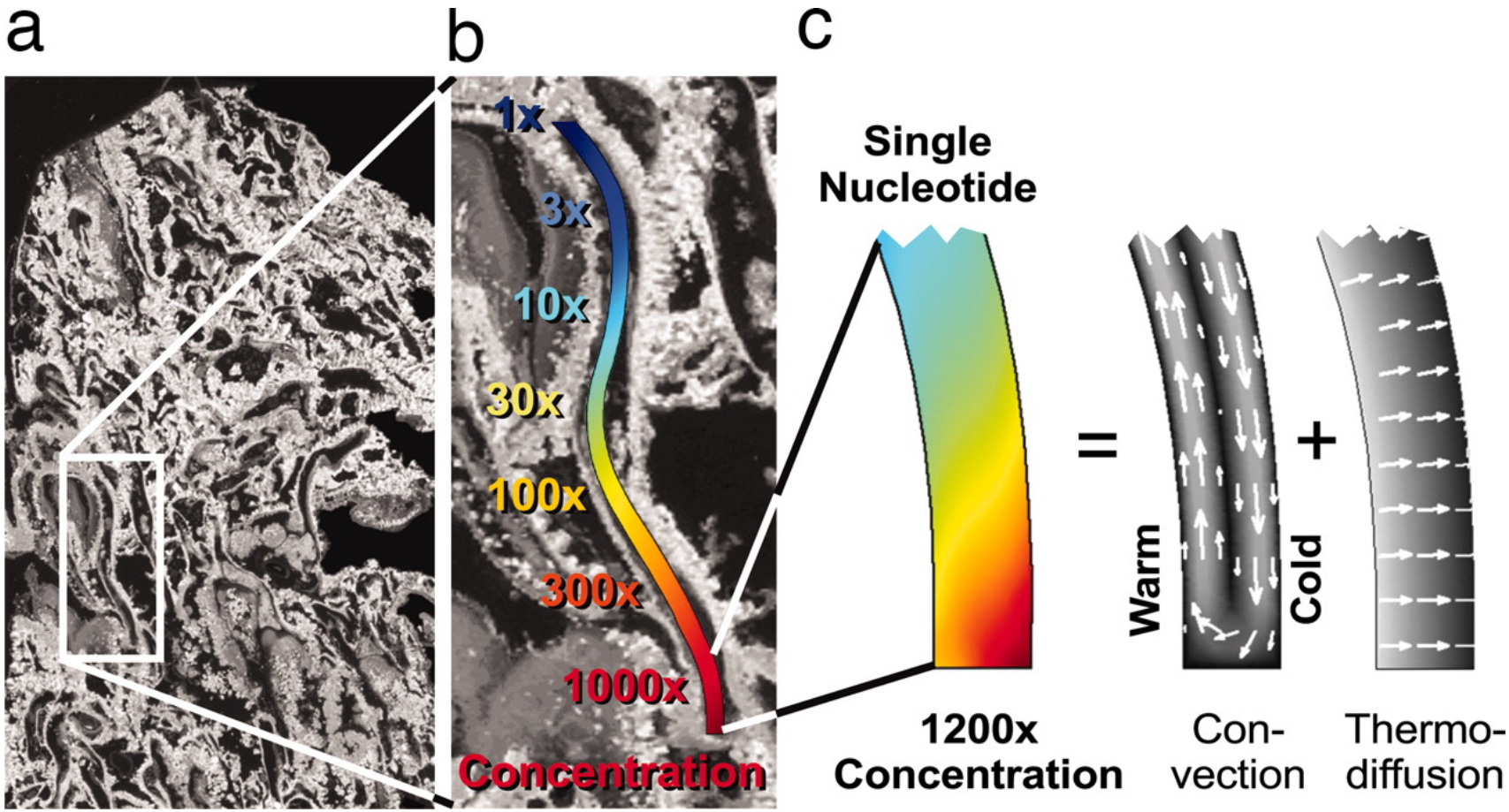

Baaske P et al. PNAS 2007;104:9346-9351

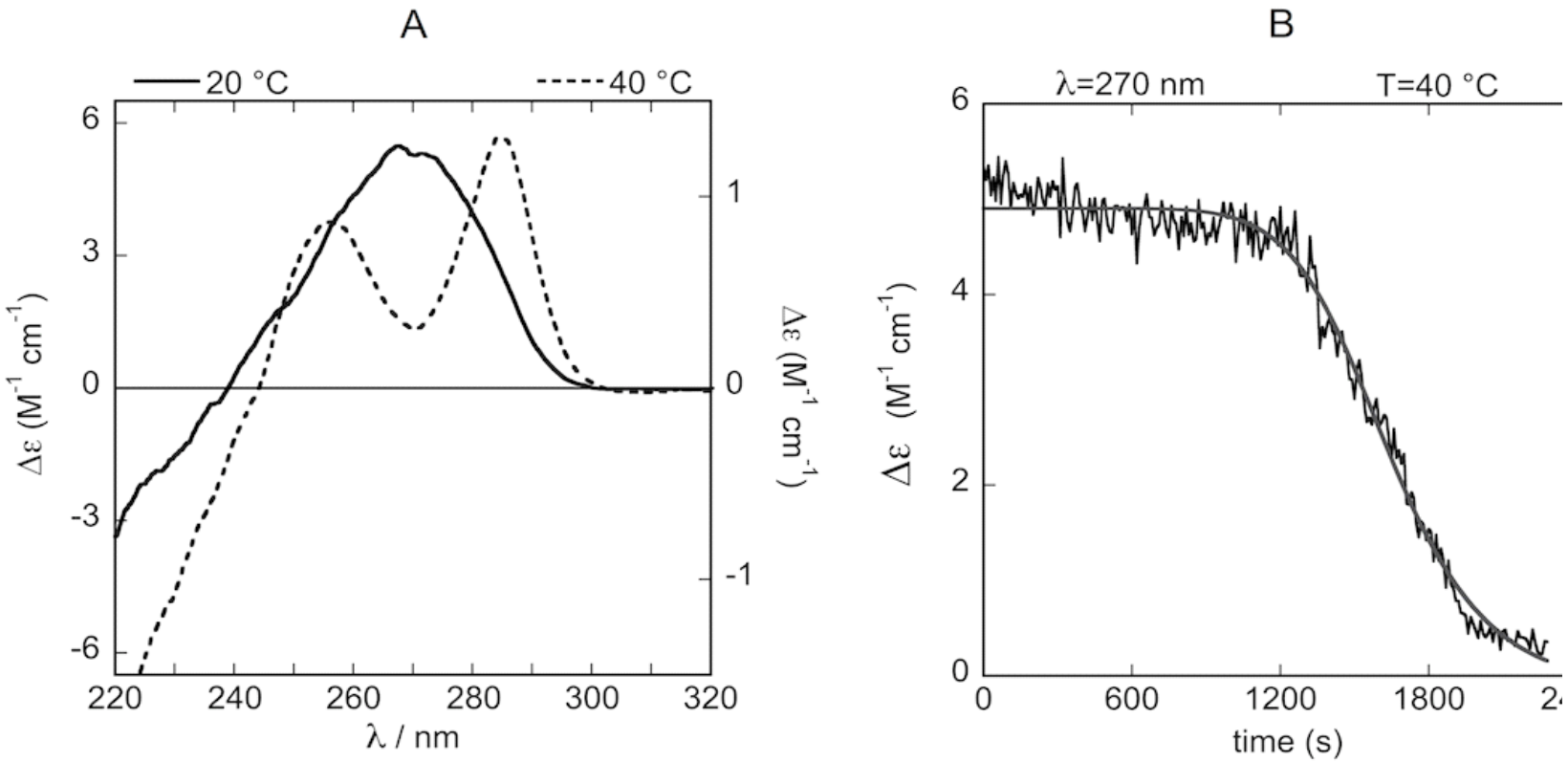

Figure S5. Persistence of the stacked state as a function of temperature. Panel A: Circular dichroism spectra 23 mM water solution of 3',5' cCMP achieved at 20 (solid line) and 40 °C (dashed line). Panel B : kinetics of stacking as a function of temperature: variation of molar circular dichroism of 23 mM water solution of 3',5 cCMP measured at 270 nm and 40 °C as a function of time. The interpolating line is drawn as a guide to the ey

polymerizing 3',5'-cyclic GMP: boosting by bases

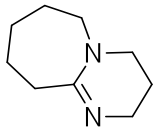

1,8-Diazabicycloundec-7-ene DBU

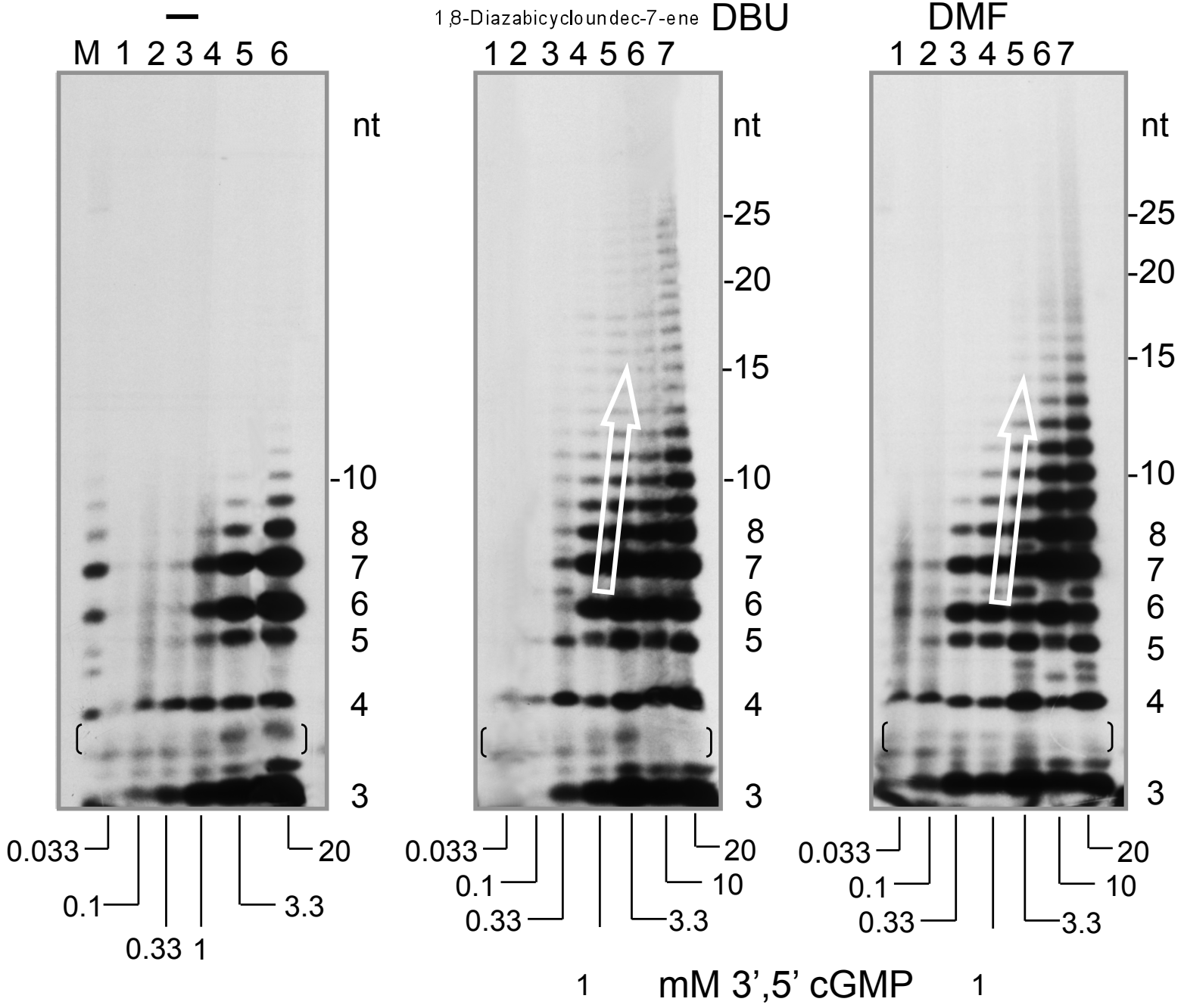

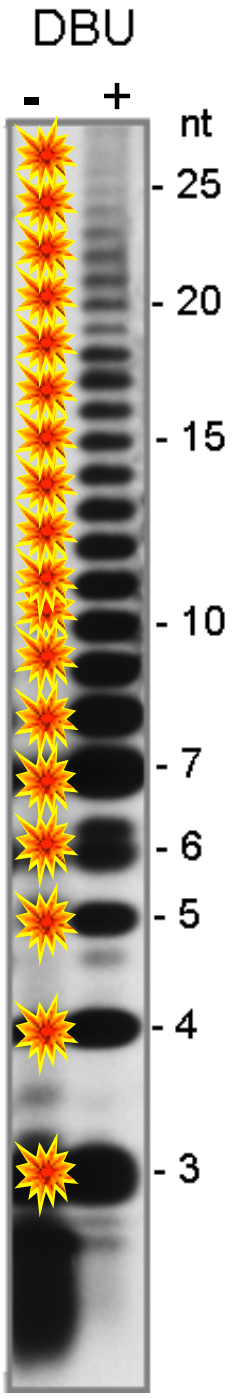

Polymerization of 3',5'-cGMP

Selectively produces 3',5'-linkages

3',5'-cGMP: prebiotic building block, can be synthesized from formamide

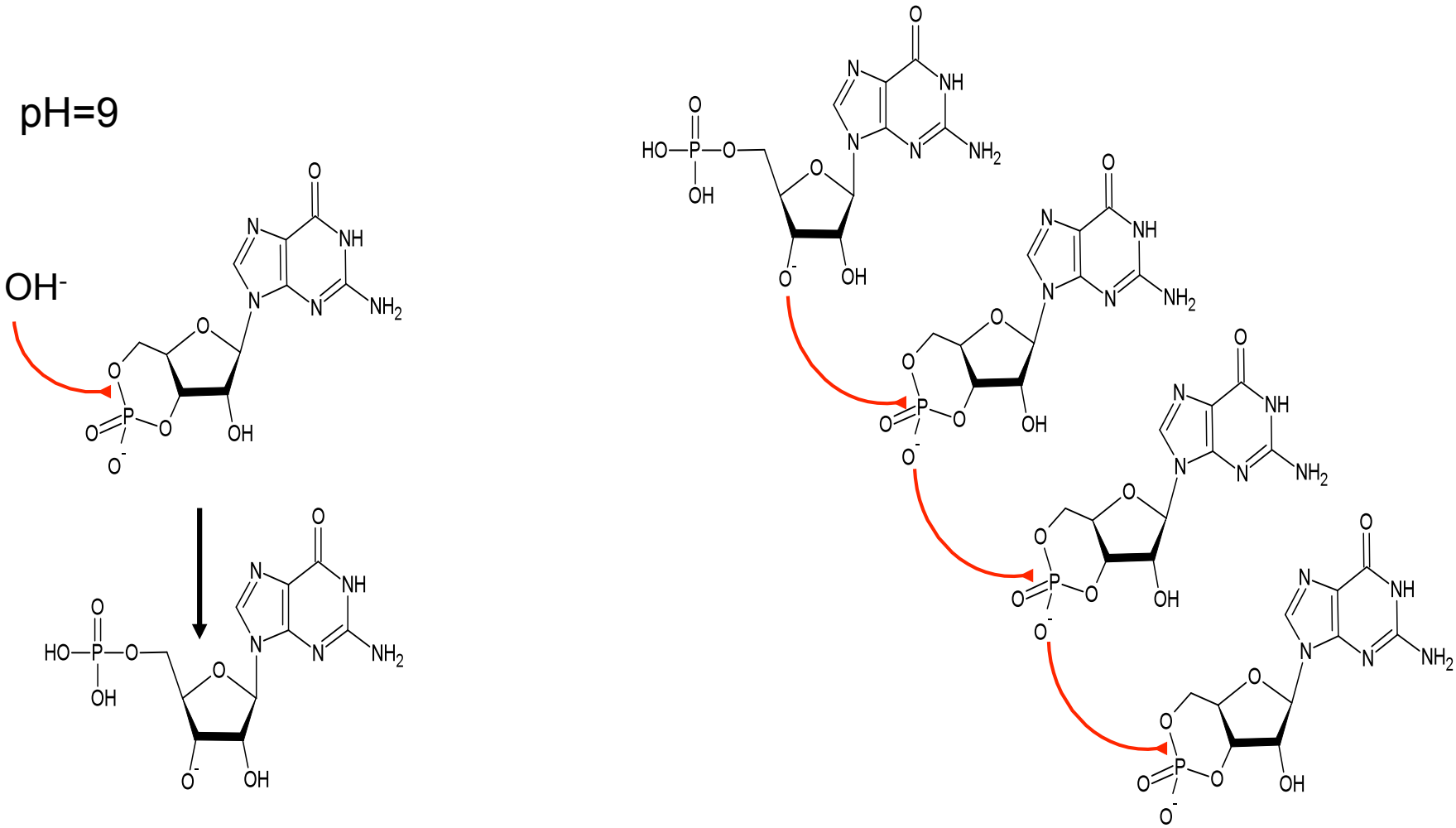

G. Costanzo, R. Saladino, G. Botta, A. Giorgi, A. Scipioni, S. Pino and E. Di Mauro, *Chembiochem*, 2012, 13, 999-1008.

MALDI ToF MS of 3',5'-cGMP polymerizations, dimer

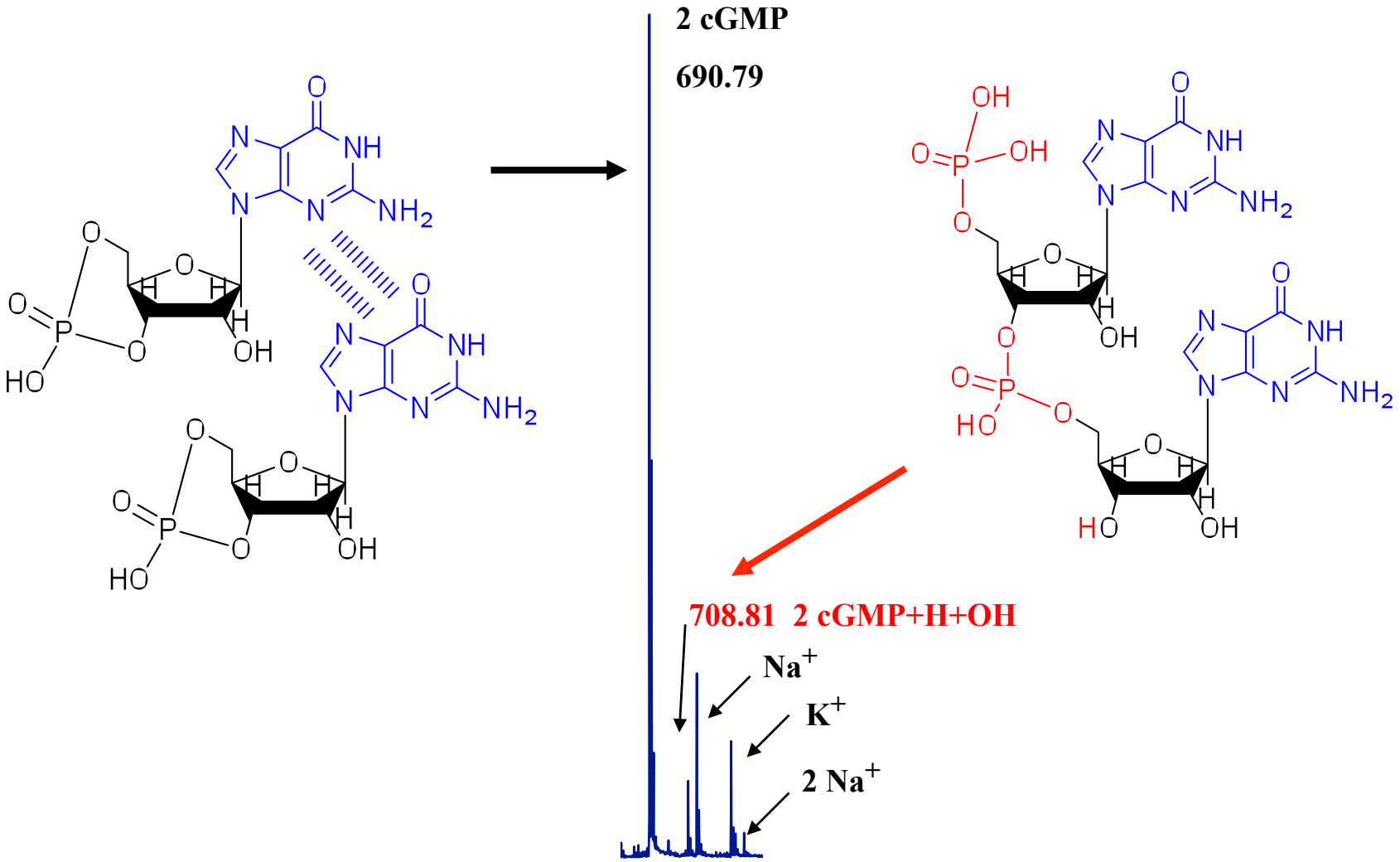

MALDI ToF MS of 3',5'-cGMP polymerizations

4 mer to 14 mer

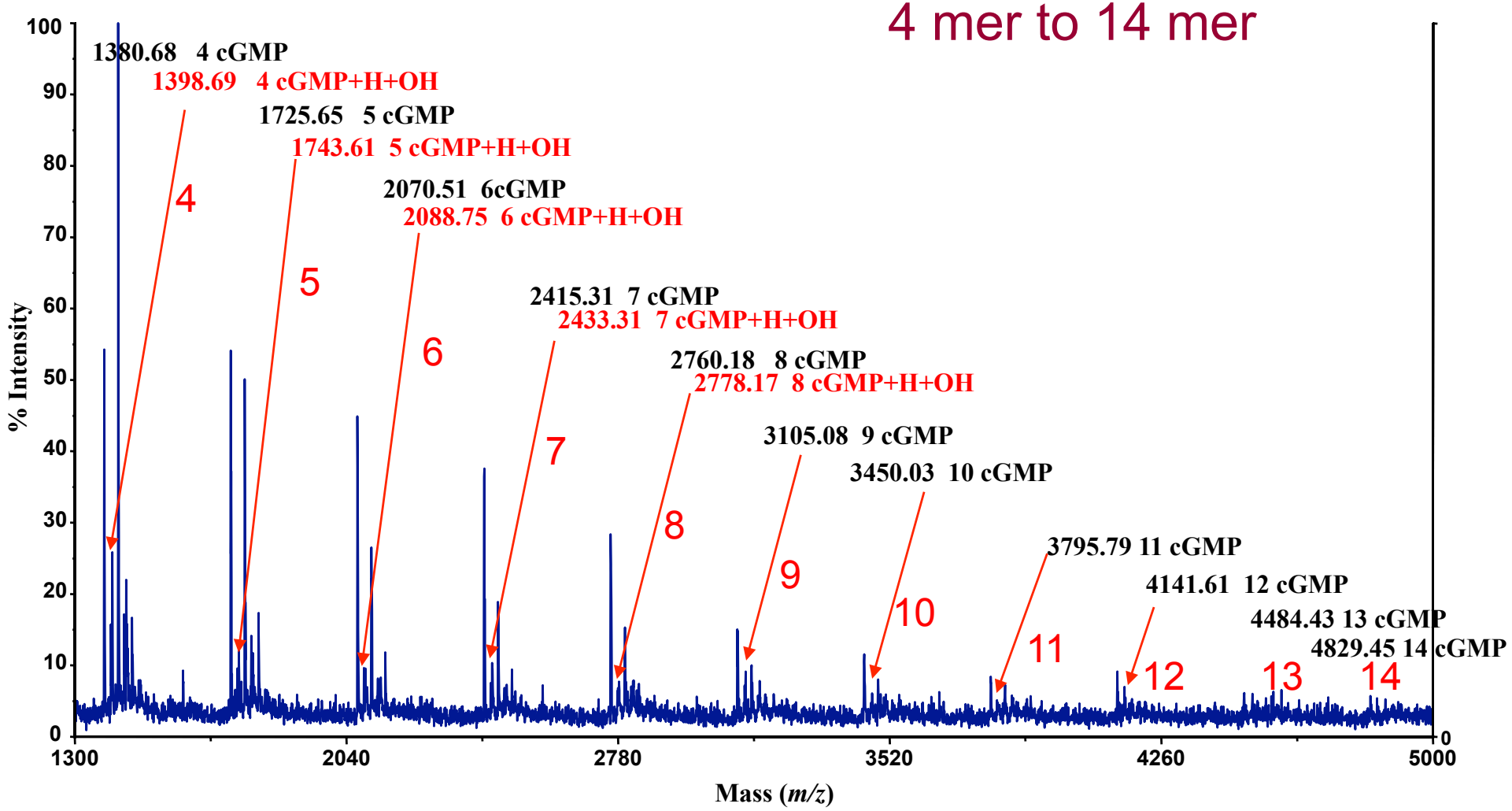

DOI: 10.1002/cbic.201200068

Generation of RNA Molecules by a Base-Catalysed Click-Like Reaction

Giovanna Costanzo,[a] Raffaele Saladino,[b] Giorgia Botta,[b] Alessandra Giorgi,[c] Anita Scipioni,[d] Samanta Pino,[e] and Ernesto Di Mauro*[e]

The problem of the abiotic origin of RNA from prebiotically plausible compounds remains unsolved. As a potential partial solution, we report the spontaneous polymerization of 3′,5′-cyclic GMP in water, in formamide, in dimethylformamide, and (in water) in the presence of a Brønsted base such as 1,8-diazabicycloundec-7-ene. The reaction is untemplated, does not require enzymatic activities, is thermodynamically favoured and selectively yields 3′,5′-bonded ribopolymers containing as many as 25 nucleotides. We propose a reaction pathway on the basis of 1) the measured stacking of the 3′,5′-cyclic monomers, 2) the activation by Brønsted bases, 3) the determination (by MALDI-TOF mass spectrometry, by ^{31}P NMR, and by specific ribonucleases) of the molecular species produced. The reaction pathway has several of the attributes of a click-like reaction.

Ribozyme activity of abiotically generated RNA

Samanta Pino,[a] Giovanna Costanzo,[b] Alessandra Giorgi, [c] and Ernesto Di Mauro* [d]

((Dedication, optional))

3',5' cyclic GMP nonenzymatically spontaneously polymerizes by a base-catalyzed click-like reaction. Upon interaction with fully or partially sequence-complementary RNA, the resulting abiotically generated RNAs perform at least two ribozyme activities: Intramolecular Cleavage following Ligation (ICL) and Intermolecular Splicing (IS). Consequently, the informational content of the RNA polymeric mixture resulting from the nonenzymatic polymerization of 3',5' cyclic GMP promptly increases upon reaction with complementary-sequence oligonucleotides. In prebiotic perspective, the ability of oligoG polynucleotides to ligate and recombine with other sequences provides a simple and powerful evolutionary scenario based on the autocatalytic properties of RNA.

CHEMBIOCHEM
FULL PAPERS

ChemBioChem **2014**, *15*, 879 – 883

ChemPubSoc Europe

DOI: 10.1002/cbic.201300773

Dry Polymerization of 3′,5′-Cyclic GMP to Long Strands of RNA

Matthias Morasch,[a] Christof B. Mast,[a] Johannes K. Langer,[a] Pierre Schilcher,[b] and Dieter Braun*[a]

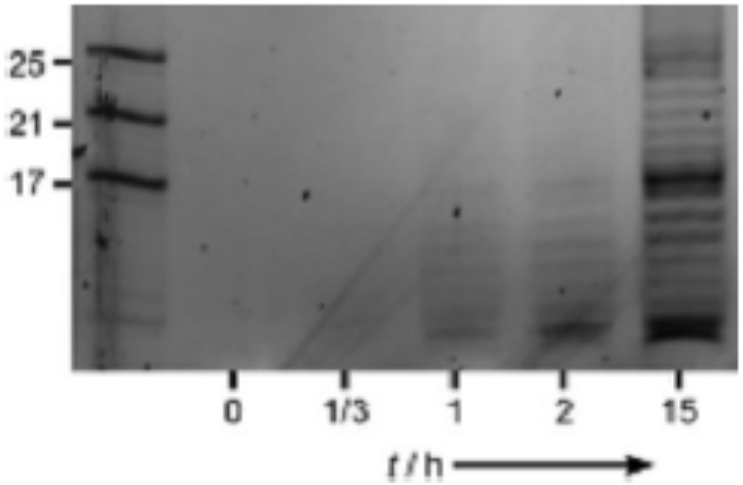

Up to 40 Gs: Long RNA strands (up to 40 nucleotides) have been formed by dry polymerization of pure 3′,5′-cyclic GMP. The mean polymer length increases with the time that the sample stays in its dry form. The reaction is considerably more efficient than cGMP polymerization in bulk water.

A

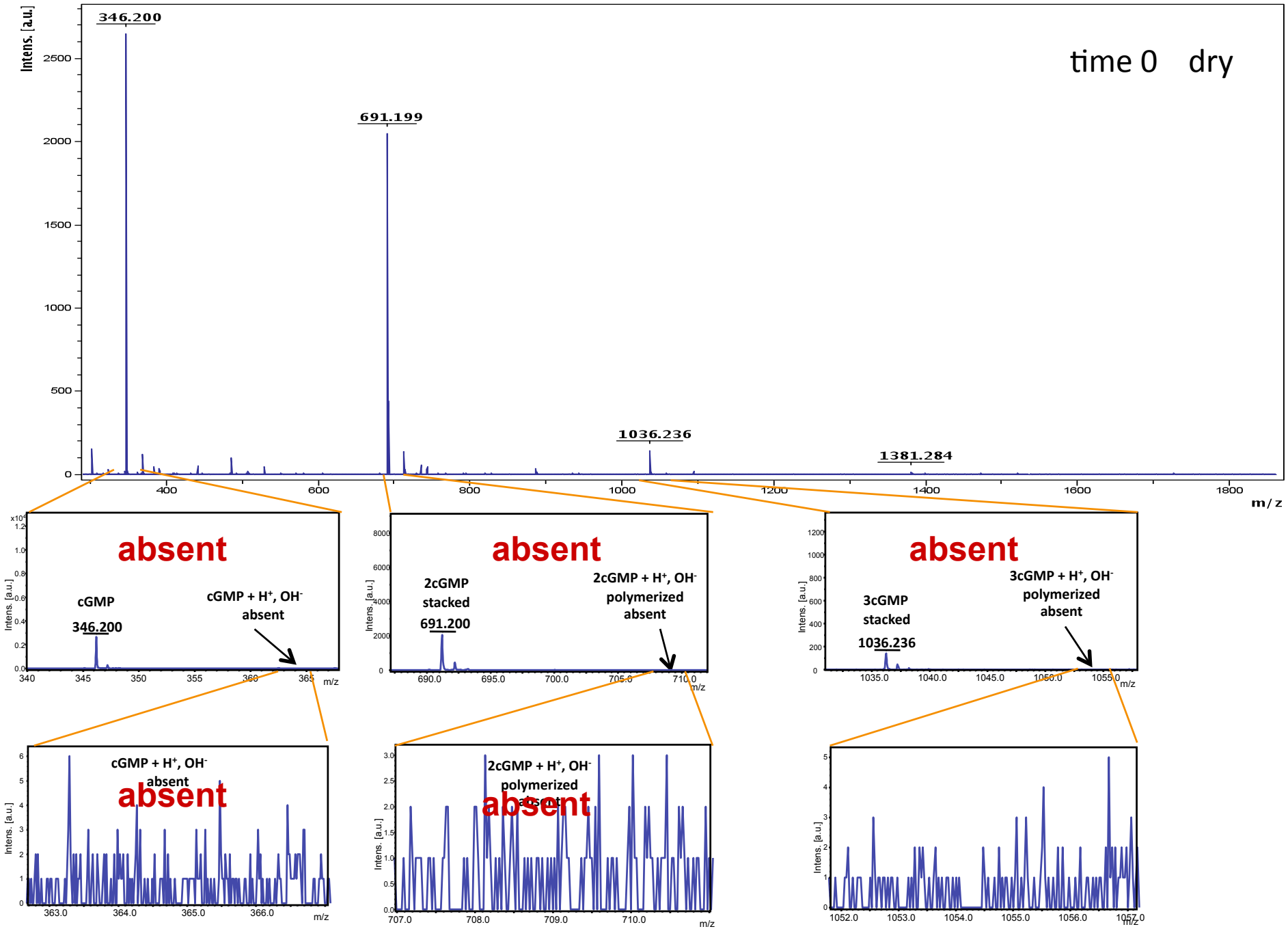
346.200
691.199
1036.236
1381.284
time 0 dry
Intens. [a.u.]
m/z
absent
cGMP
346.200
cGMP + H+, OH-
absent
2cGMP
stacked
691.200
2cGMP + H+, OH-
polymerized
absent
3cGMP
stacked
1036.236
3cGMP + H+, OH-
polymerized
absent
cGMP + H+, OH-
absent
absent
2cGMP + H+, OH-
polymerized
absent
absent

B

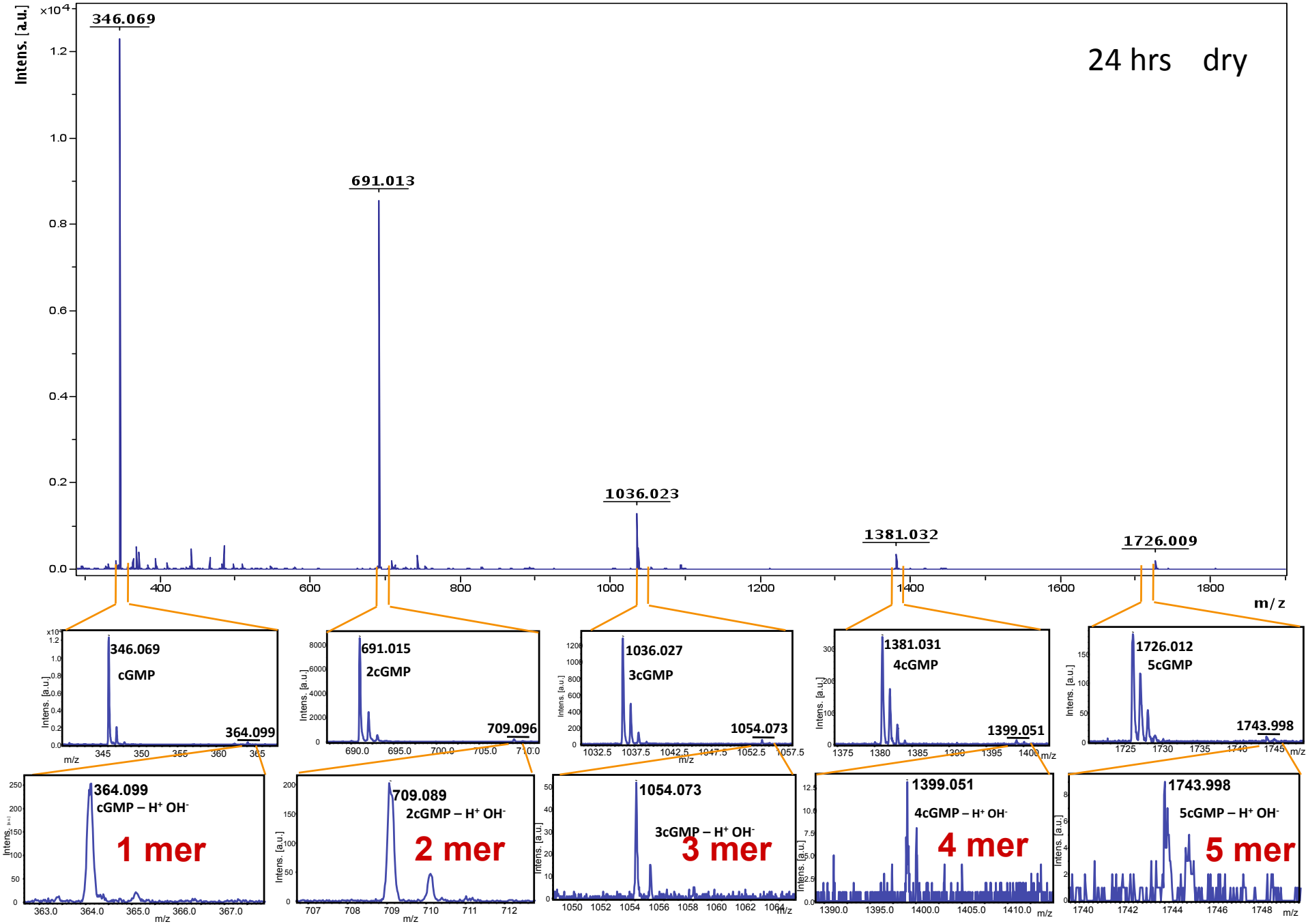
24 hrs dry
Intens. [a.u.]
m/z
346.069
691.013
1036.023
1381.032
1726.009
346.069
cGMP
364.099
691.015
2cGMP
709.096
1036.027
3cGMP
1054.073
1381.031
4cGMP
1399.051
1726.012
5cGMP
1743.998
364.099
cGMP – H+ OH-
1 mer
709.089
2cGMP – H+ OH-
2 mer
1054.073
3cGMP – H+ OH-
3 mer
1399.051
4cGMP – H+ OH-
4 mer
1743.998
5cGMP – H+ OH-
5 mer

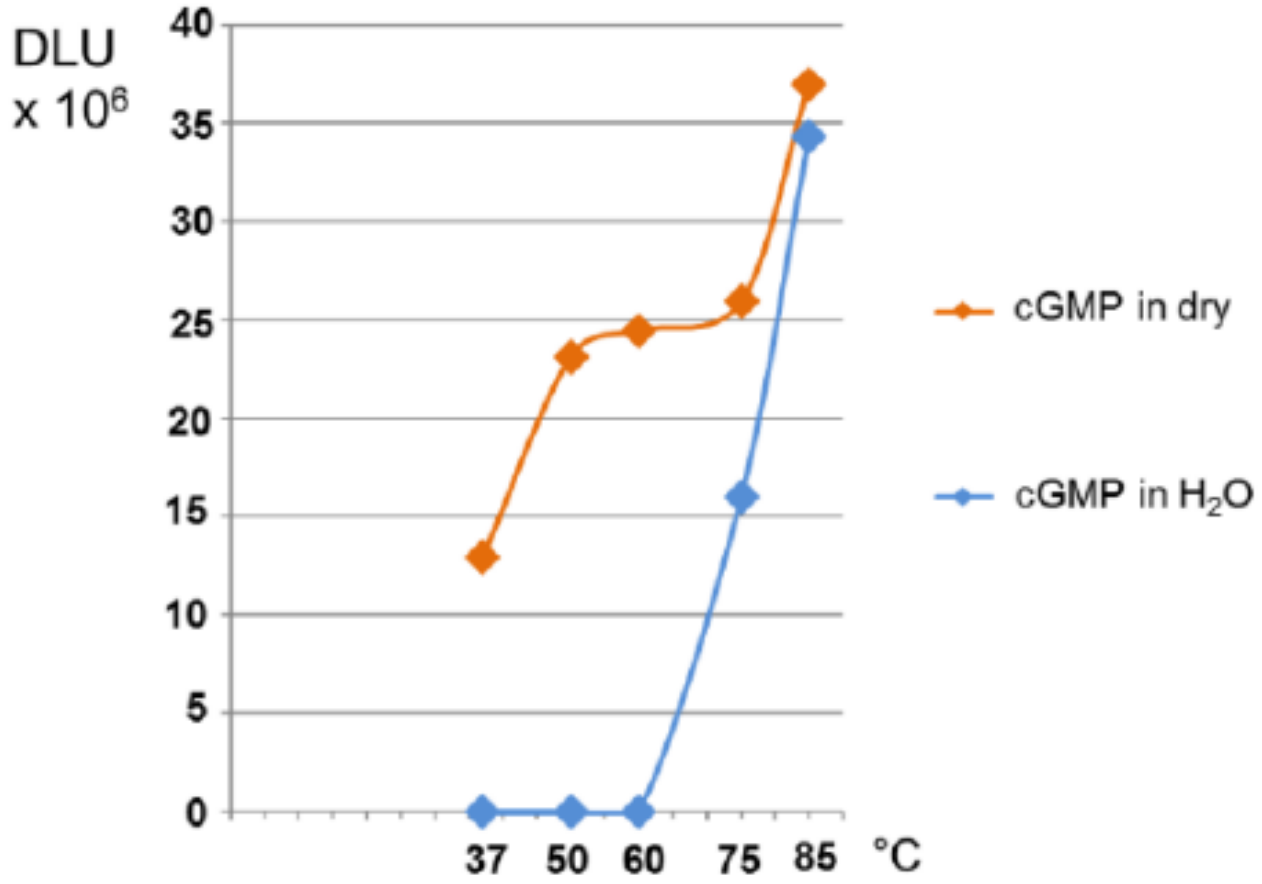

Figure 3. The temperature-dependent transition in polymerization efficiency depends on the medium. The plot shows the total amount of RNA obtained (DLU) in 5 hours reactions in dry (orange diamonds) and in water (7.5mM 3',5'cGMP) (blue diamonds).

Mechanism of the polymerization of 3',5'-cGMPs from quantum chemical calculations

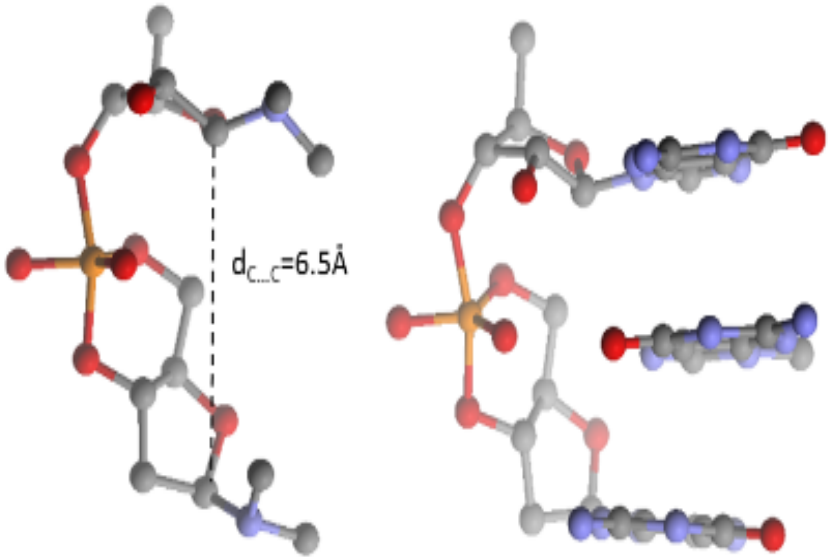

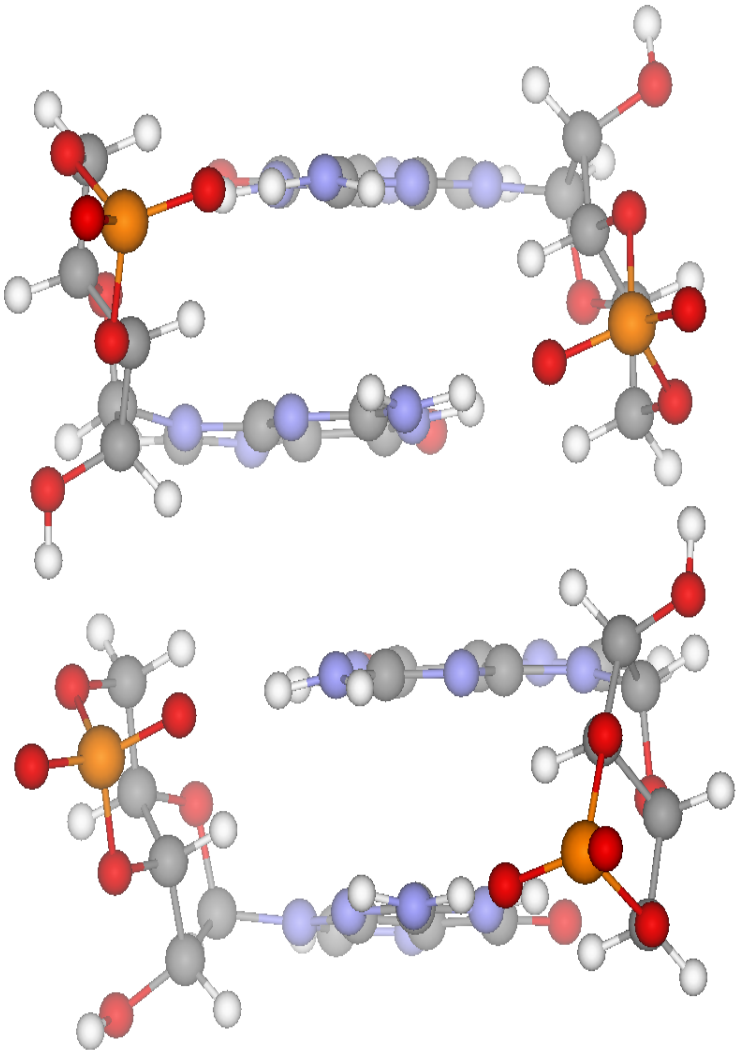

(TPSS-D2/TZVP level of theory)

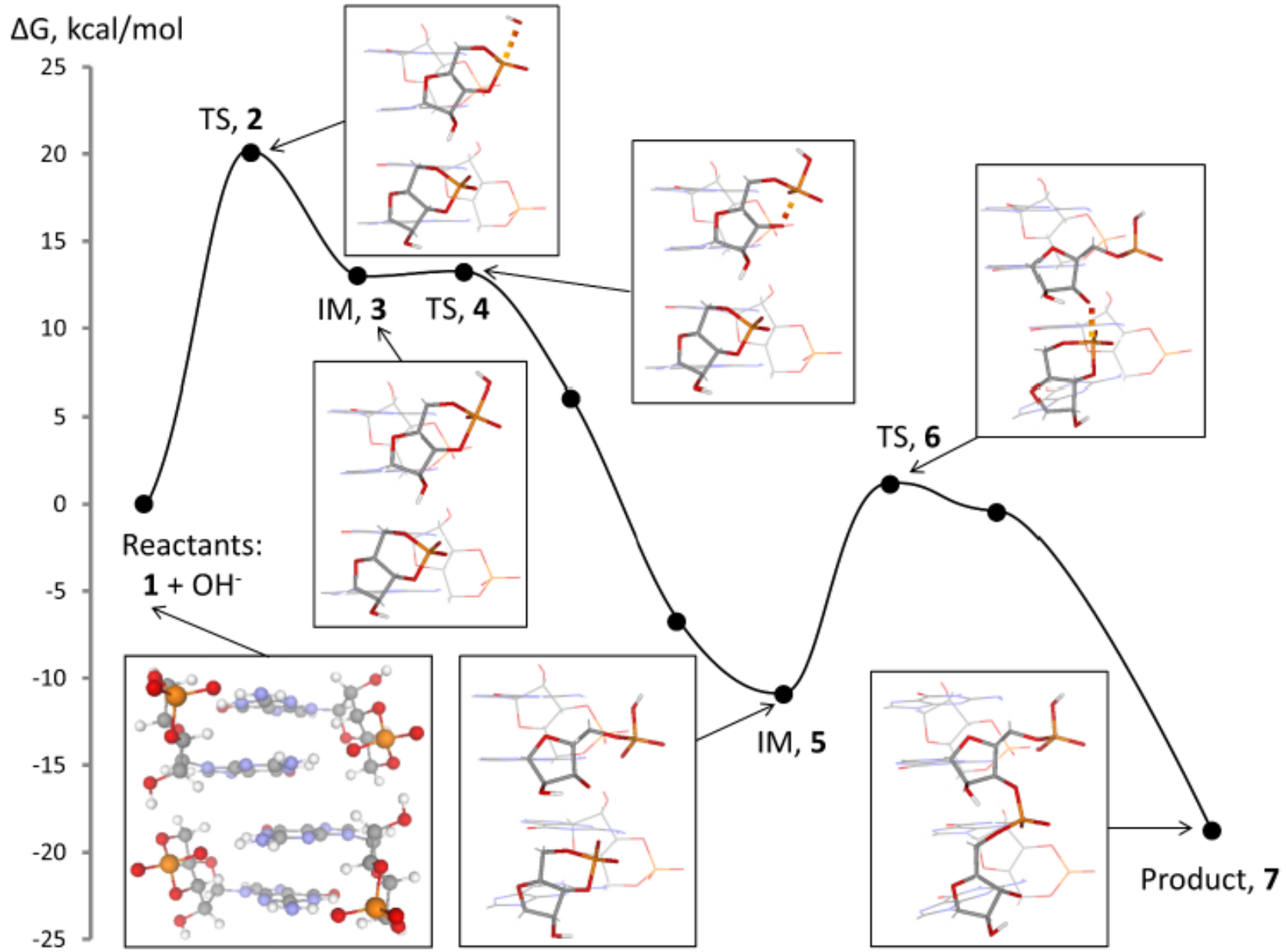

Figure 4. Computed free energy profile of the polymerization reaction from TPSS-D2 calculations with the TZVP basis set. IM: intermediate, TS: transition state. For

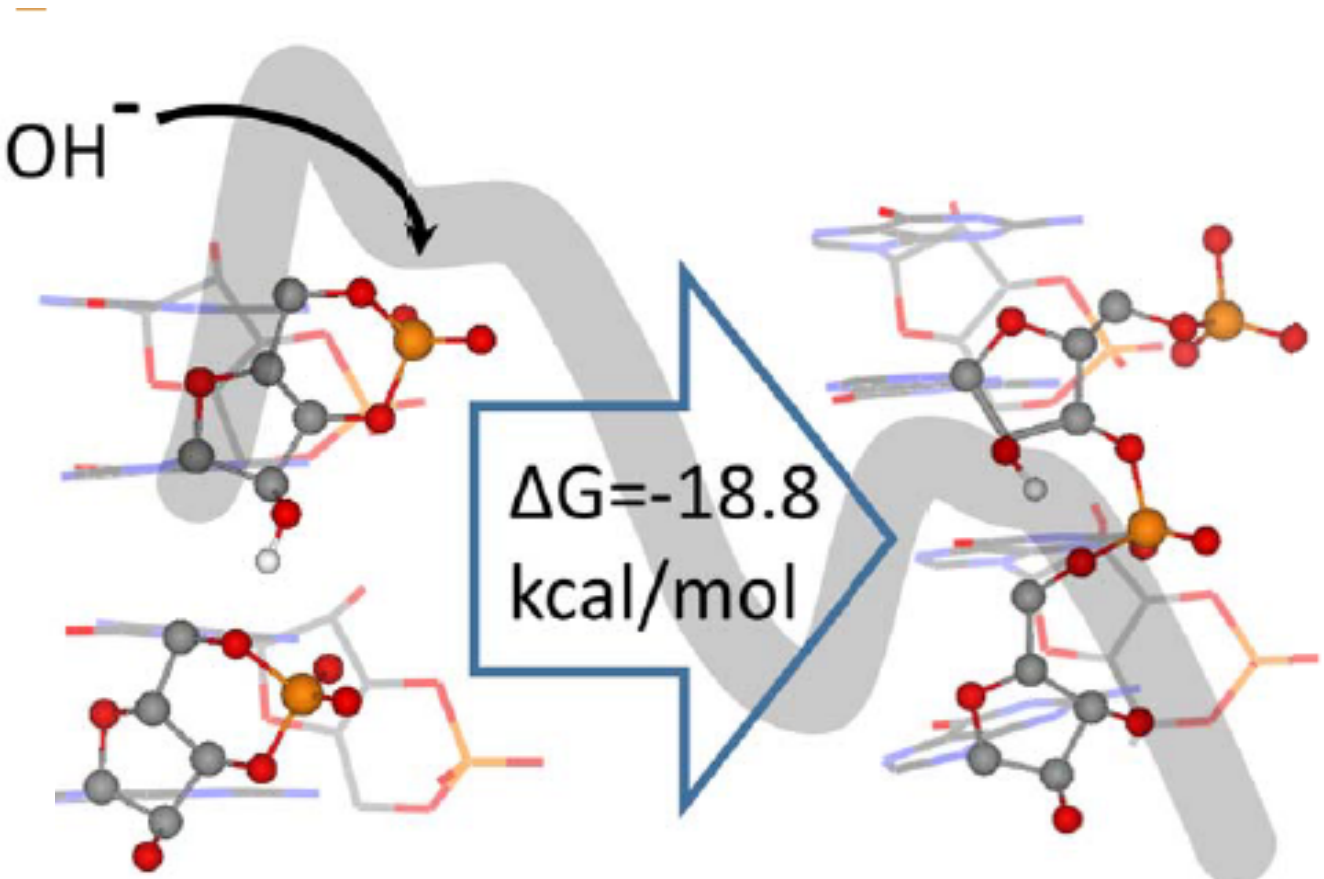

Jiří Šponer, Judit E. Šponer, Peter Stadlbauer, Brno

Polymerization of 3',5' cyclic GMP

(AutoFlex II Bruker) MALDI Dr Alessandra Giorgi, Rome
MALDI of 3',5'cGMP
UNREACTED Rome→ Dubna → Rome

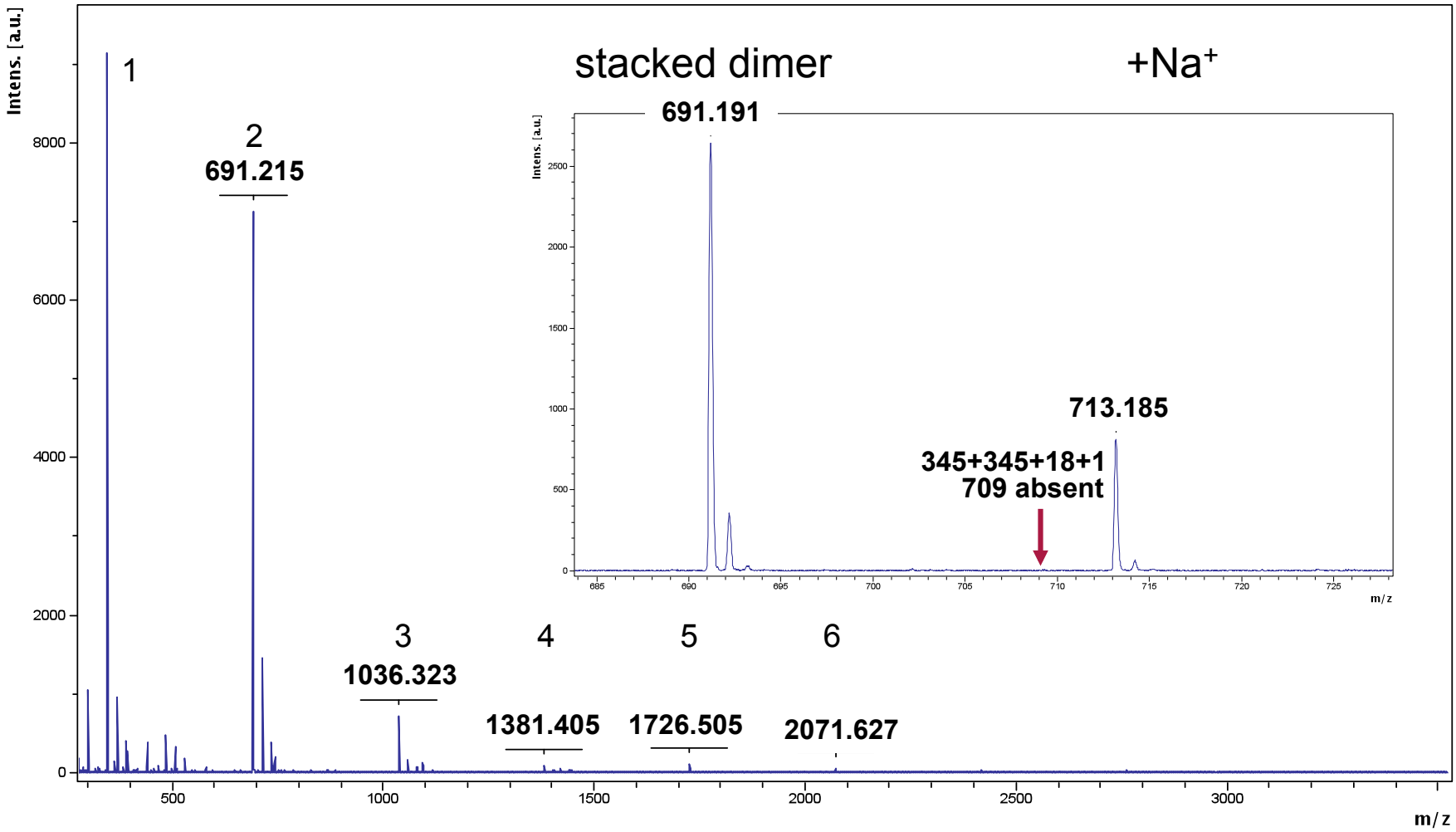

Polymerization of 3',5' cyclic GMP

(AutoFlex II Bruker) MALDI Dr Alessandra Giorgi, Rome
MALDI of 3',5'cGMP
Proton irradiation at Phasotron, Dubna

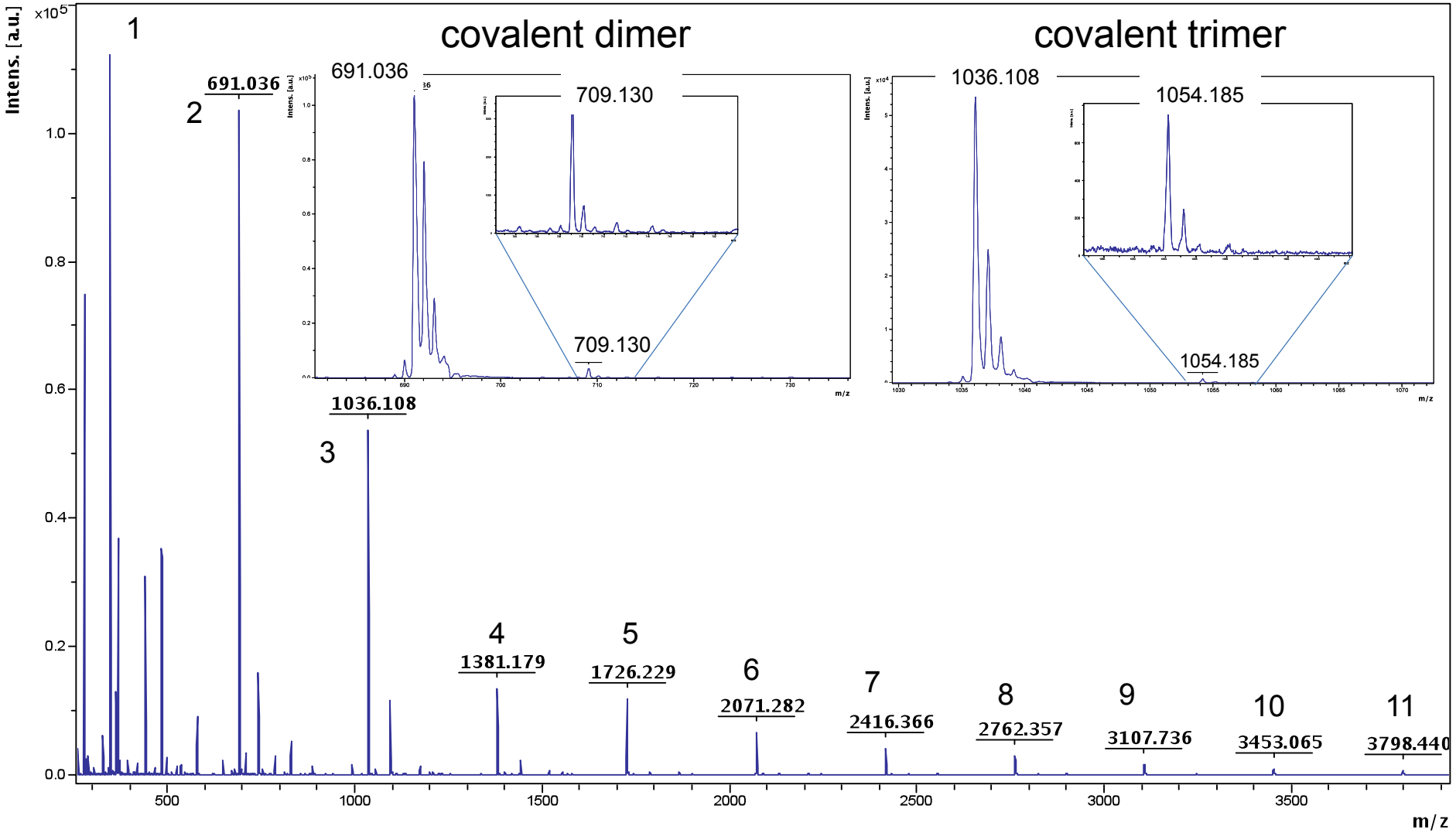

Polymerization of 3’,5’ cyclic GMP

(AutoFlex II Bruker) MALDI Dr Alessandra Giorgi, Rome
MALDI of 3’,5’cGMP
Proton irradiation at Phasotron, Dubna

covalent tetramer

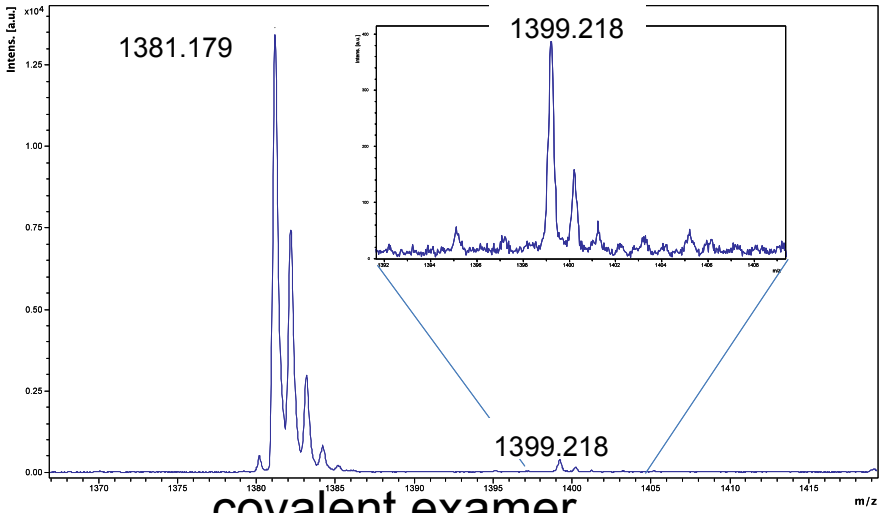

covalent pentamer

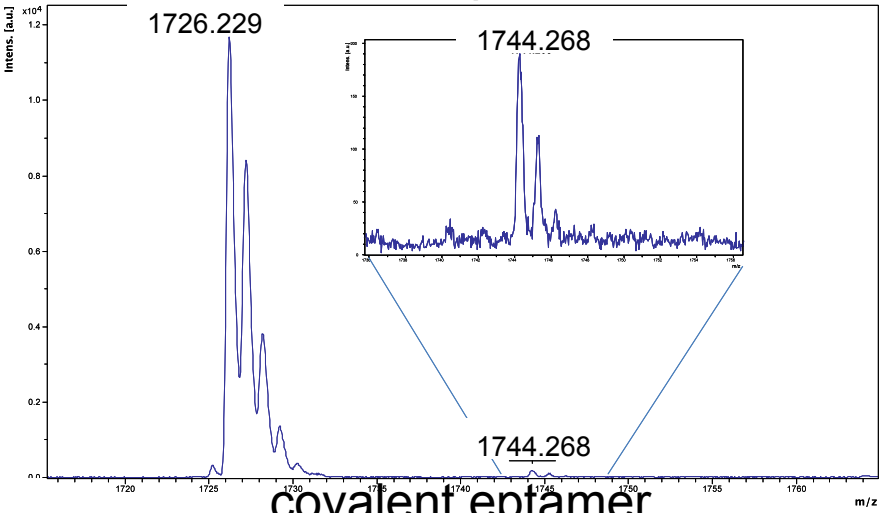

covalent examer

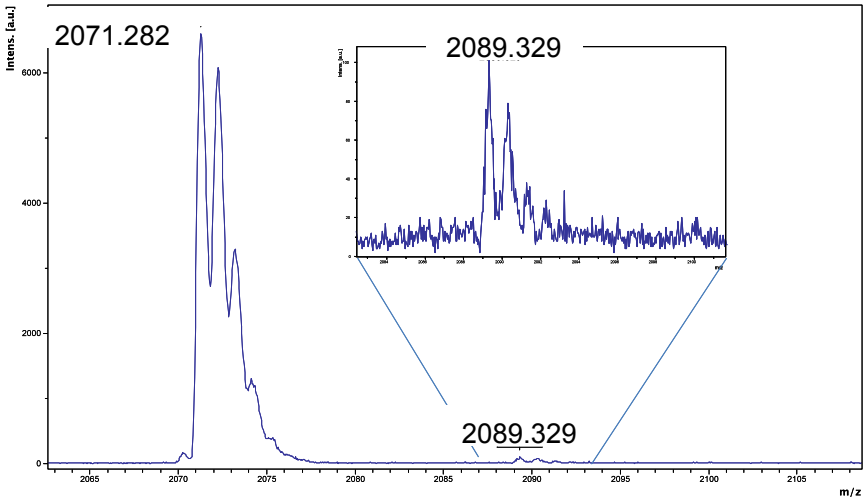

covalent eptamer

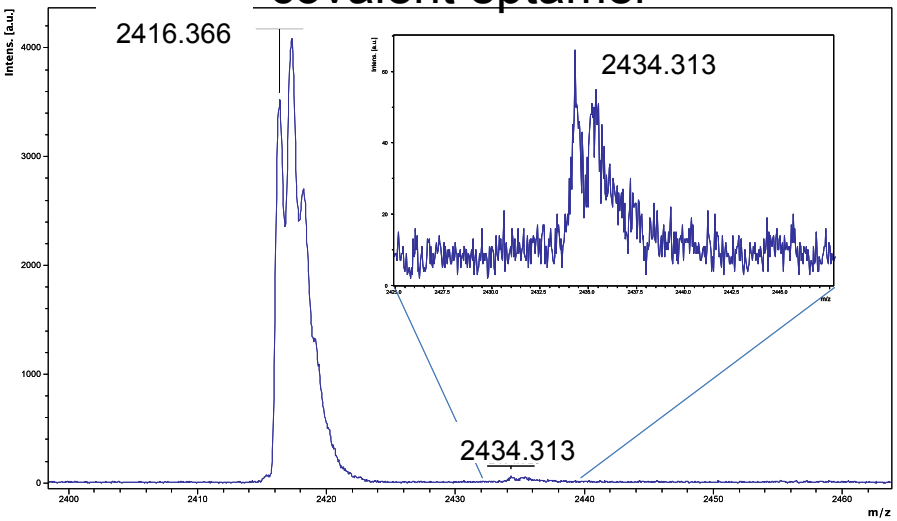

Polymerization of 3’,5’ cyclic GMP

(AutoFlex II Bruker) MALDI Dr Alessandra Giorgi, Rome
MALDI of 3’,5’cGMP
Proton irradiation at Phasotron, Dubna

covalent octamer

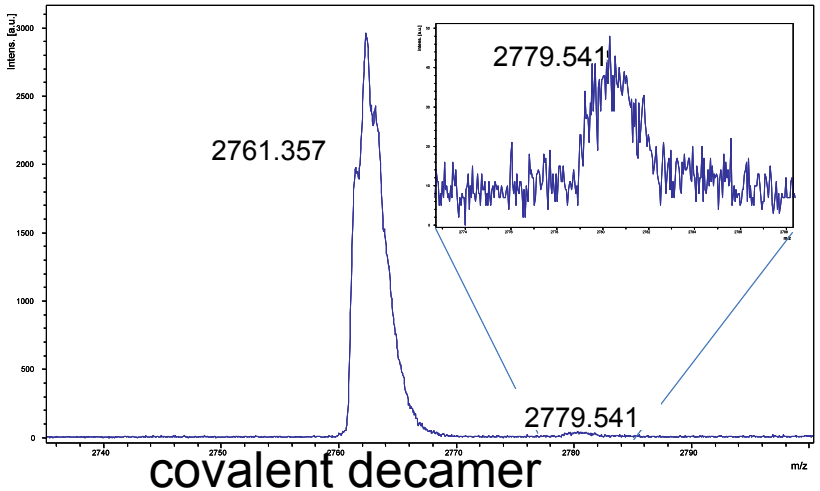

covalent nonamer

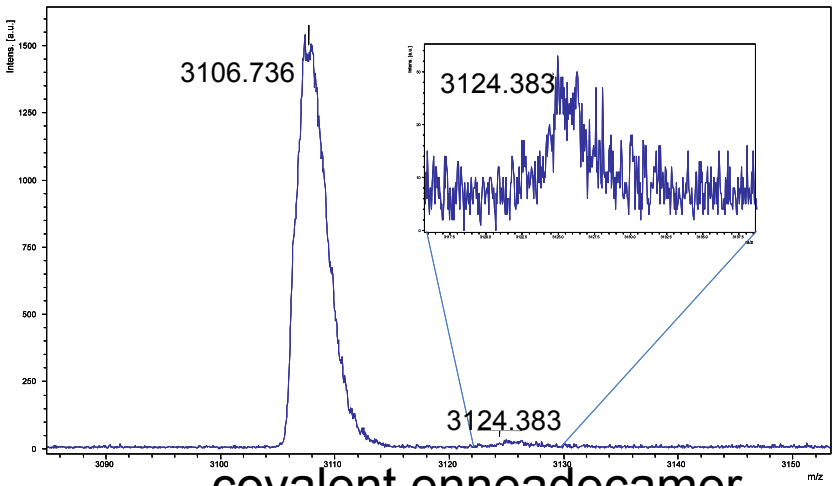

covalent decamer

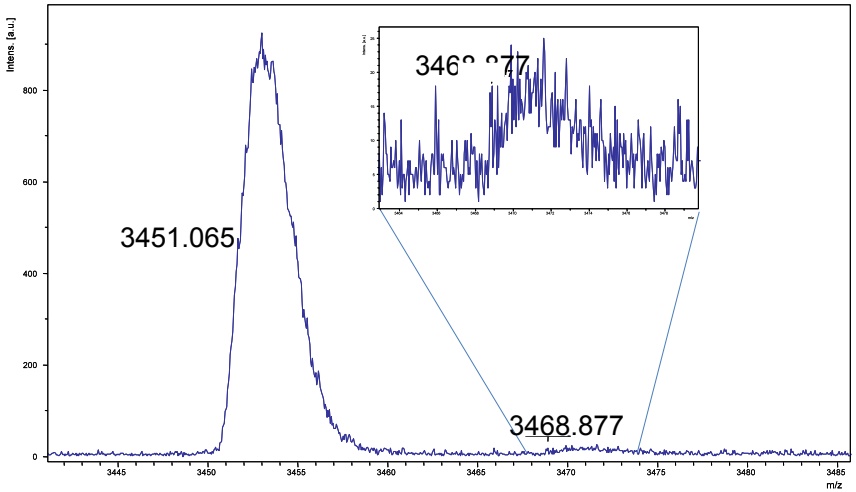

covalent enneadecamer

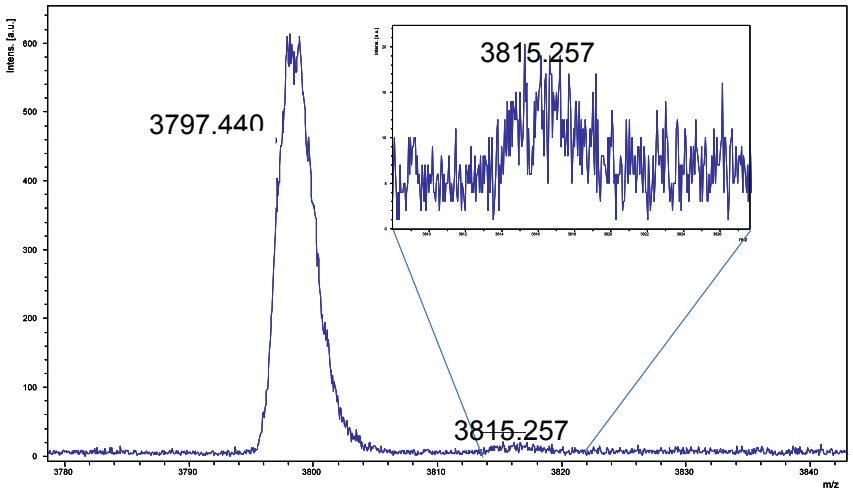

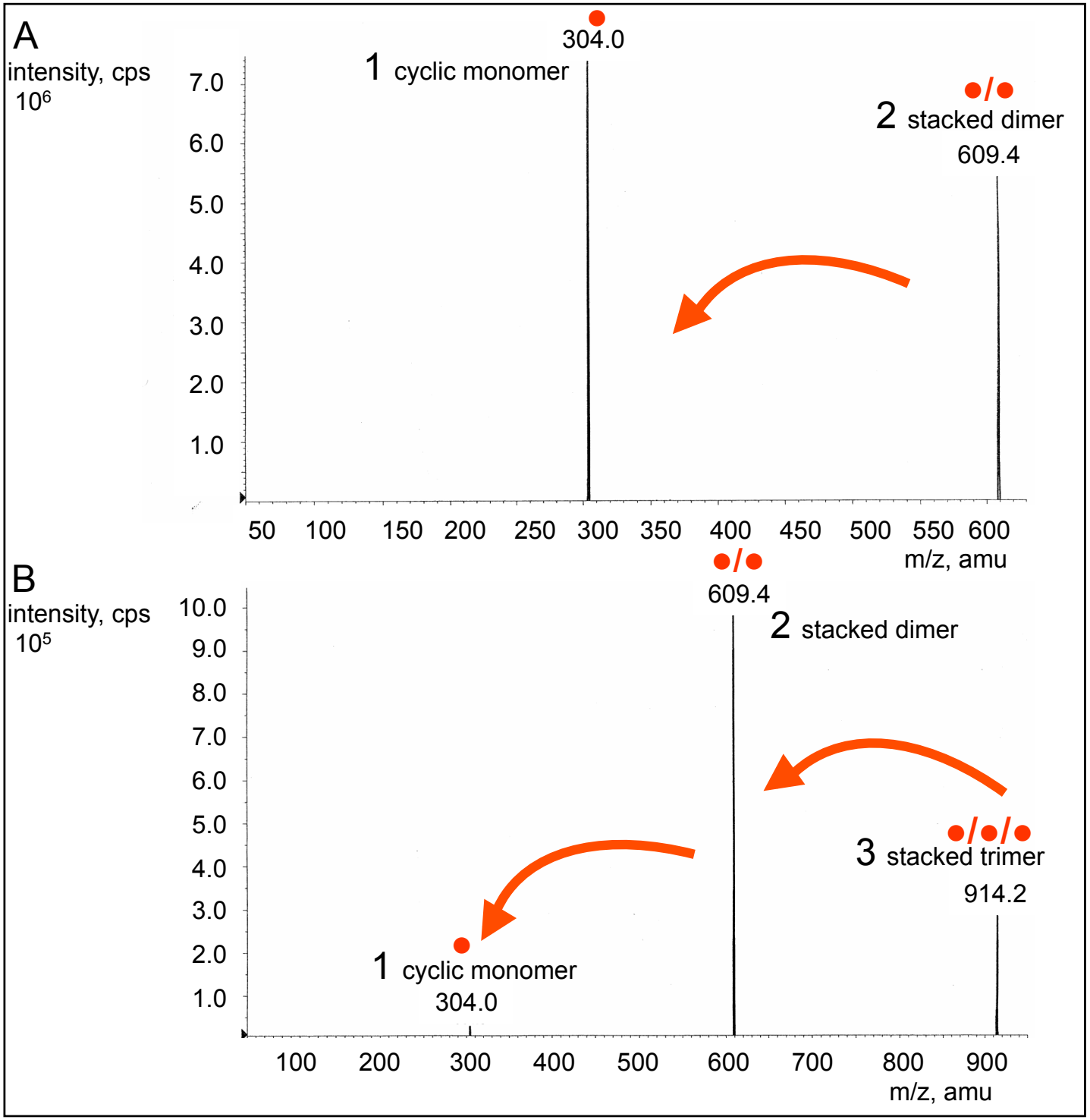

fragmentation (stacked)

Product Ion Scan Spectra
CE - 20

fragmentation
(covalents)

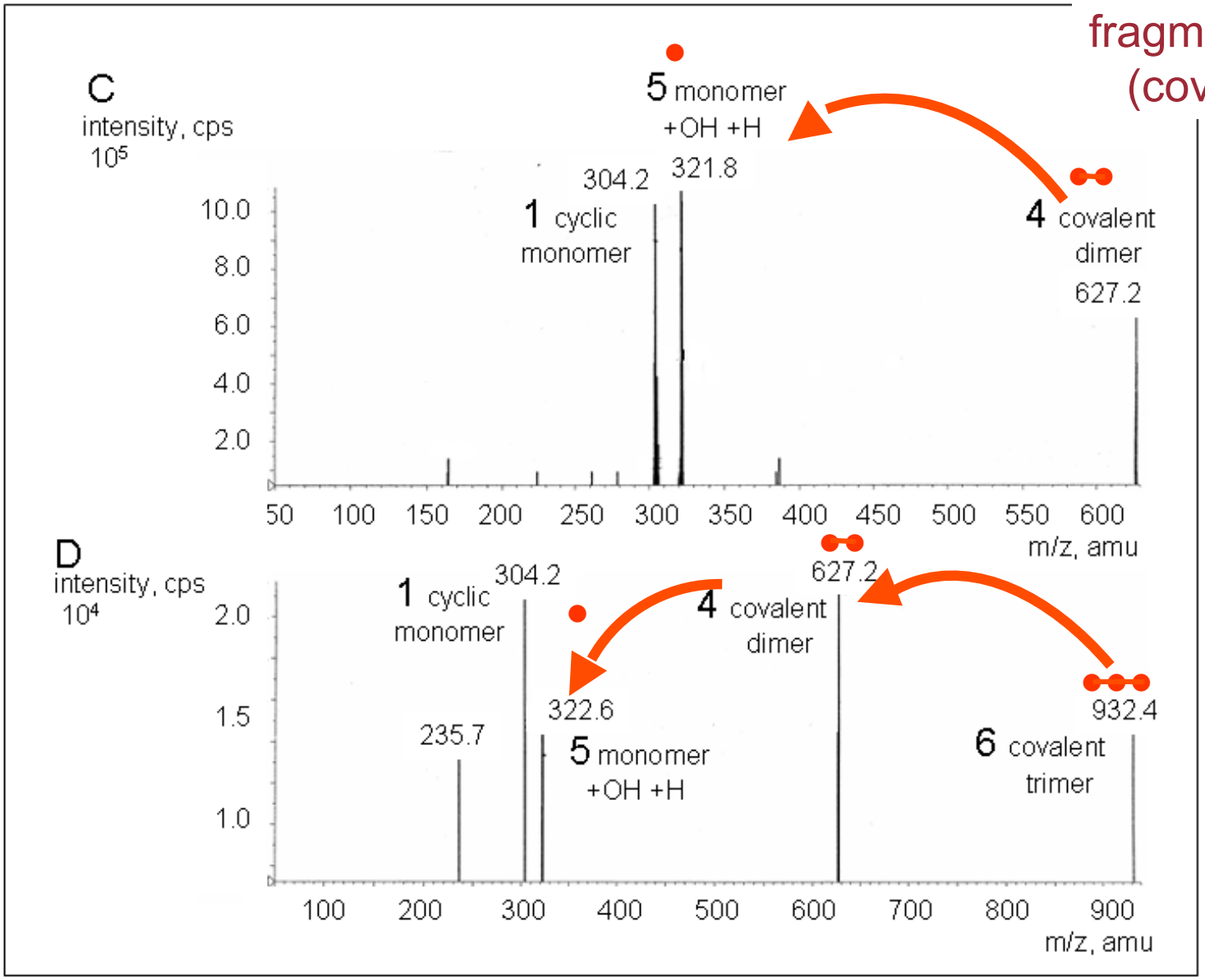

Polymerization of 3’,5’ cyclic GMP

(AutoFlex II Bruker) MALDI Dr Alessandra Giorgi, Rome
MALDI of 3’,5’cGMP
γ irradiation at Nuclotron, Dubna

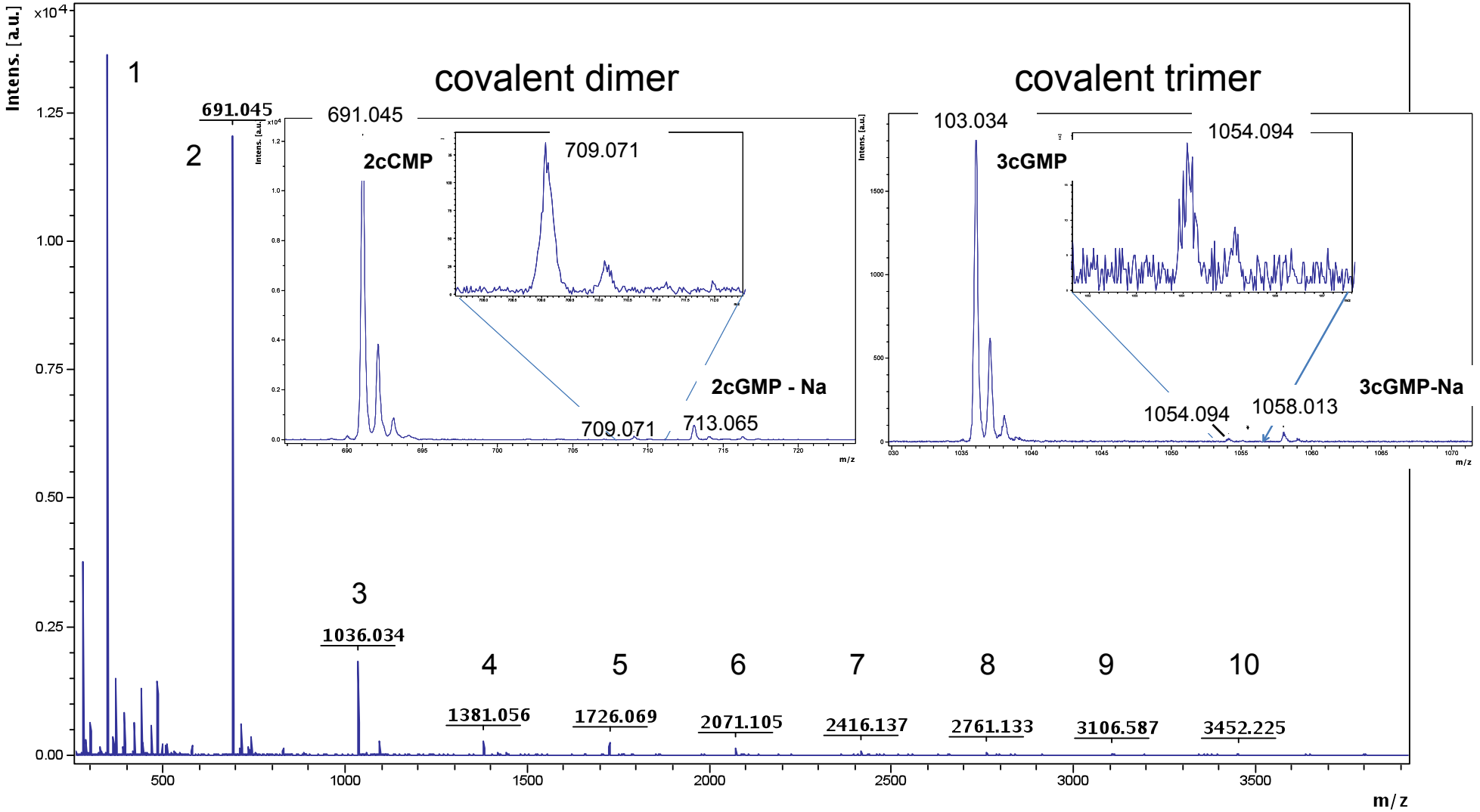

Sodium-effect

Anionic mechanism:

blocked by highly mobile cations H^+ and Na^+

but not by HNR_3^+

↓

formamide-based scenario

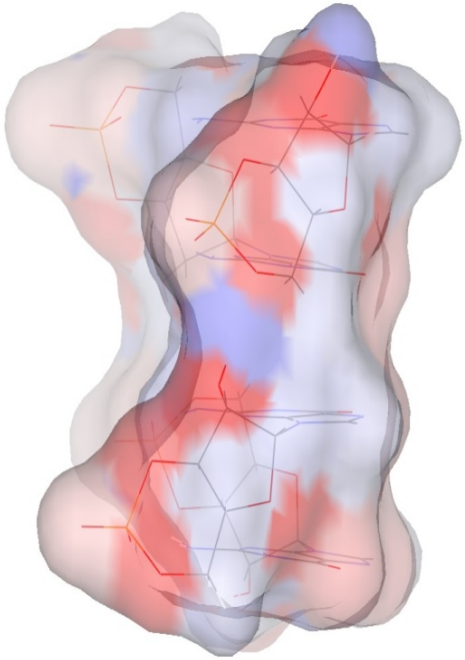

Low sodium-concentration, non-specific binding residency time : 1-30 ps (quantum molecular dynamicsby Kolev et al. ACS Chem. Biol. 2013, 8, 1578.)

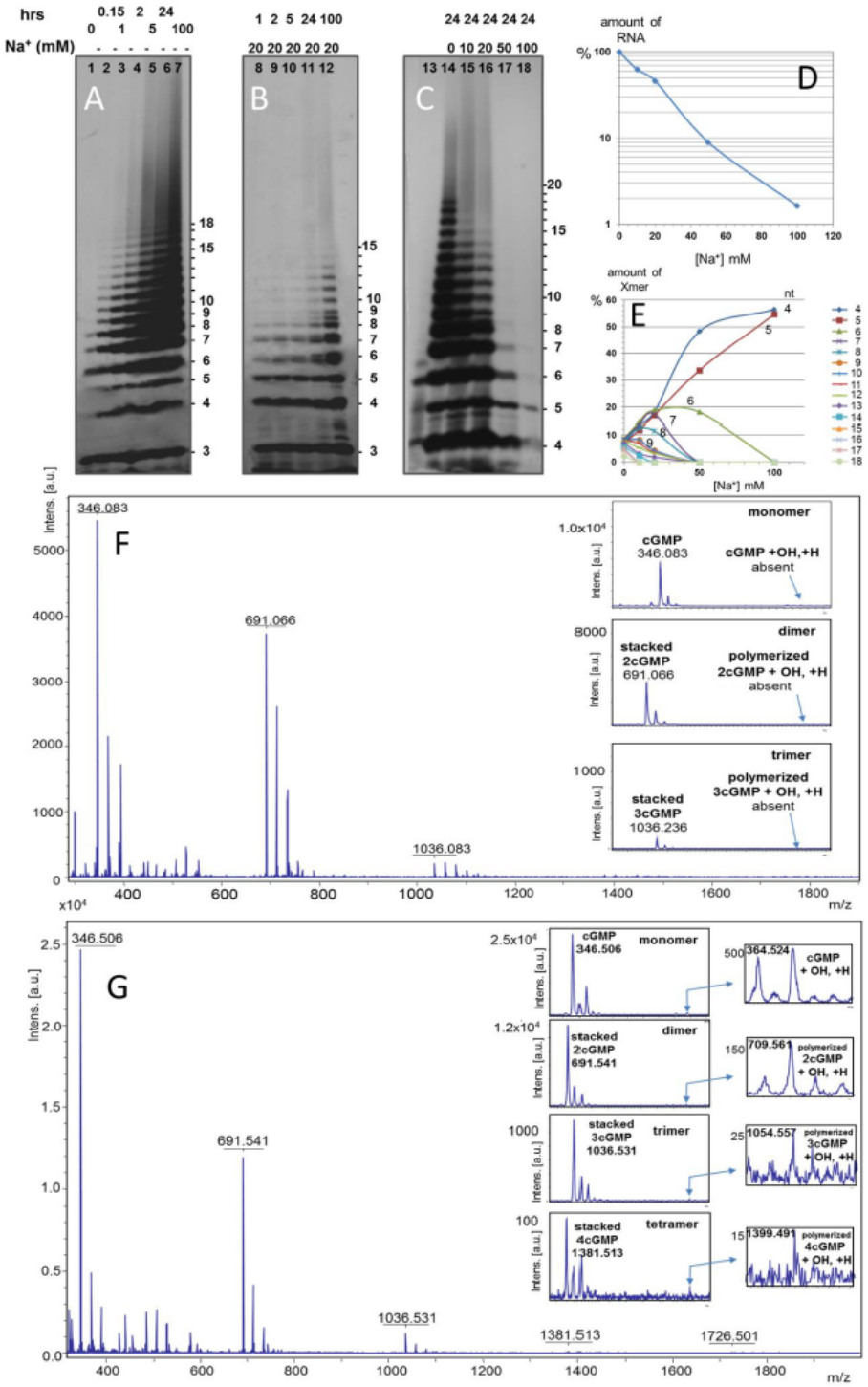

Polymerization of 3′,5′cGMP is inhibited by Na^+.

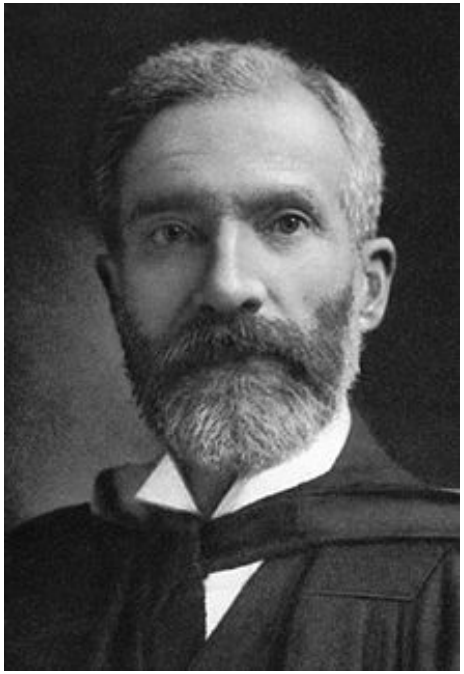

A. B. Macallum

The cell… has endowments transmitted from
a past almost remote as the origin of life on earth

The paleochemistry of the body fluids and tissues. Physiol Rev, 1926

Armen Mulkidjanian

Michael Y. Galperin

The chemical traits of organisms are more conservative than the changing environment and hence retain information about ancient environment conditions

The chemistry conservation principle, 2007

Origin of first cells at terrestrial, anoxic geothermal fields

Pnas, 2012

Armen Y. Mulkidjanian[a,b,1], Andrew Yu. Bychkov[c], Daria V. Dibrova[a,d], Michael Y. Galperin[e], and Eugene V. Koonin[e,1]

Table 1. Approximate concentrations of key ions in various environments

Ion, mol/L	Modern sea water	Anoxic water of primordial ocean	Cell cytoplasm
Na^+	0.4	>0.4	0.01
K^+	0.01	~0.01	0.1
Ca^{2+}	0.01	~0.01	0.001
Mg^{2+}	0.05	~0.01	0.01
Fe	10^{-8} (mostly Fe^{3+})	10^{-5}	10^{-3} to 10^{-4}
Mn^{2+}	10^{-8}	10^{-6} to 10^{-8}	10^{-6}
Zn^{2+}	10^{-9}	$<10^{-12}$	10^{-3} to 10^{-4}
Cu	10^{-9} (Cu^{2+})	$<10^{-20}$ (Cu^{1+})	10^{-5}
Cl^-	0.5	>0.1	0.1
PO_4^{3-}	10^{-6} to 10^{-9}	$<10^{-5}$	~10^{-2} (mostly bound

The intracellular concentration is defined here as the total content of a particular element divided by the ce volume and should be discriminated from the much lower free ion concentration, which does not account for th ions that are bound to biological molecules. The reconstructed chemical composition of the anoxic ocea includes data from refs. 14, 15, 58, 141. The data on intracellular concentrations of different chemical element are based on refs. 14, 142–145.

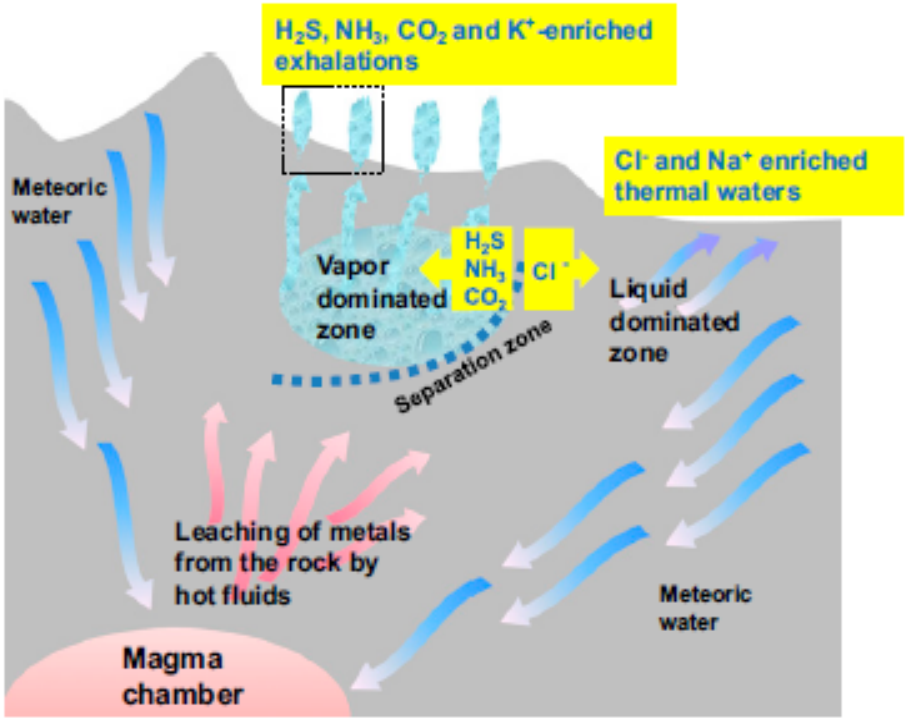

Fig. 1. A terrestrial geothermal system (scheme based on refs. 52, 53, 62 138) that is fed mostly by water from rain and snow (meteoric water) which when it is deep underground, mixes with cation- and anion-enriched mag matic fluids and becomes heated to 300 to 500 °C; such hot fluids can lead diverse ions from the hot rock.

MOLECULAR STRUCTURE OF NUCLEIC ACIDS

A Structure for Deoxyribose Nucleic Acid

It has not escaped our notice that the specific pairing we have postulated immediately suggests a possible copying mechanism for the genetic material.

J. D. WATSON
F. H. C. CRICK

CONTENTS

THE DEAD PAST 7
THE FOUNDATION OF S.F. SUCCESS 55
FRANCHISE 57
GIMMICKS THREE 75
KID STUFF 83
THE WATERY PLACE 97

THE MESSAGE

HELL-FIRE 137
THE LAST TRUMP 139
THE FUN THEY HAD 157
JOKESTER 161
THE IMMORTAL BARD 175
SOMEDAY 179
THE AUTHOR'S ORDEAL 189
DREAMING IS A PRIVATE THING 193

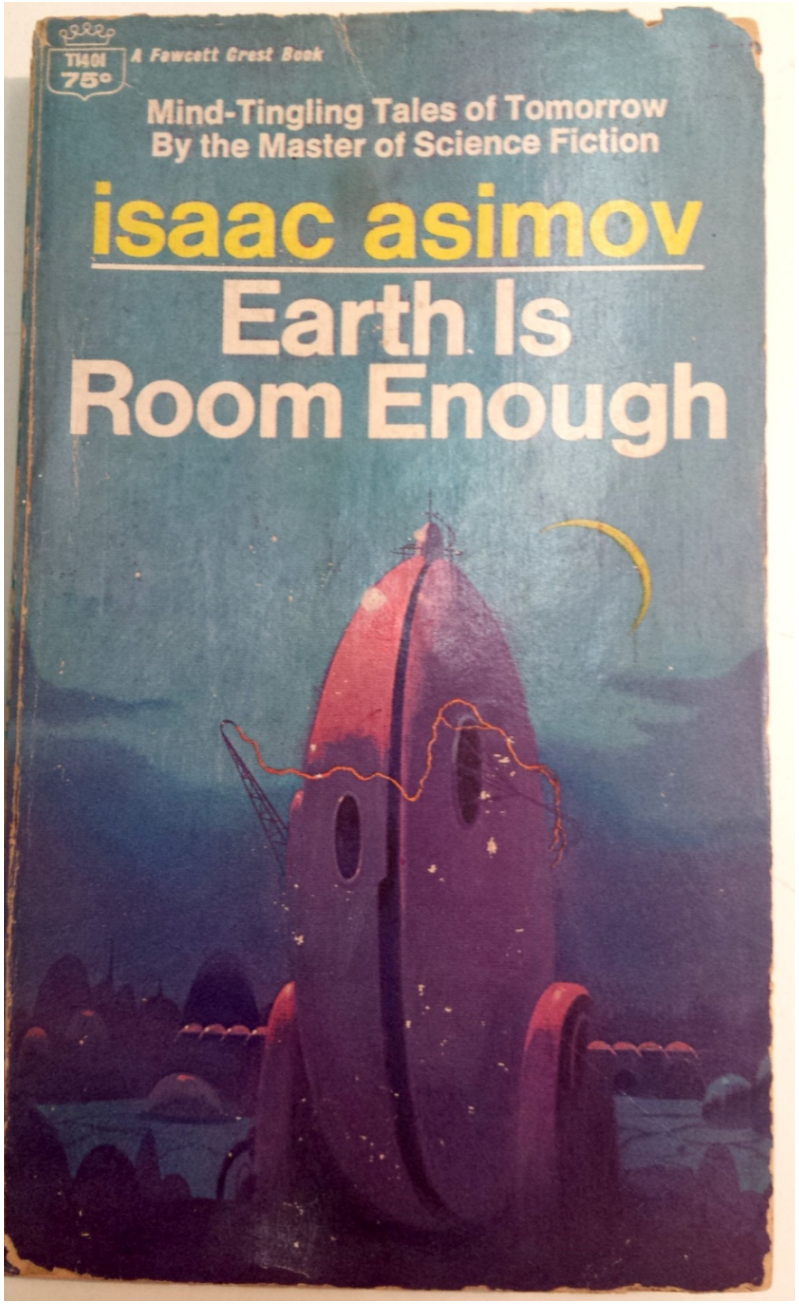

Polymerization of 3',5' cyclic CMP

(AutoFlex II Bruker) MALDI Dr Alessandra Giorgi, Rome

MALDI of 3',5'cCMP

UNREACTED Rome → Dubna → Rome

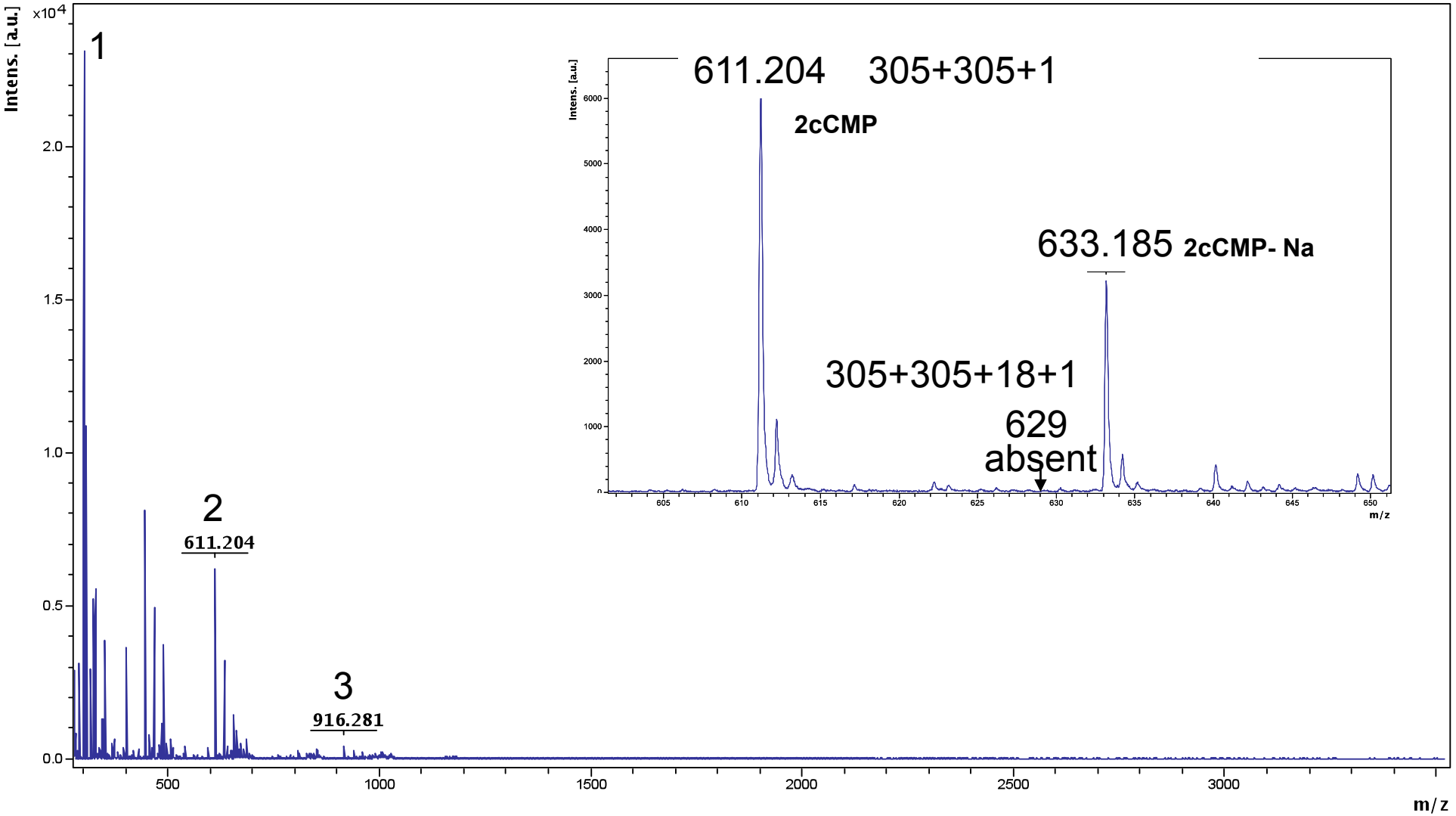

Polymerization of 3',5' cyclic CMP

(AutoFlex II Bruker) MALDI Dr Alessandra Giorgi, Rome
MALDI of 3',5'cCMP
Proton irradiation at Phasotron, Dubna

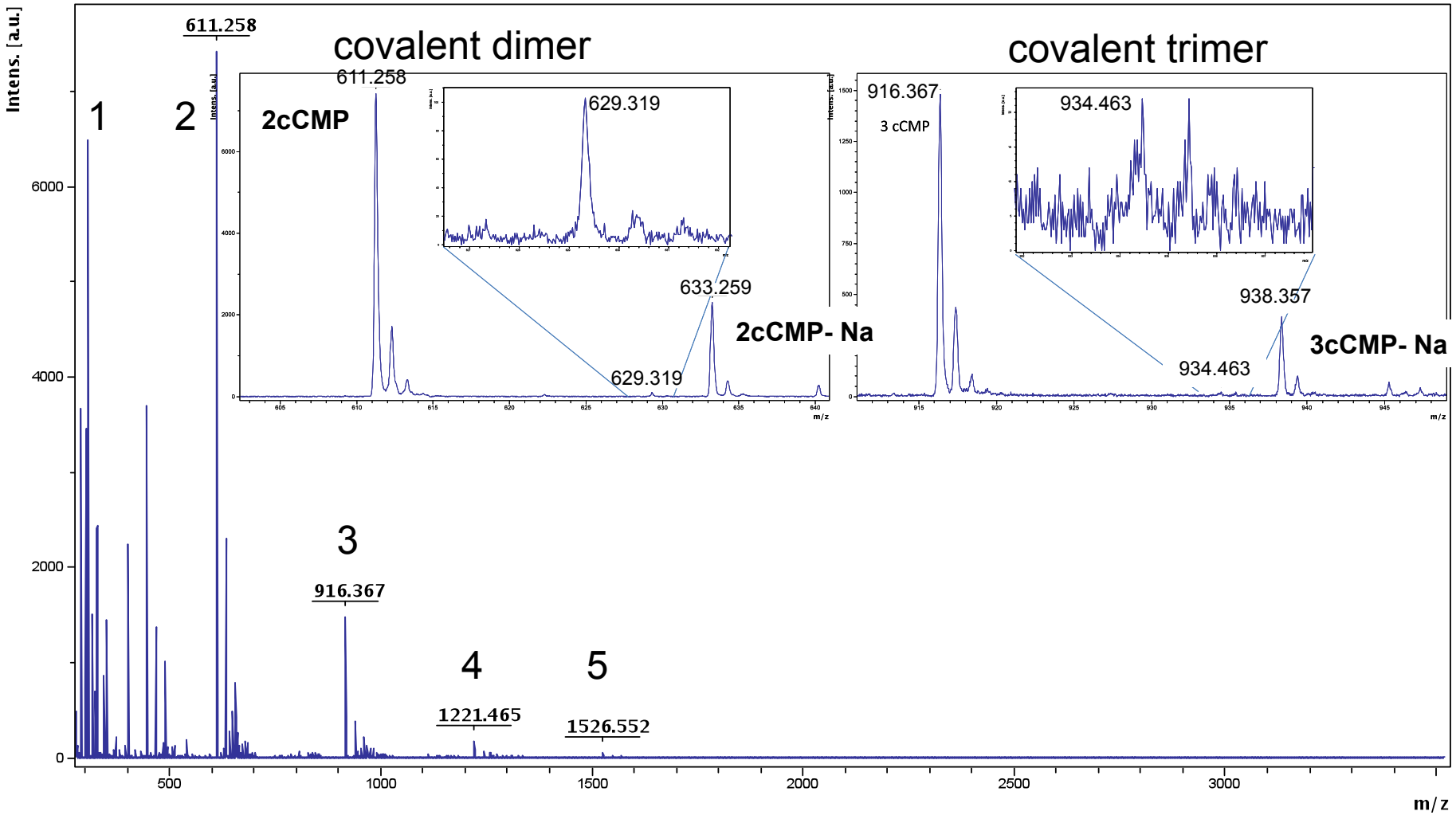

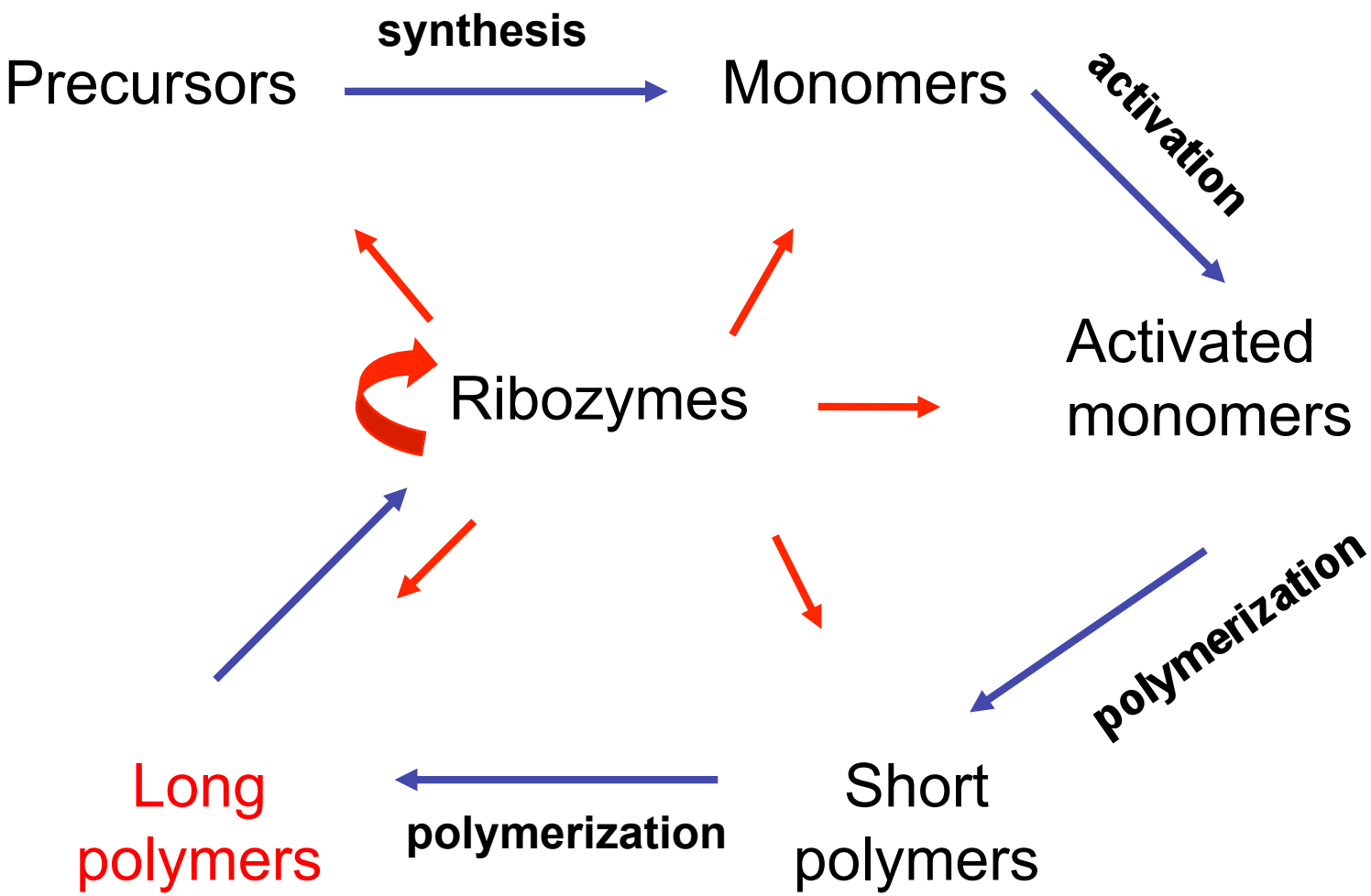
Precursors
synthesis
Monomers
activation
Activated monomers
Ribozymes
polymerization
Short polymers
polymerization
Long polymers

Driving force of the polymerization

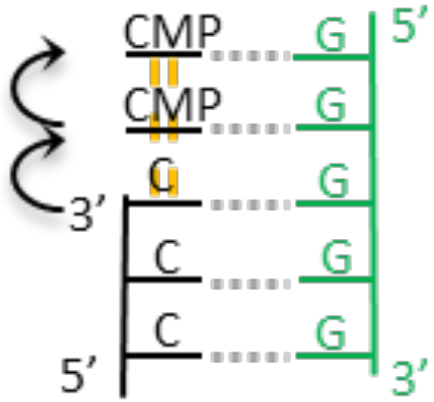

templated

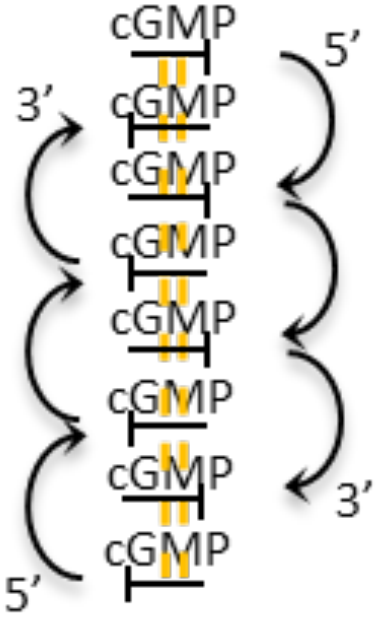

non-templated

synthesis of oligo Gs from 3',5'-cGMP on $5'A_{12}C_{12}3'$

60°C; TrisHCl pH 5,3
6hrs

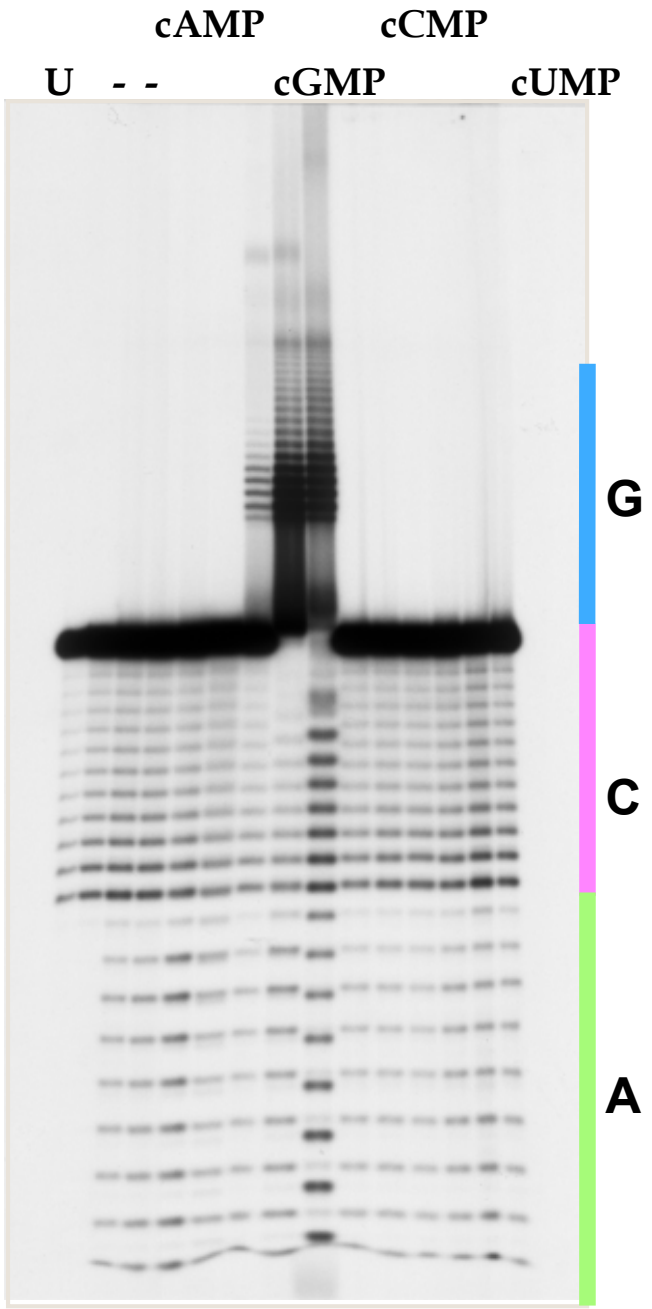

Biochemistry, 2011
J Biol Chem,2009
Biochemistry,2008

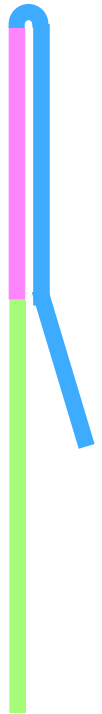

polymerization on the polyC 3’-end by removal of the 3’-H proton through a base (B^-).

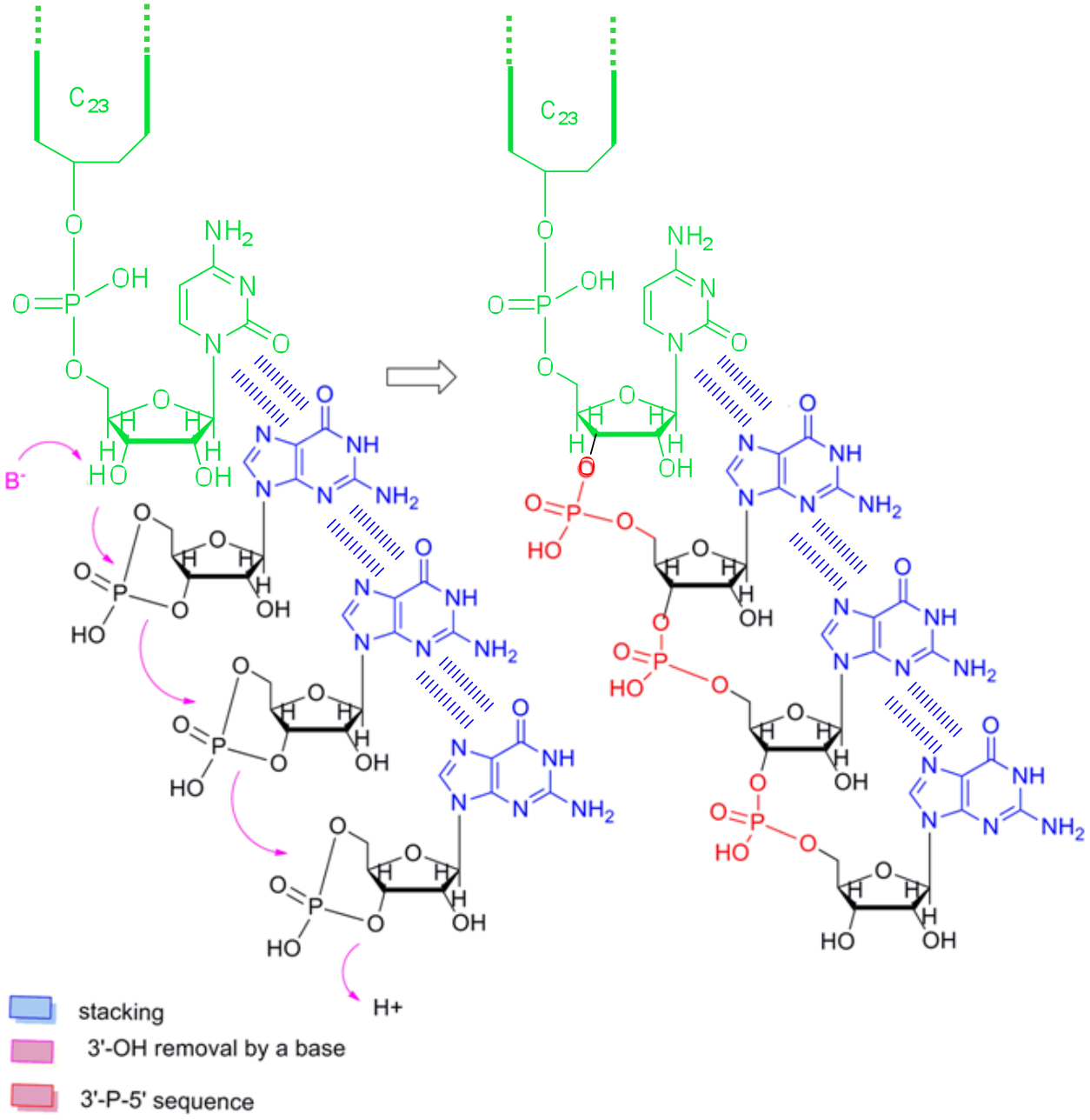

polymerization of 3',5'-cGMP on the 3' end of C_{24} MALDI ToF MS

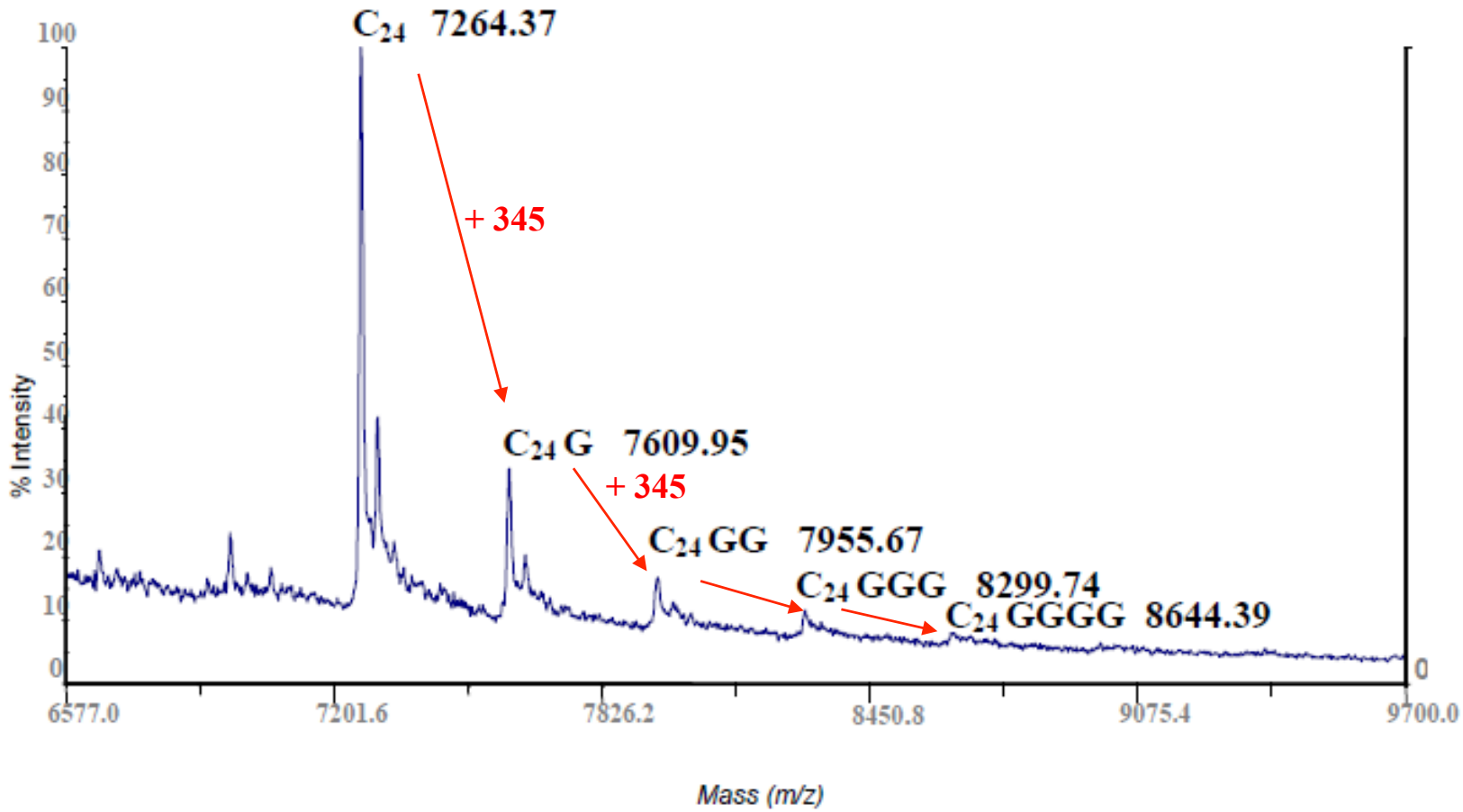

in non-enzymatic RNA
self-polymerization
base complementarity
wins over stacking,
but stacking came first

sequence complementarity-driven terminal ligation

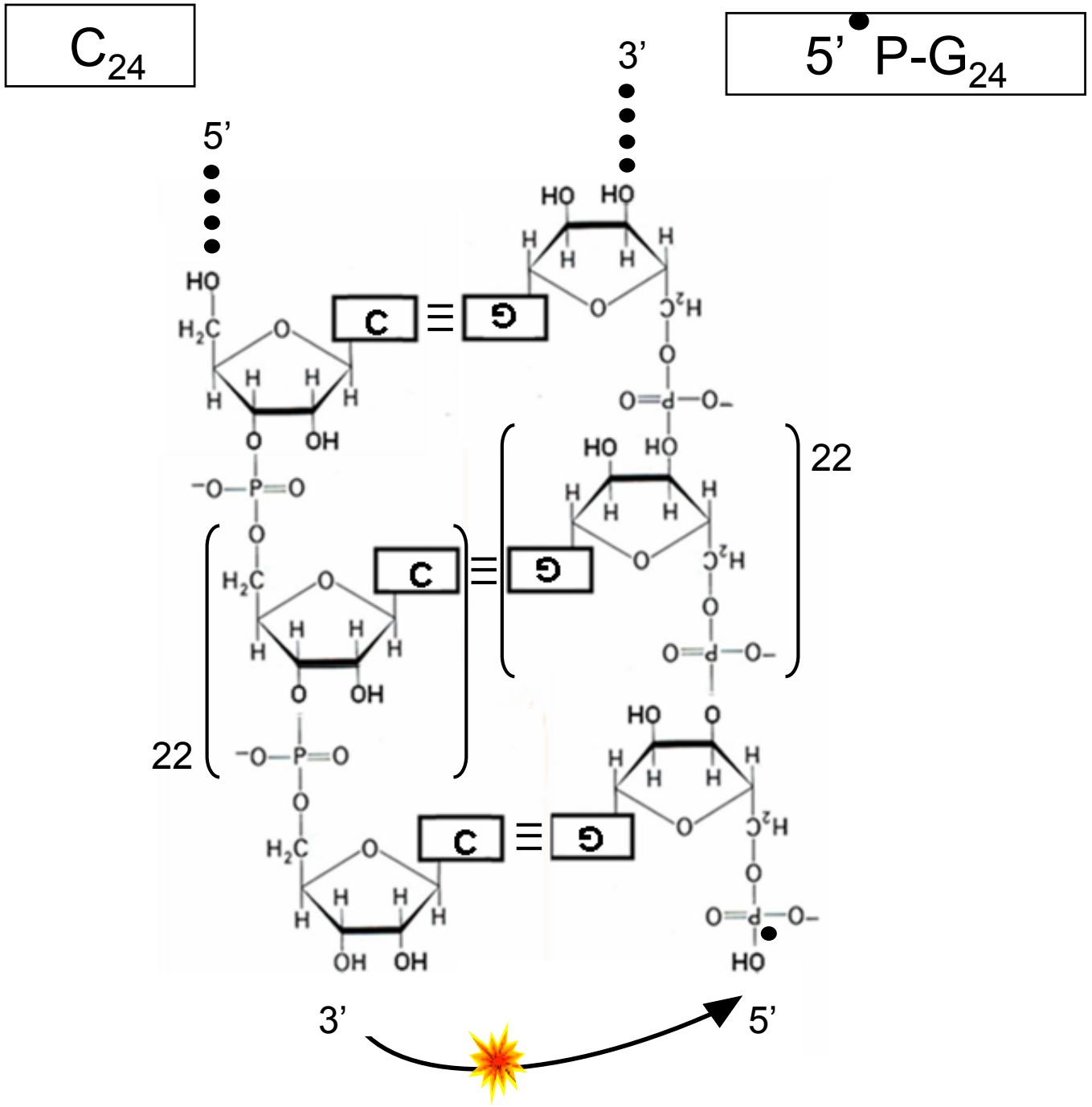

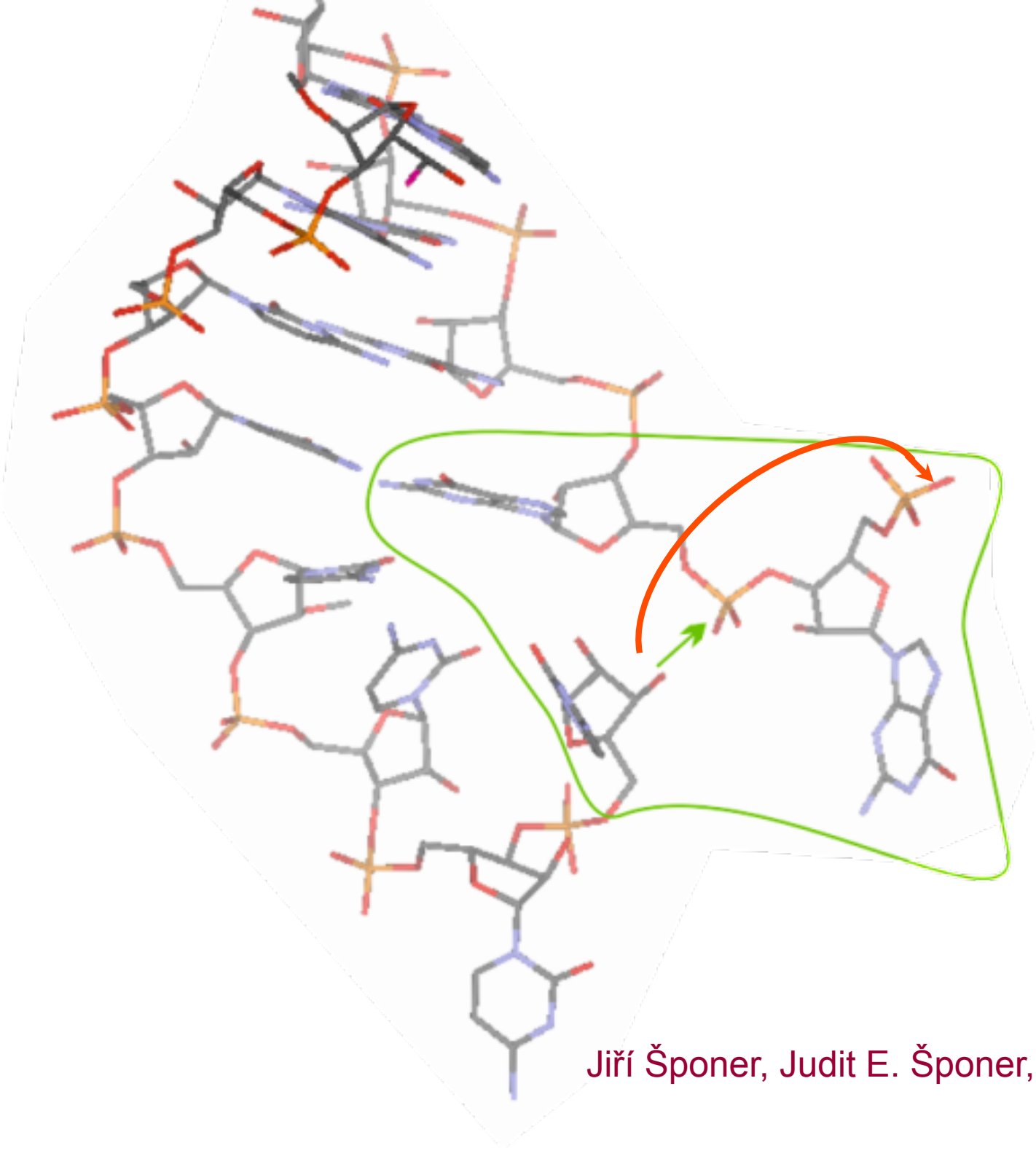

Jiří Šponer, Judit E. Šponer, Peter Stadlbauer, Brno

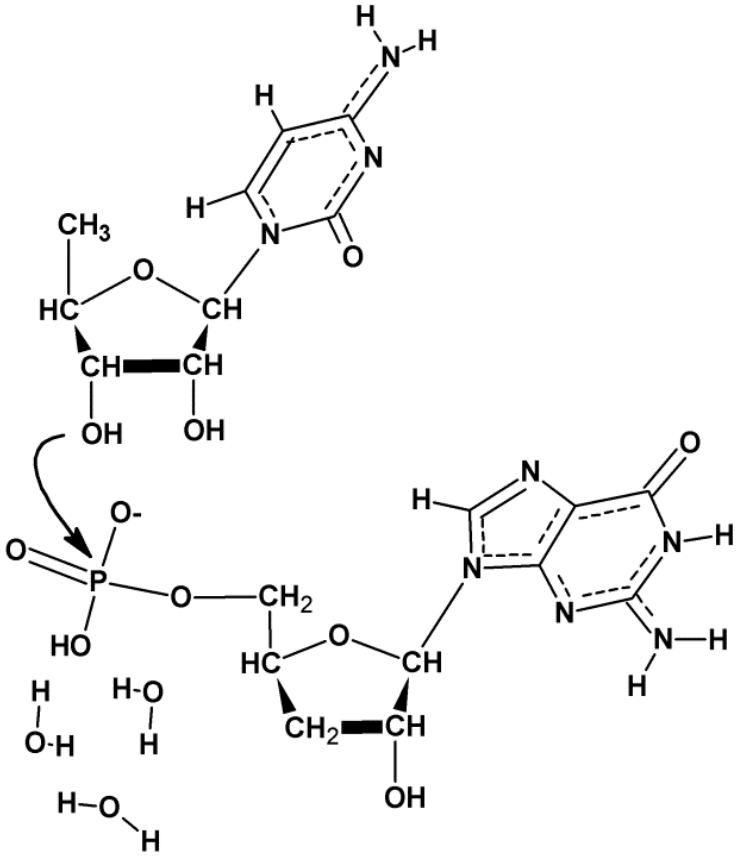

(a)

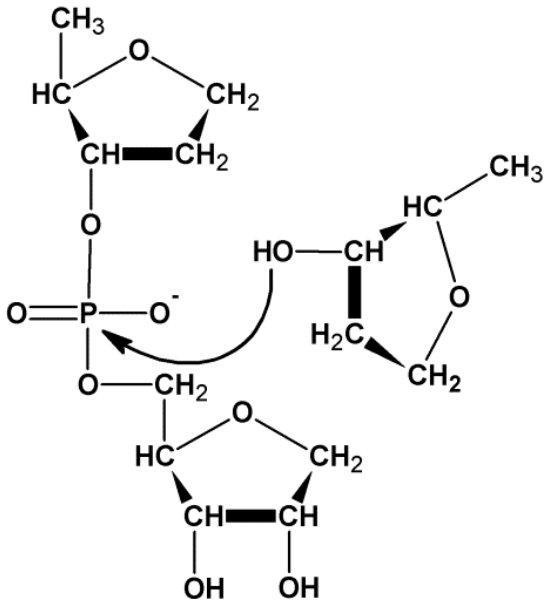

(b)

For the theoretical description of the ligation reaction
we considered a model consisting
of a donor cytidine-phosphate nucleotide and an acceptor guanosine,
which were stabilized by interbase stacking.

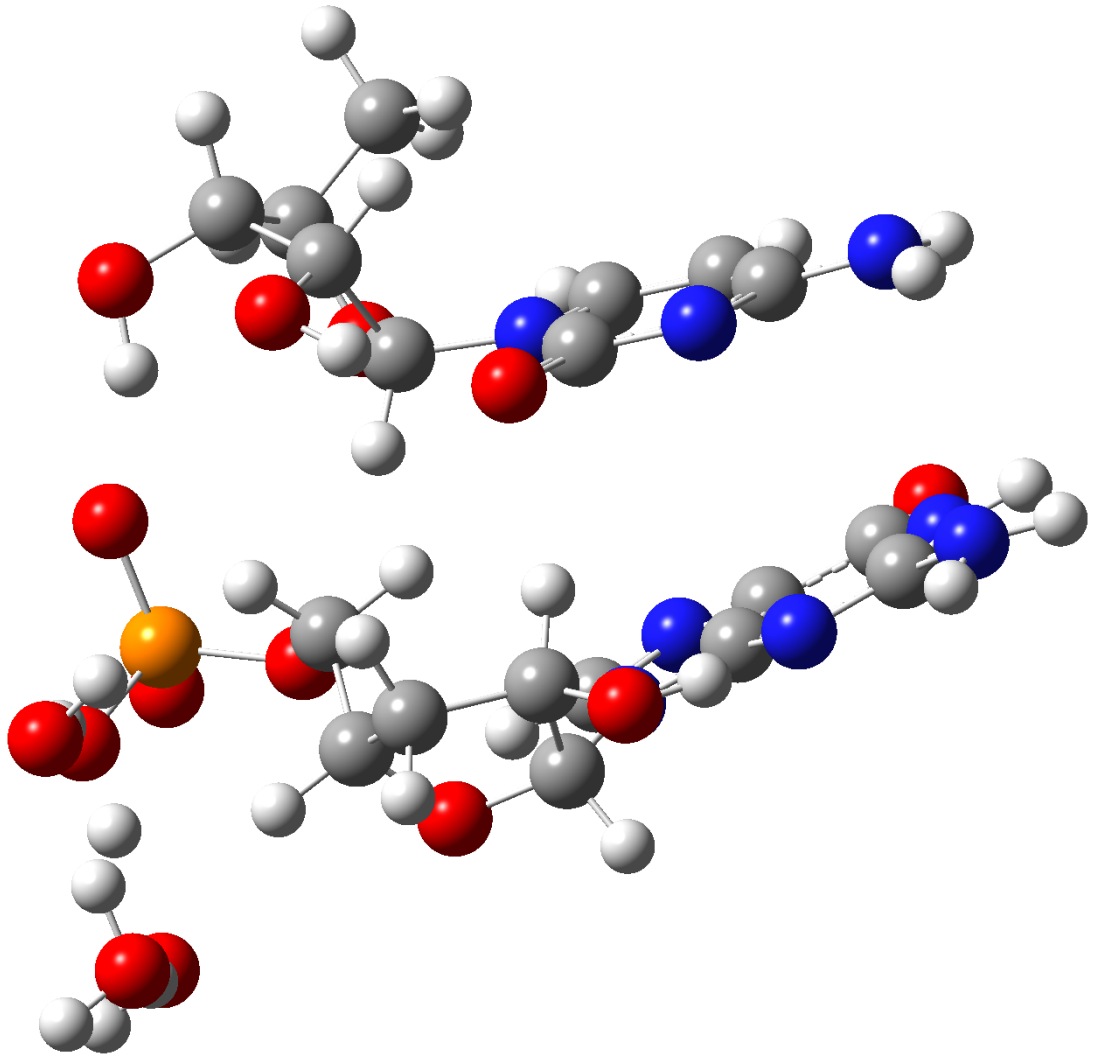

ligation-with-direct-stacking

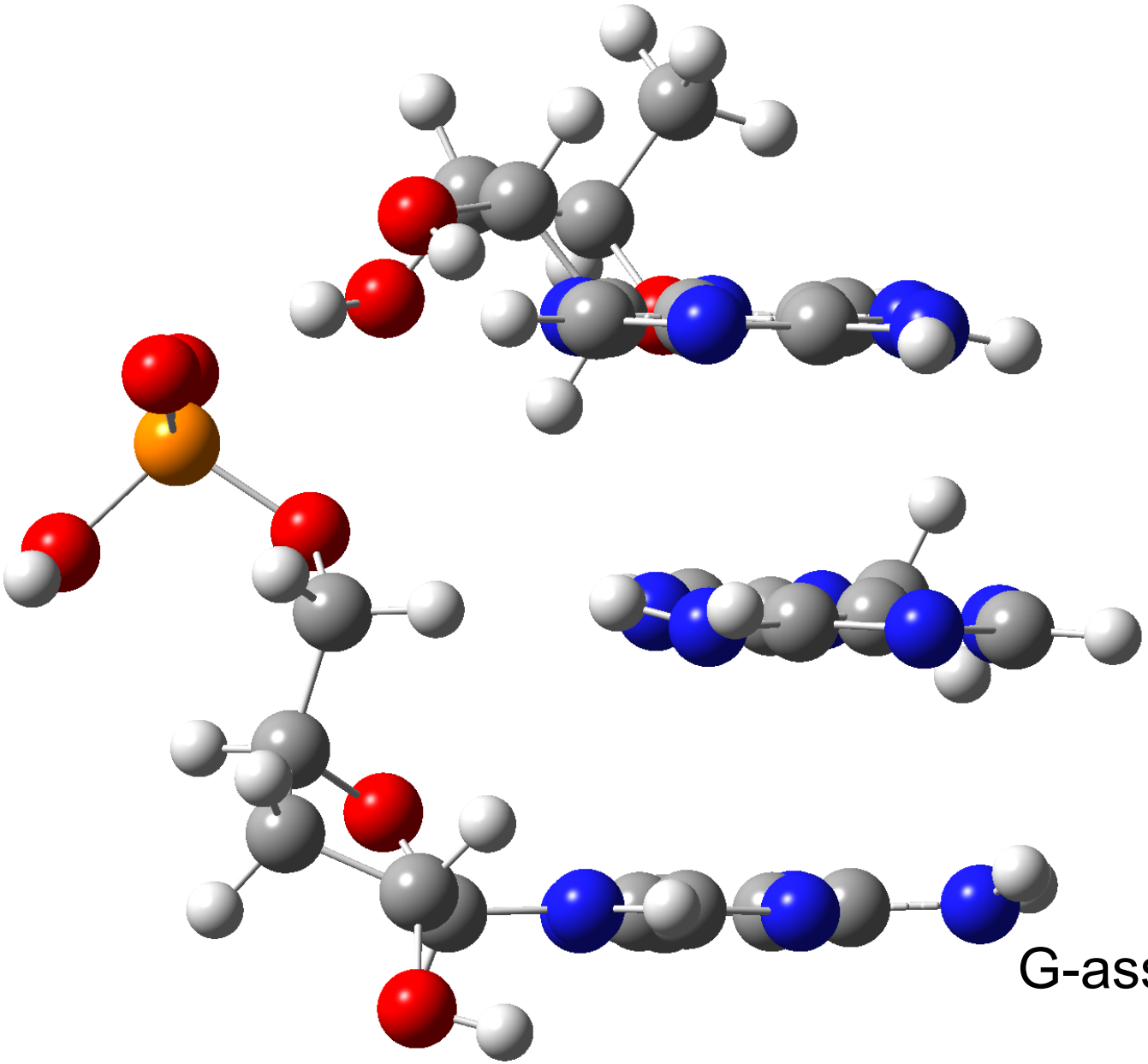

G-assisted-ligation

polyG^{P} + polyC sequence-directed terminal ligation

Pino et al. Biochemistry 2011

PolyC$_{24}$ pH 5 60°C

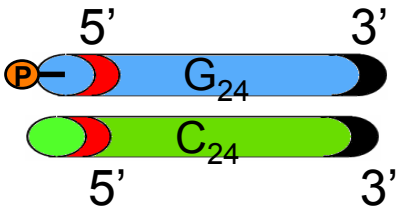

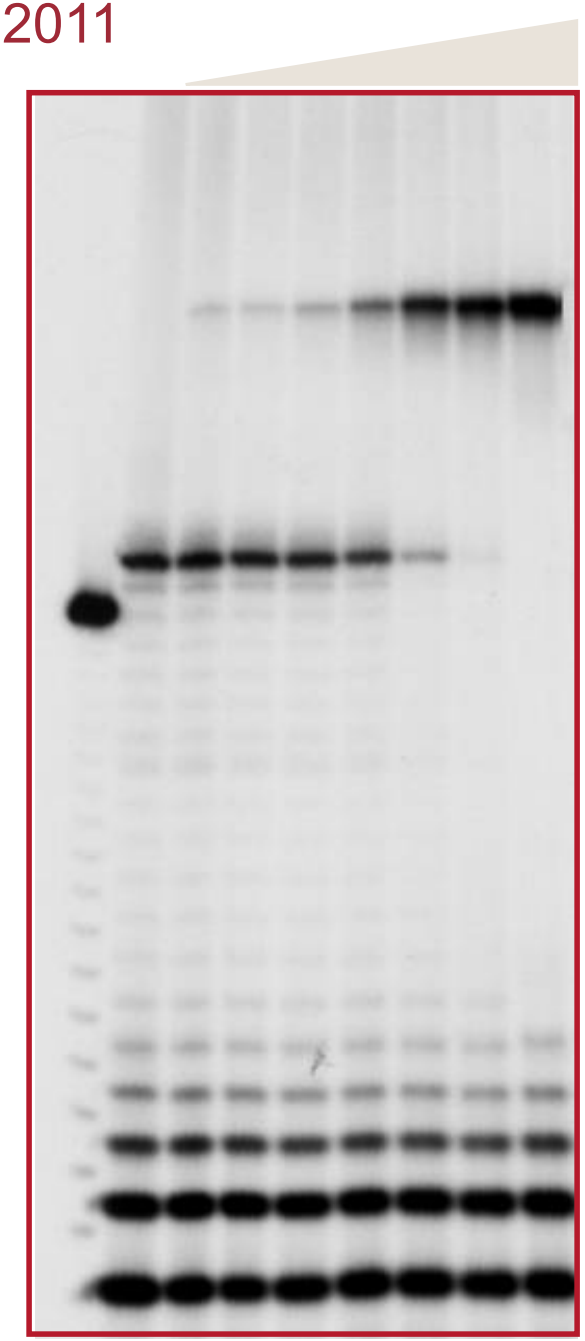

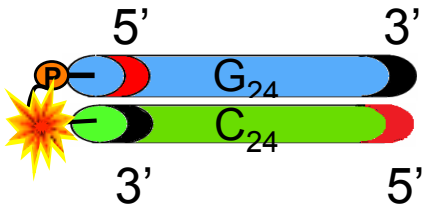

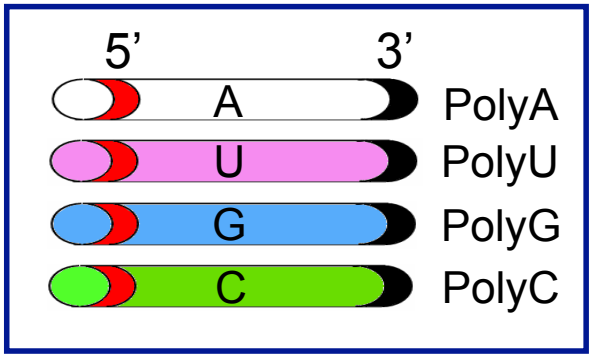

RNA ligation in H_2O

23-, 24-mer

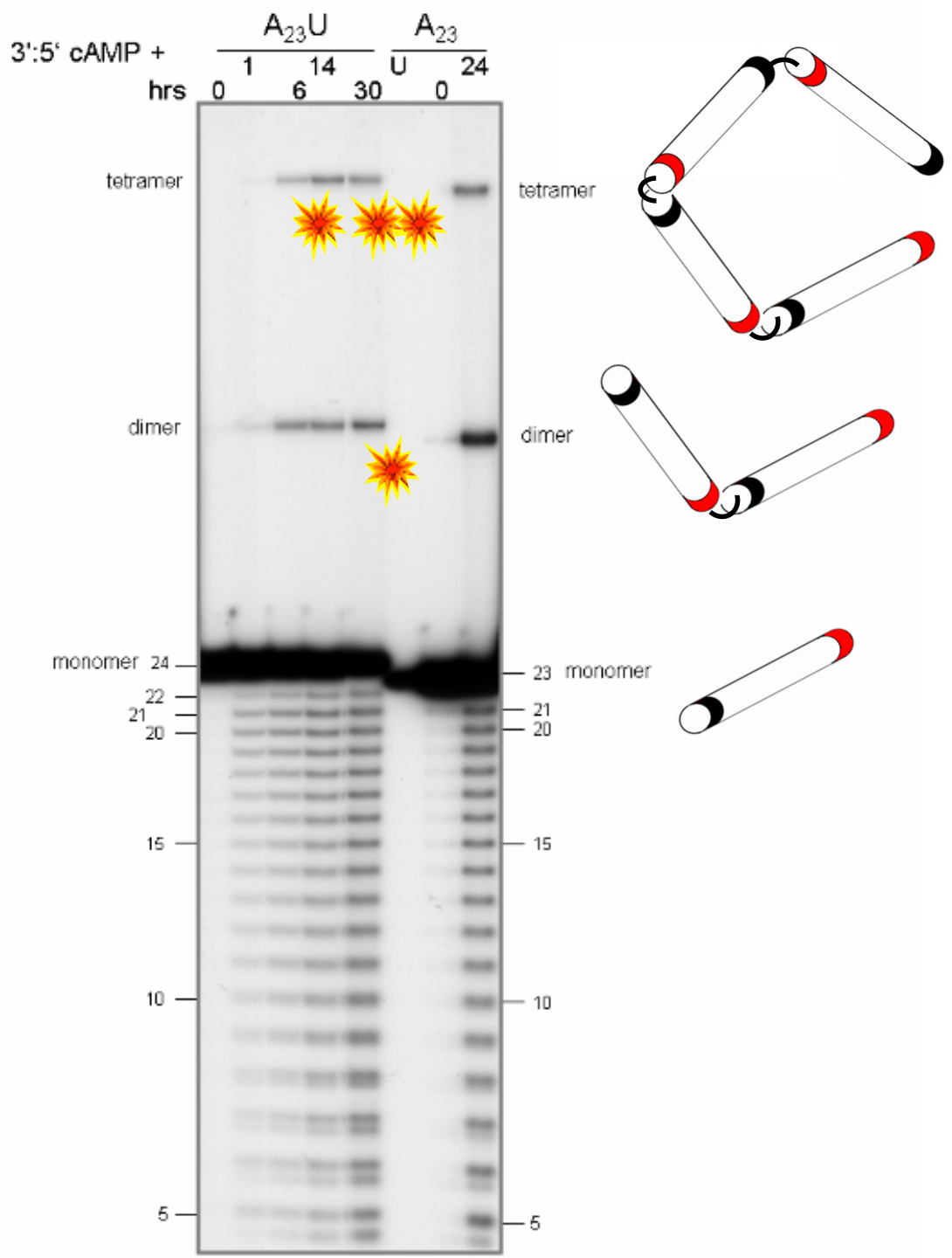

formation of complex RNA populations

Multimerization reaction performed with mixtures of oligomers results in the formation of dimers, tetramers and of additional fragments. The size of these fragments corresponds to the combinations expected for the case of heterogeneous ligation events.

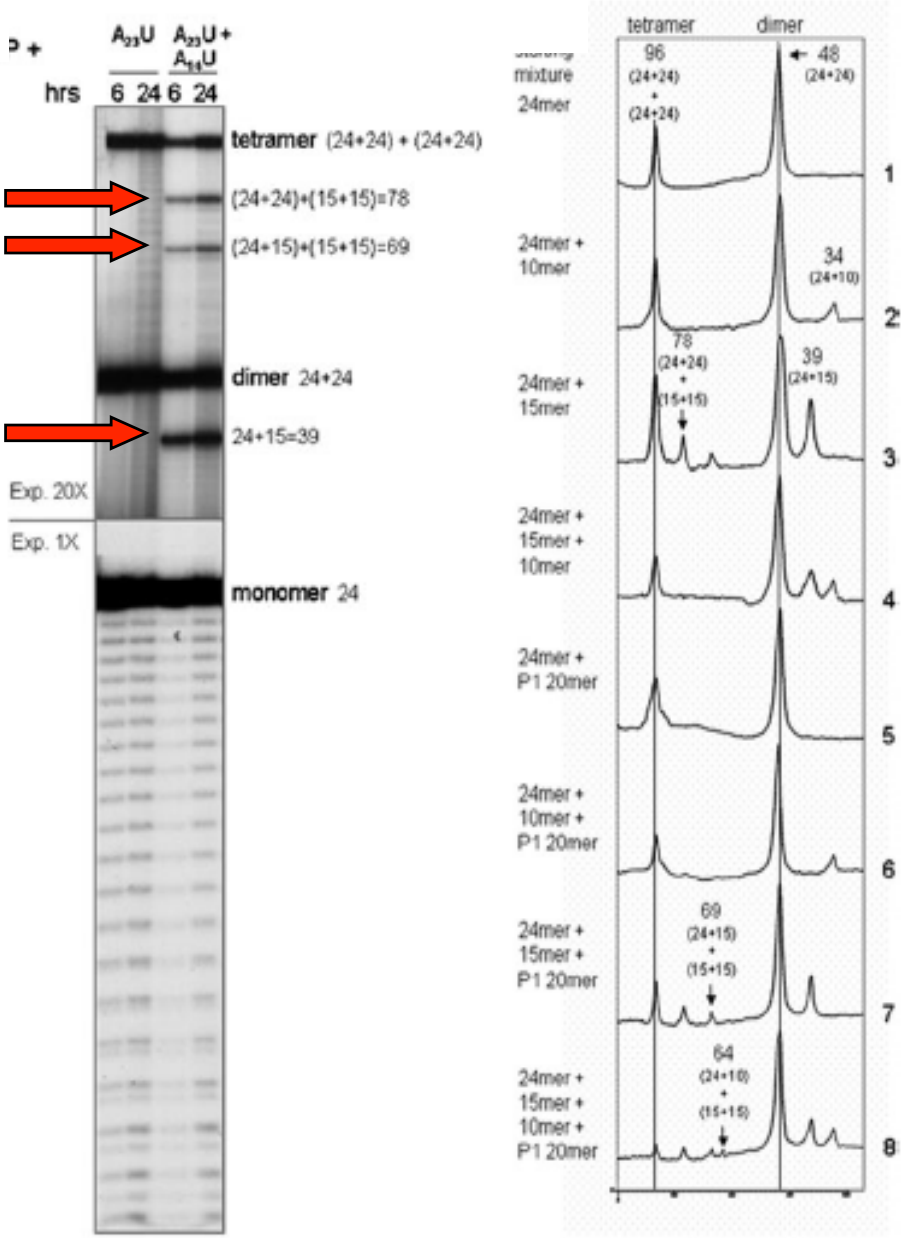

RNA ligation in H_2O

coadjutors

A_{23}

3':5' cAMP

60°C, 6 hrs

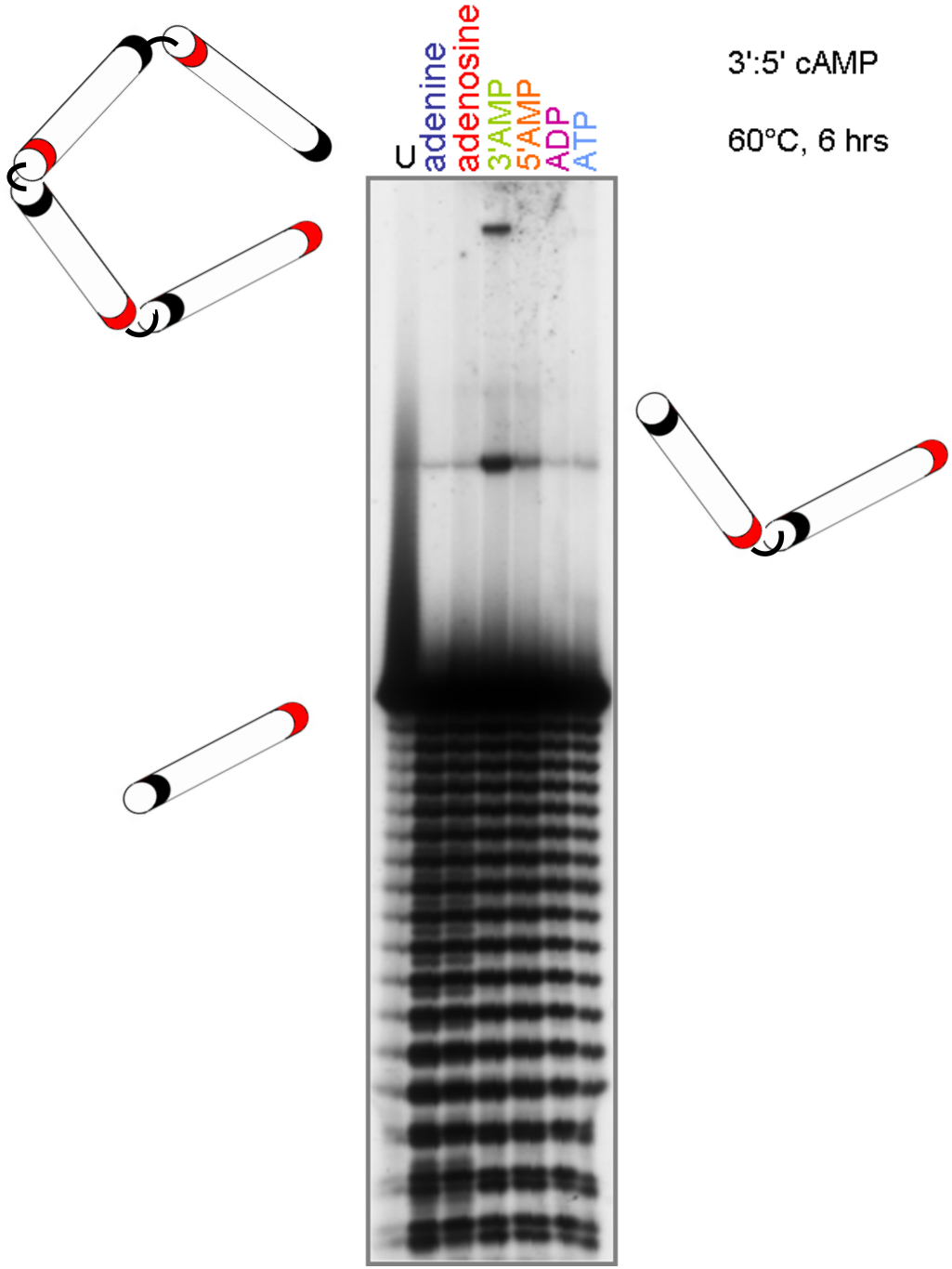

Role of co-factors in the ligation of non-WC-complementary sequences

Experiments by S. Pino, F. Ciciriello, G. Costanzo and E. Di Mauro, *J. Biol. Chem.*, 2008, 283, 36494-36503.

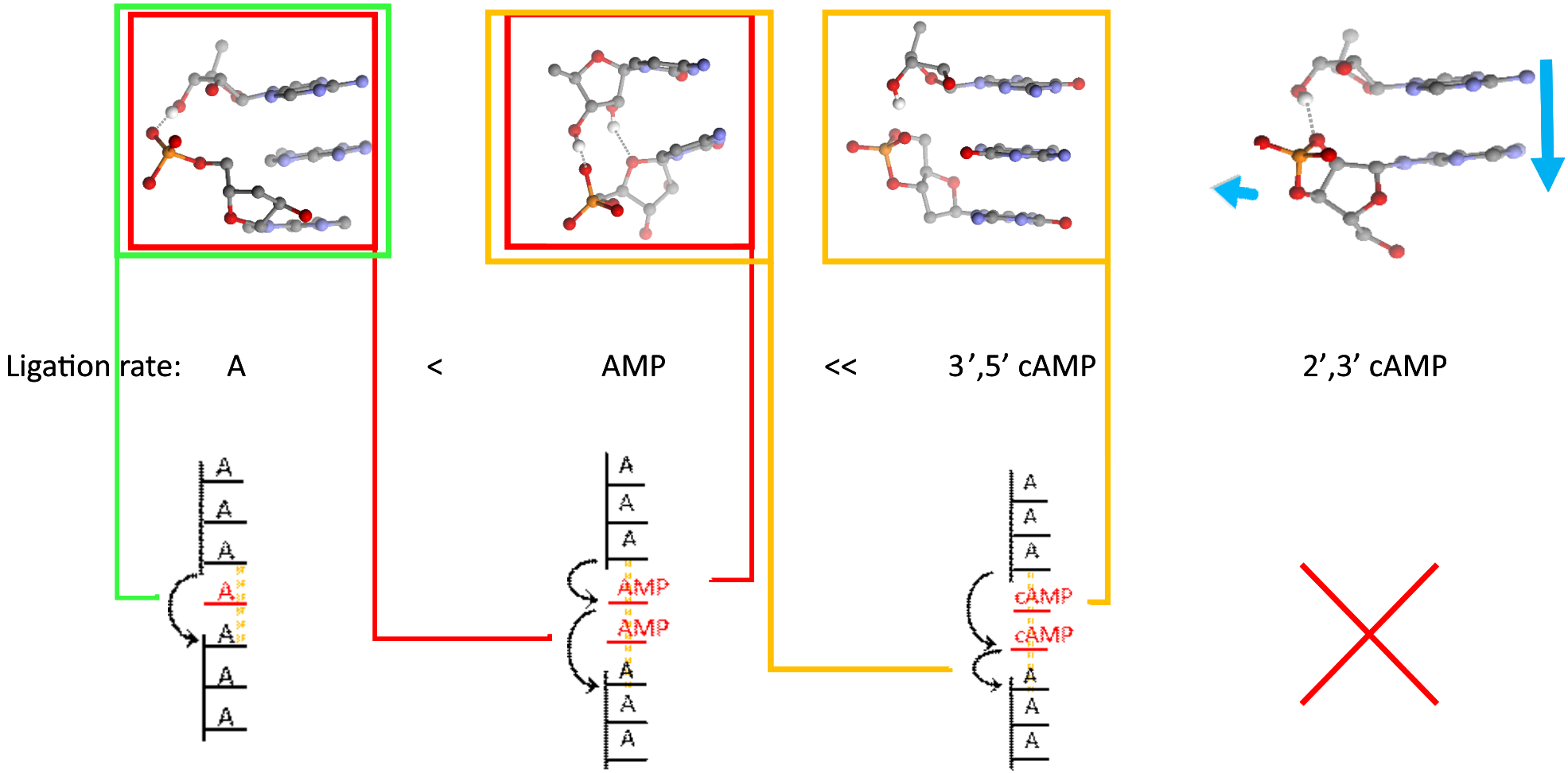

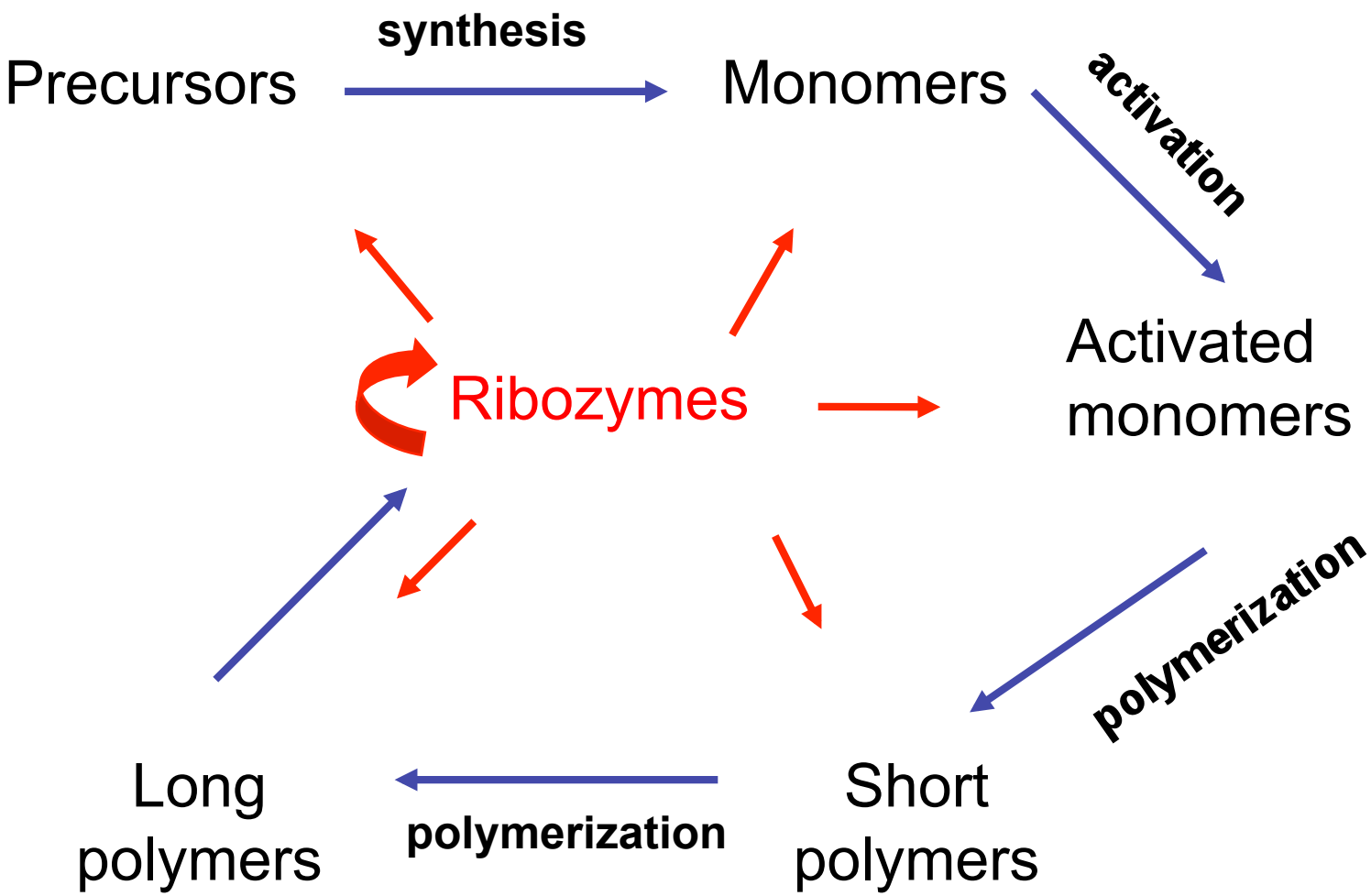
Precursors
synthesis
Monomers
activation
Activated monomers
Ribozymes
polymerization
Short polymers
polymerization
Long polymers

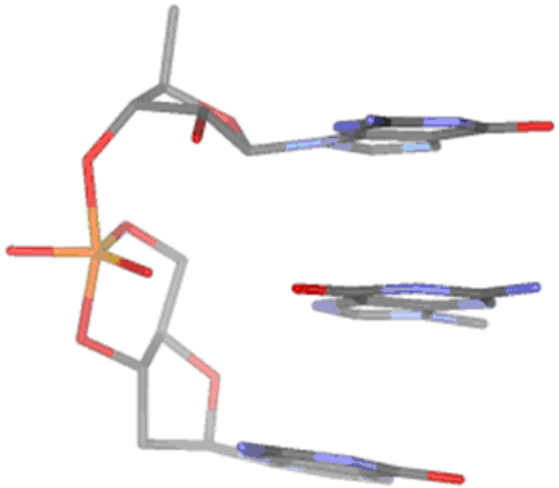

polymerization

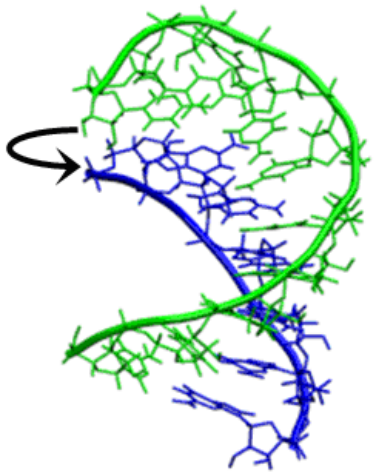

ligation

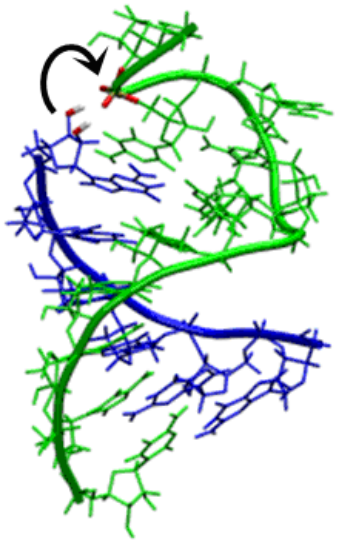

catalysis

The Intervening Sequence RNA of *Tetrahymena* Is an Enzyme

SCIENCE, 1986, Vol 231: 470-475

ARTHUR I. ZAUG AND THOMAS R. CECH

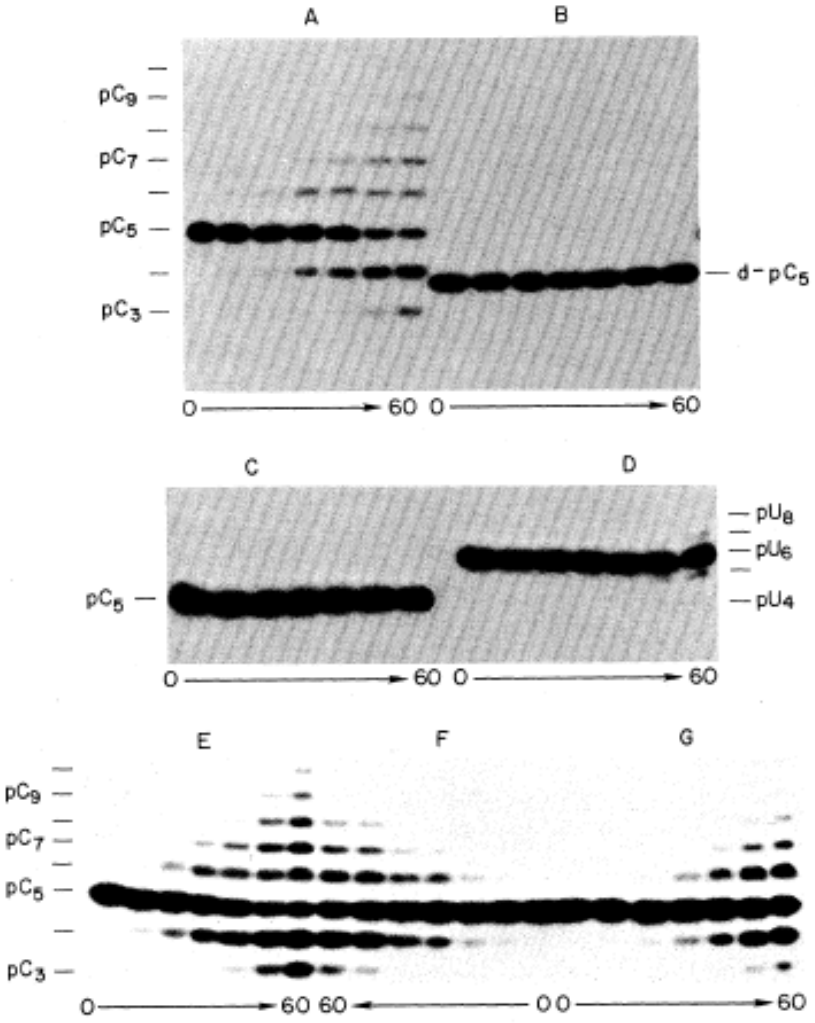

Fig. 1. The L – 19 IVS RNA catalyzes the cleavage and rejoining of oligoribonucleotide substrates;

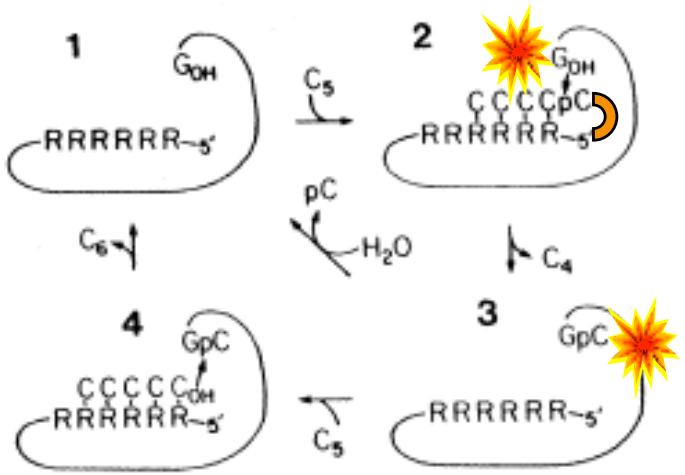

Fig. 4. Model for the enzymatic mechanism of the L – 19 IVS RNA.

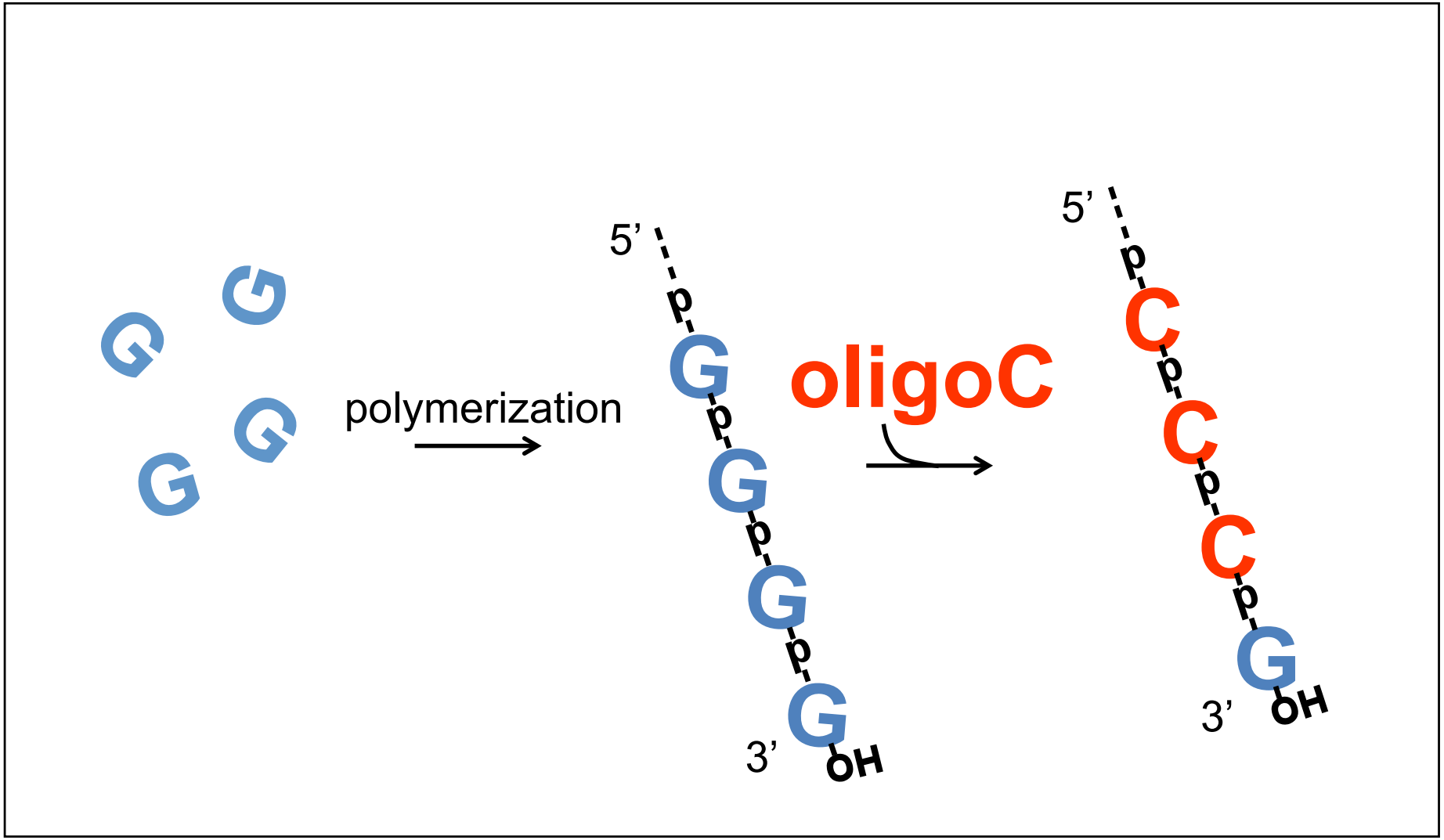
G
G
G
G
polymerization
5’
p
G
p
G
p
G
p
G
OH
3’
oligoC
5’
p
C
p
C
p
C
p
G
OH
3’

self-modification of abiotically polymerized RNA
one-nucleotide RNA terminal transfer, here: model system

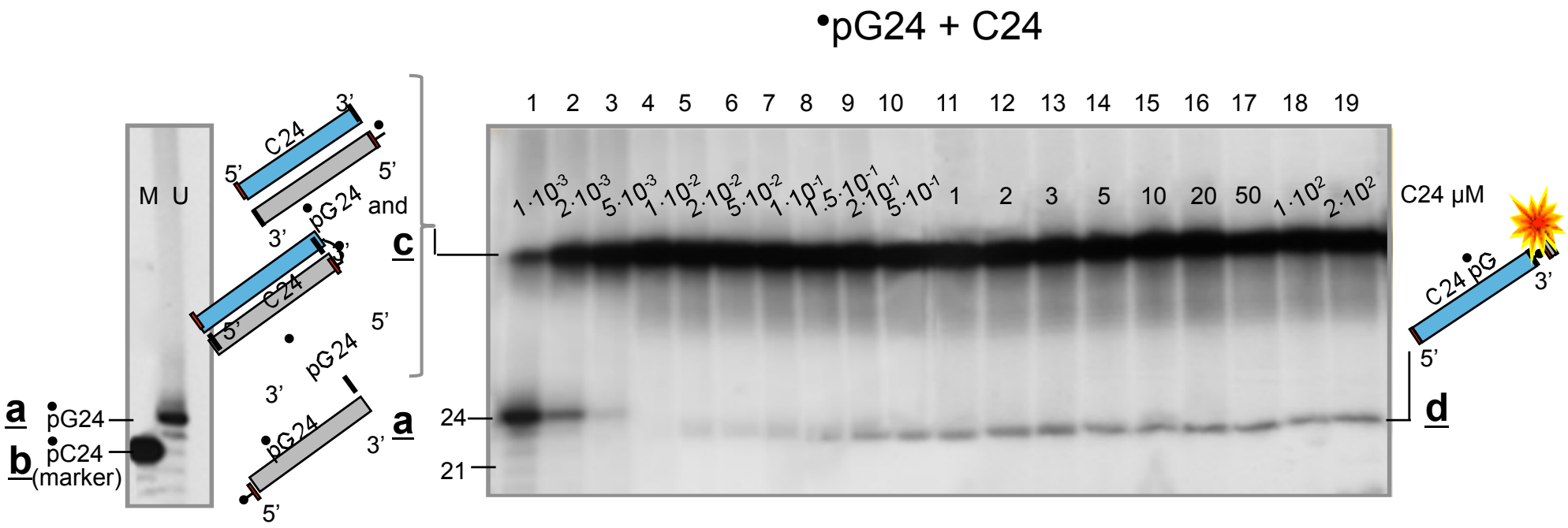

The same loop geometry can give rise to ligation as well as terminal cleavage

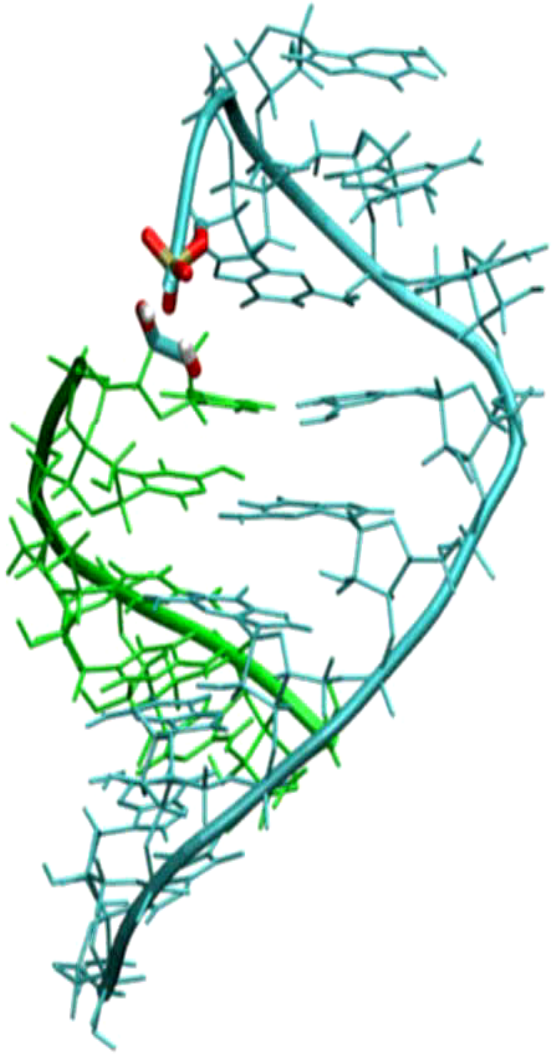

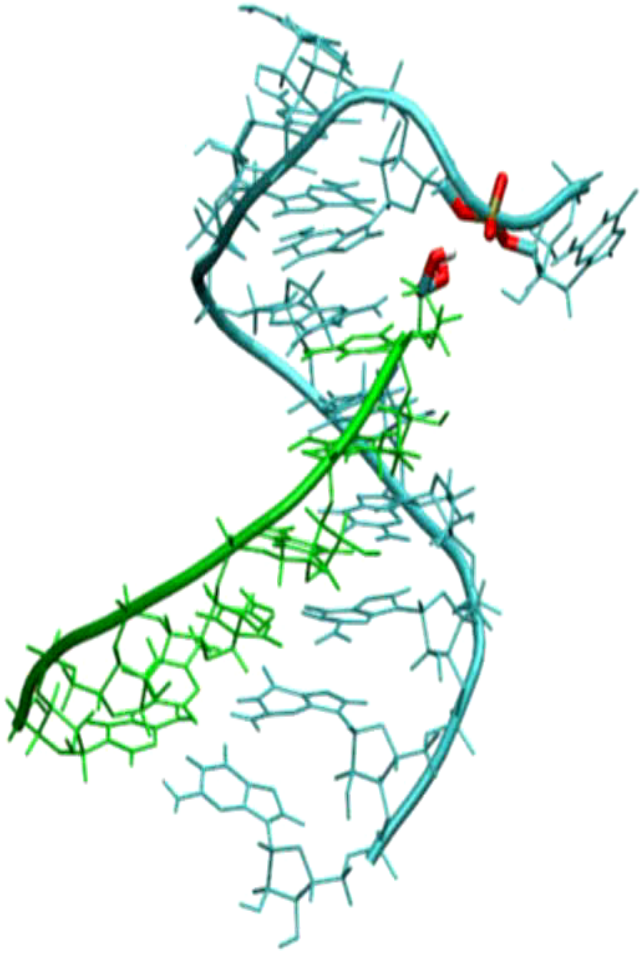

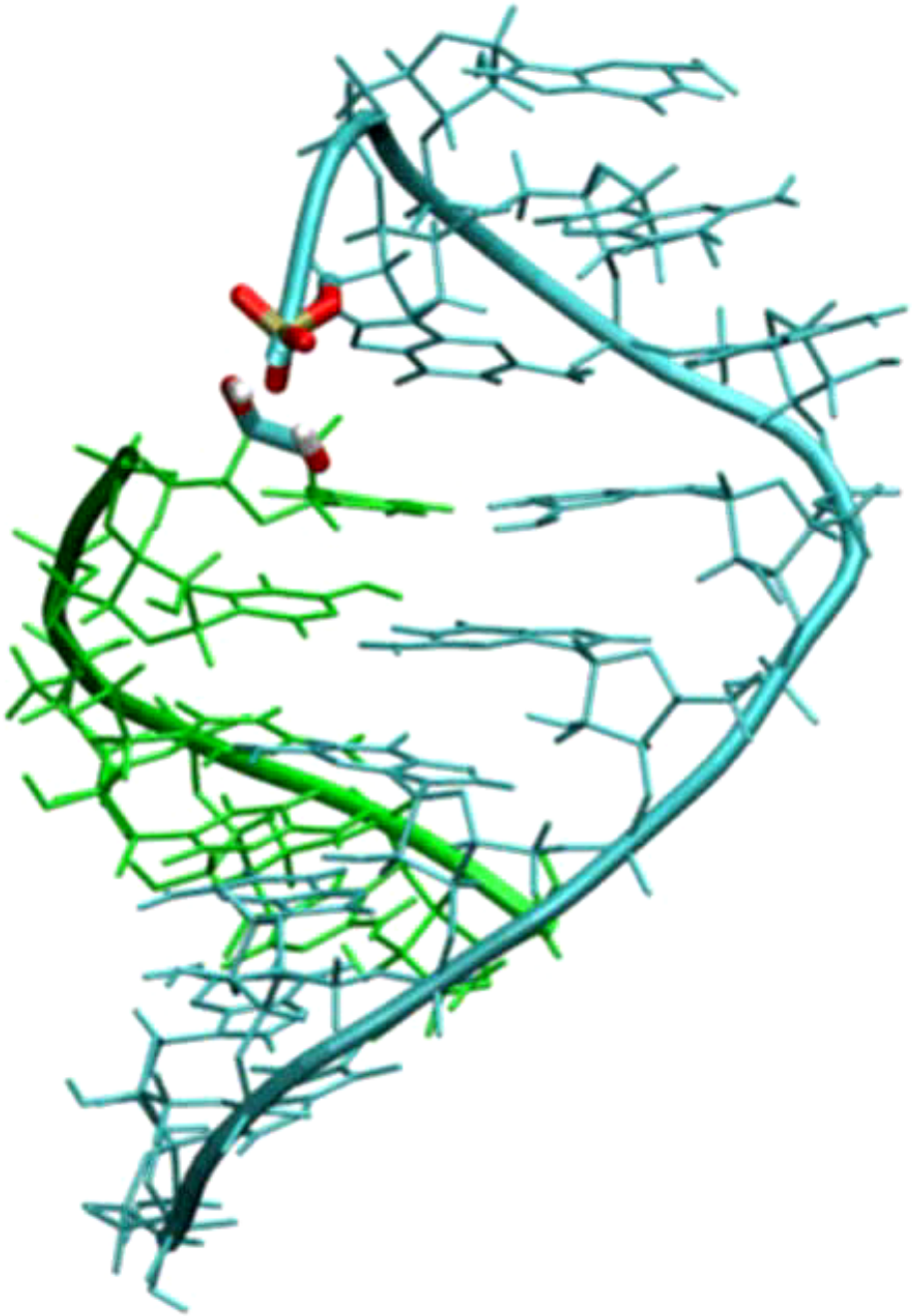

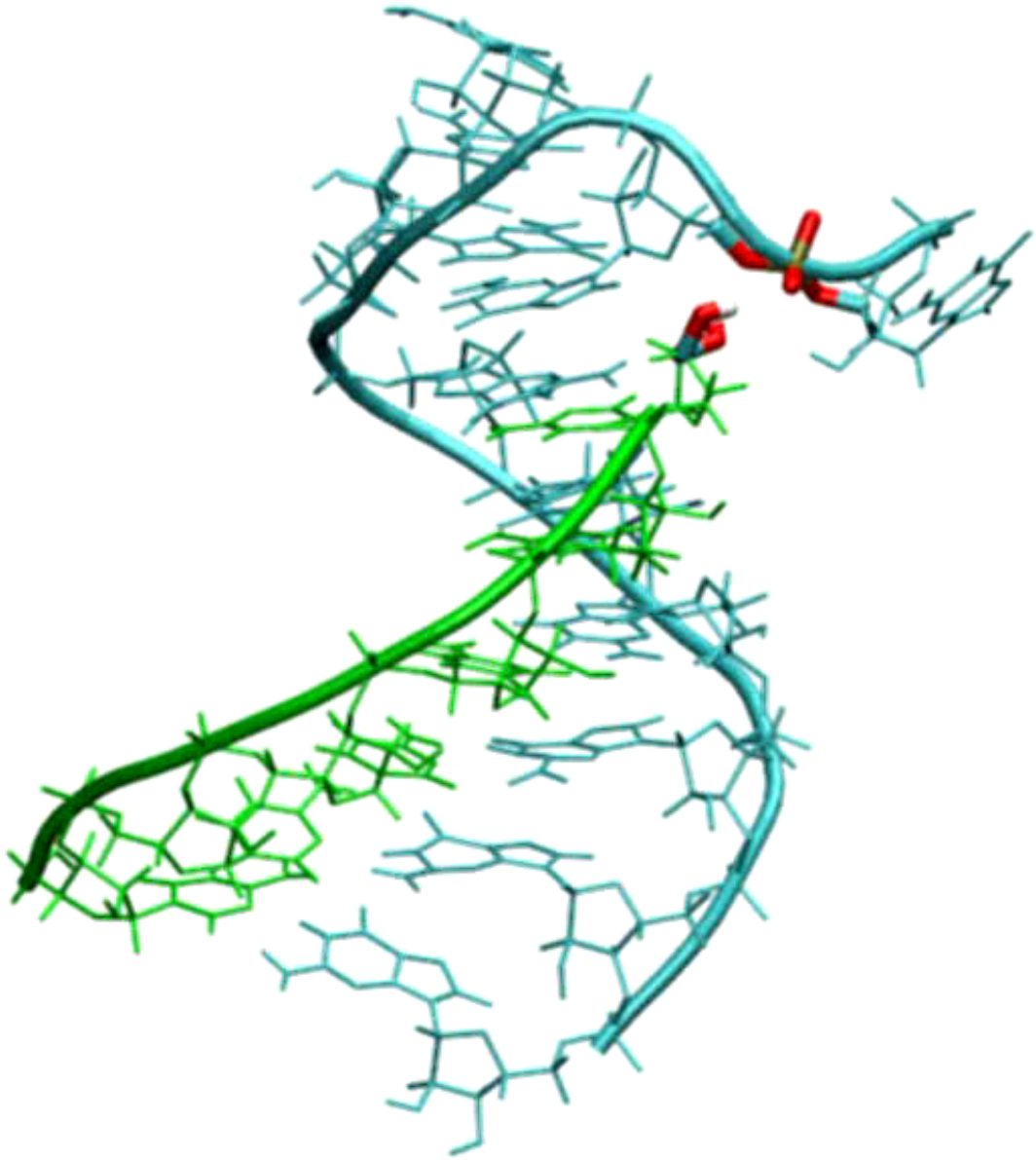

The “Ligation following Intermolecular Cleavage” (LIC) mechanism

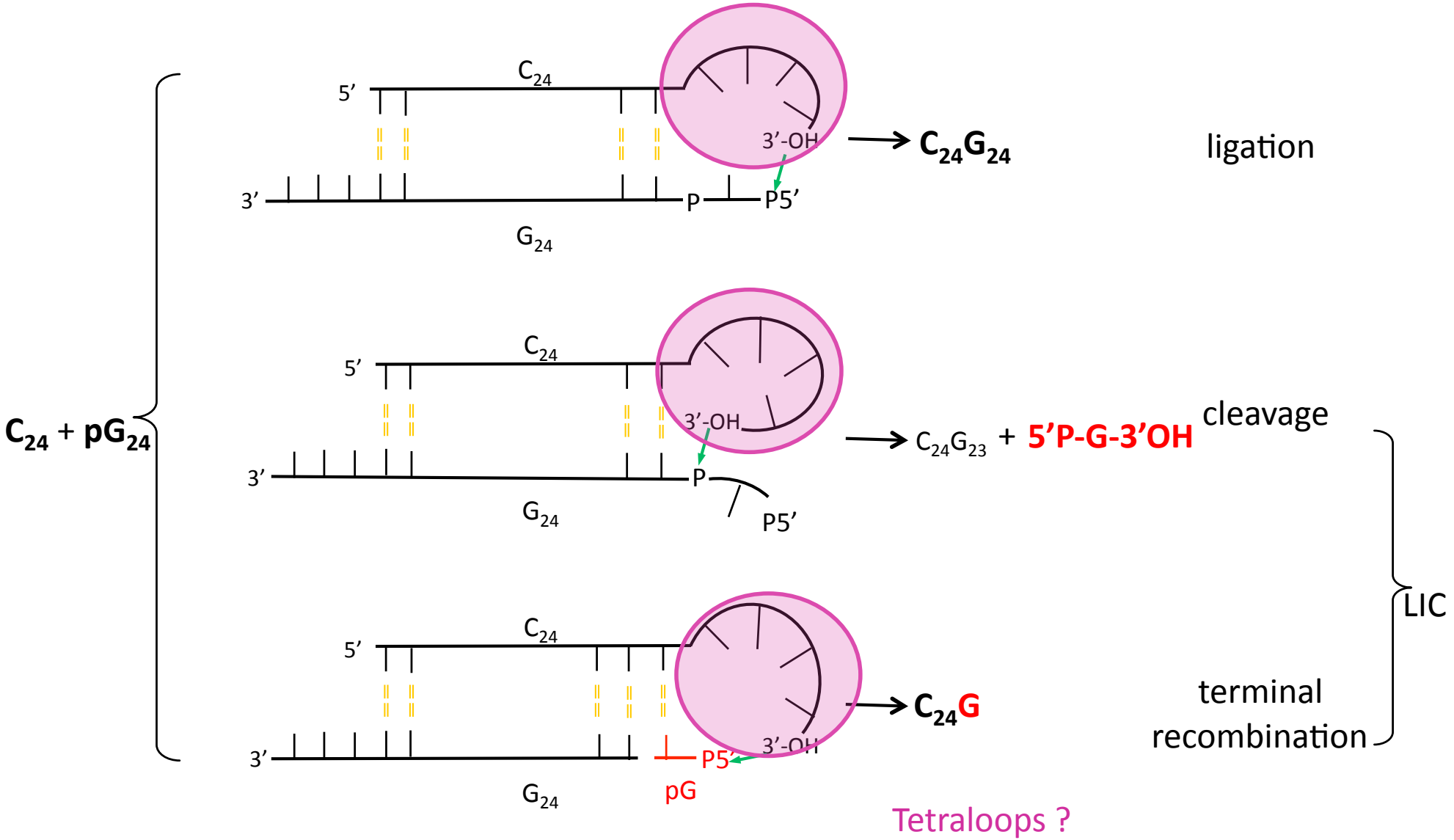

S. Pino, G. Costanzo, A. Giorgi, J. Šponer, J. E. Šponer and E. Di Mauro, *Entropy*, 2013, 15, 5362-5383.

Triloops and pentaloops?

NOT. Tetraloops !

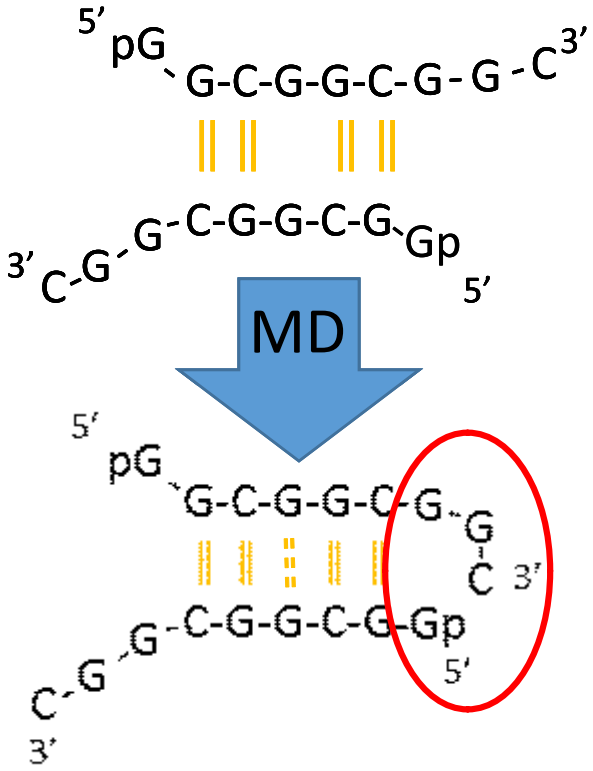

stacking

H-bond

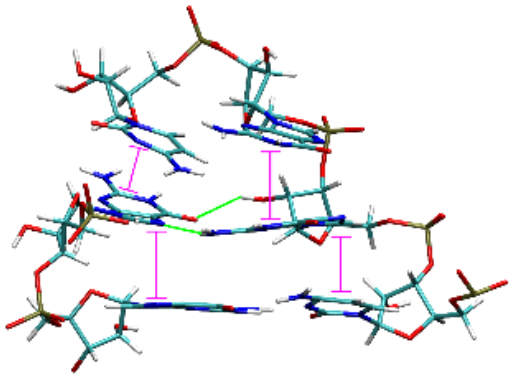

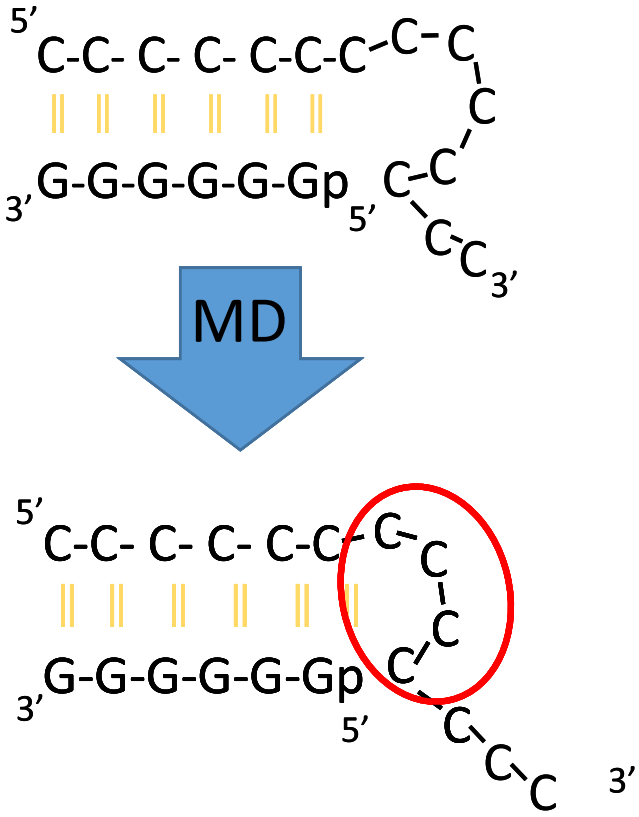

MD-simulations of tetraloop-like geometries enabling ligation and terminal cleavage

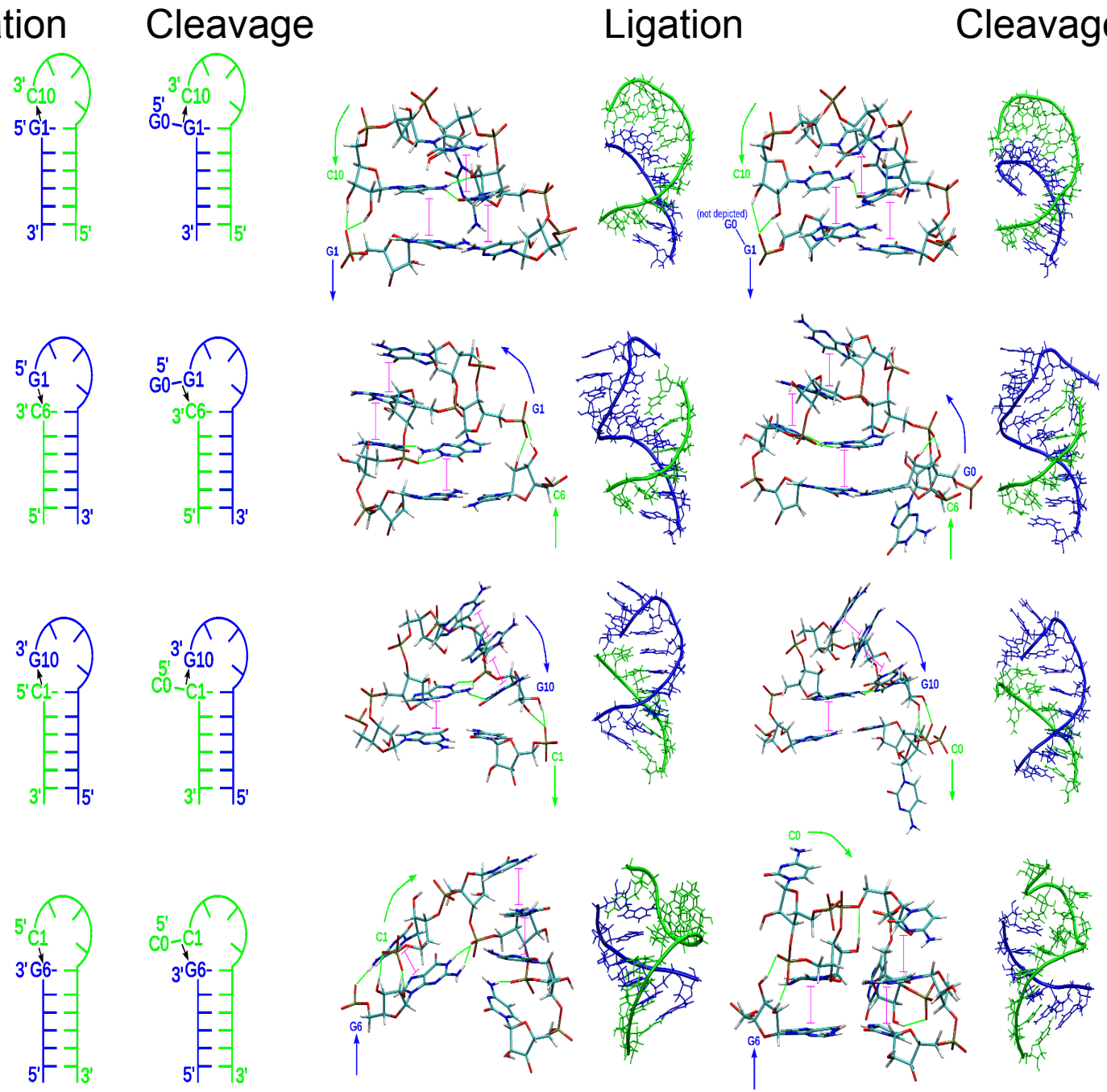

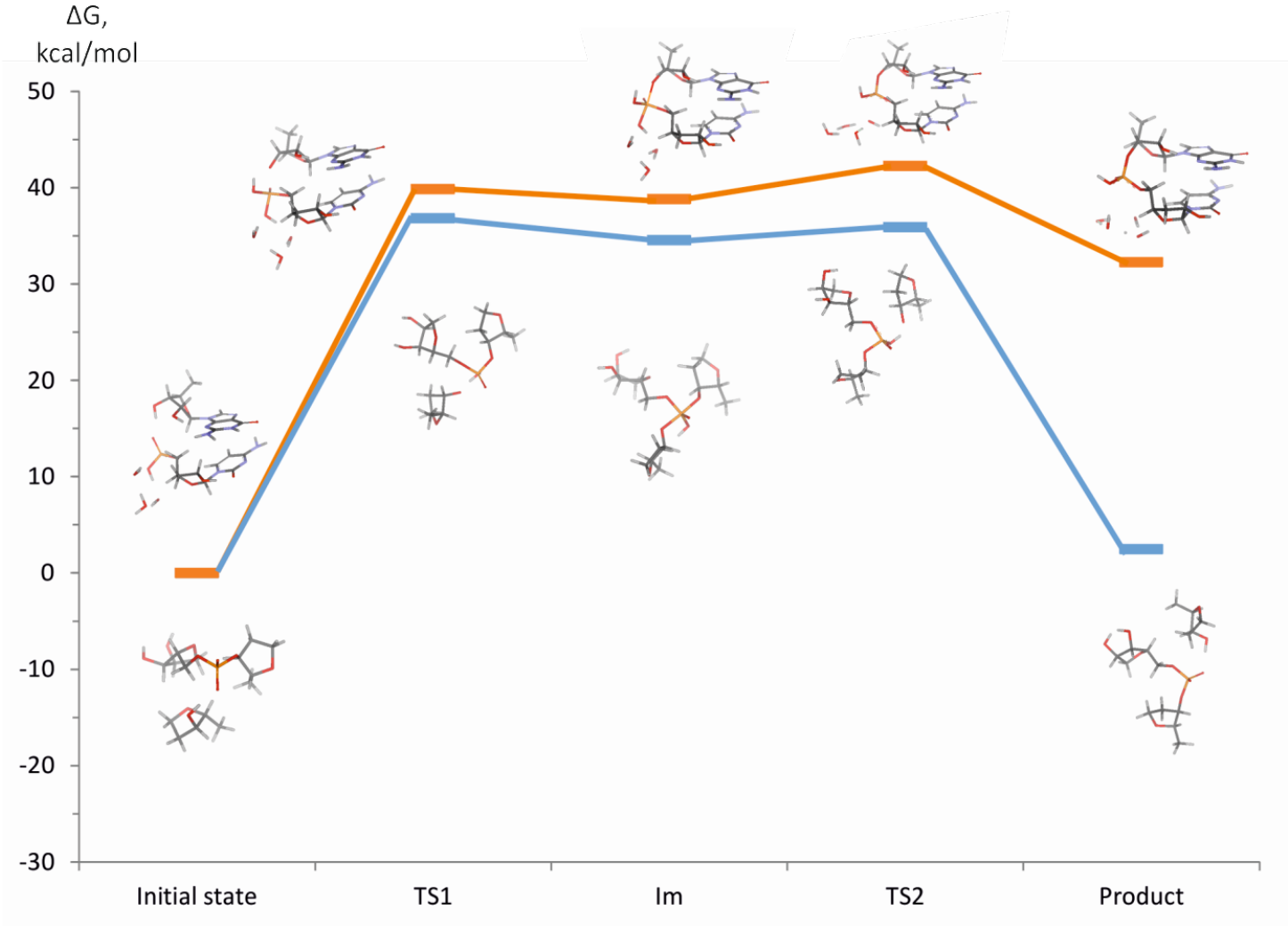

Computed free energy profile of the ligation (orange curve) and cleavage (blue curve) reactions. Computations were carried out at the DFT-D level of theory using the TPSS-D2 density functional, the TZVP basis set of atomic orbitals along with the C-PCM continuum solvent technique.

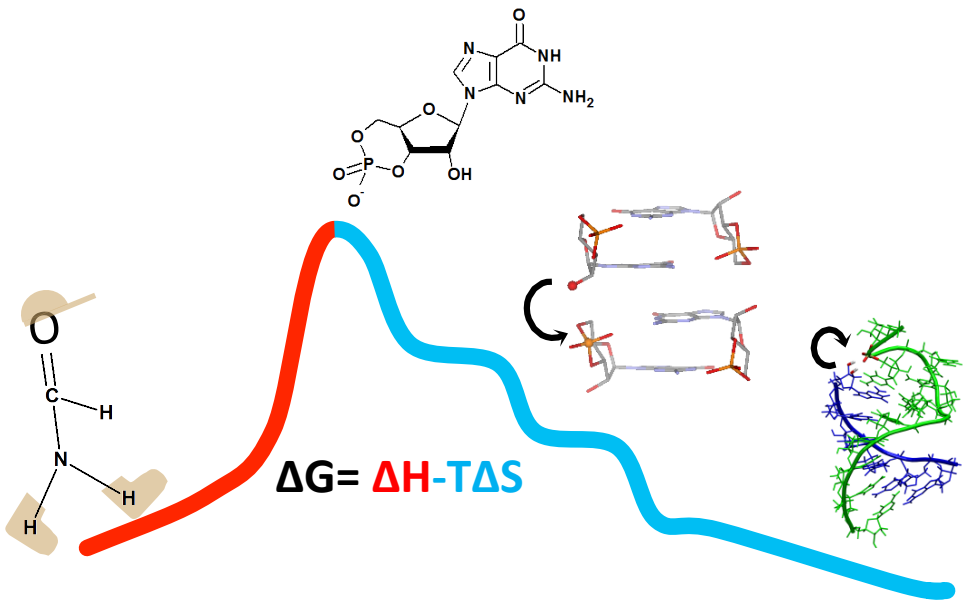
ΔG= ΔH-TΔS

CONTENTS

THE DEAD PAST

FRANCHISE 57
GIMMICKS THREE 75
KID STUFF 83
THE WATERY PLACE 97
LIVING SPACE 103
THE MESSAGE 119
SATISFACTION GUARANTEED 121
HELL-FIRE 137
THE LAST TRUMP 139
THE FUN THEY HAD 157
JOKESTER 161
THE IMMORTAL BARD 175
SOMEDAY 179
THE AUTHOR'S ORDEAL 189
DREAMING IS A PRIVATE THING 193

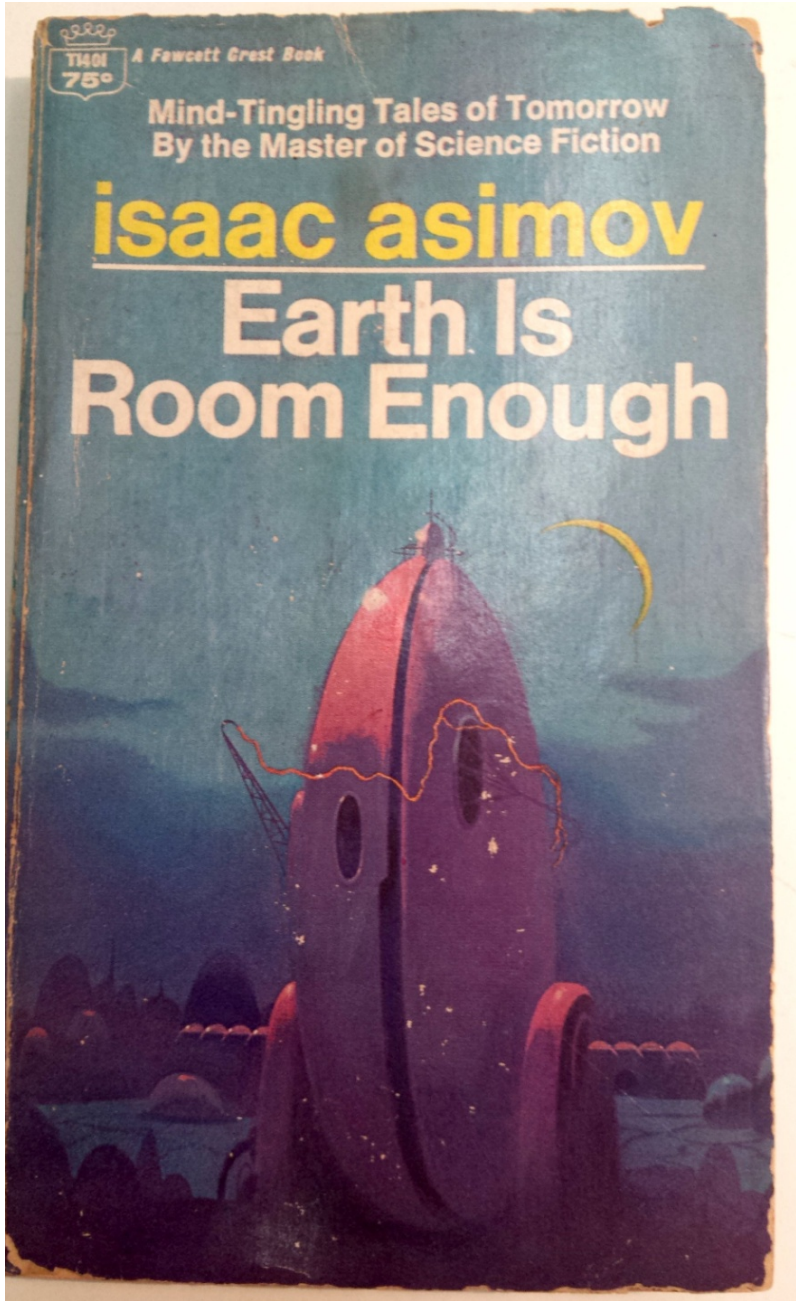

Features of Spliceosome Evolution and Function Inferred from an Analysis of the Information at Human Splice Sites

R. Michael Stephens[1,2]† and Thomas Dana Schneider[1]‡

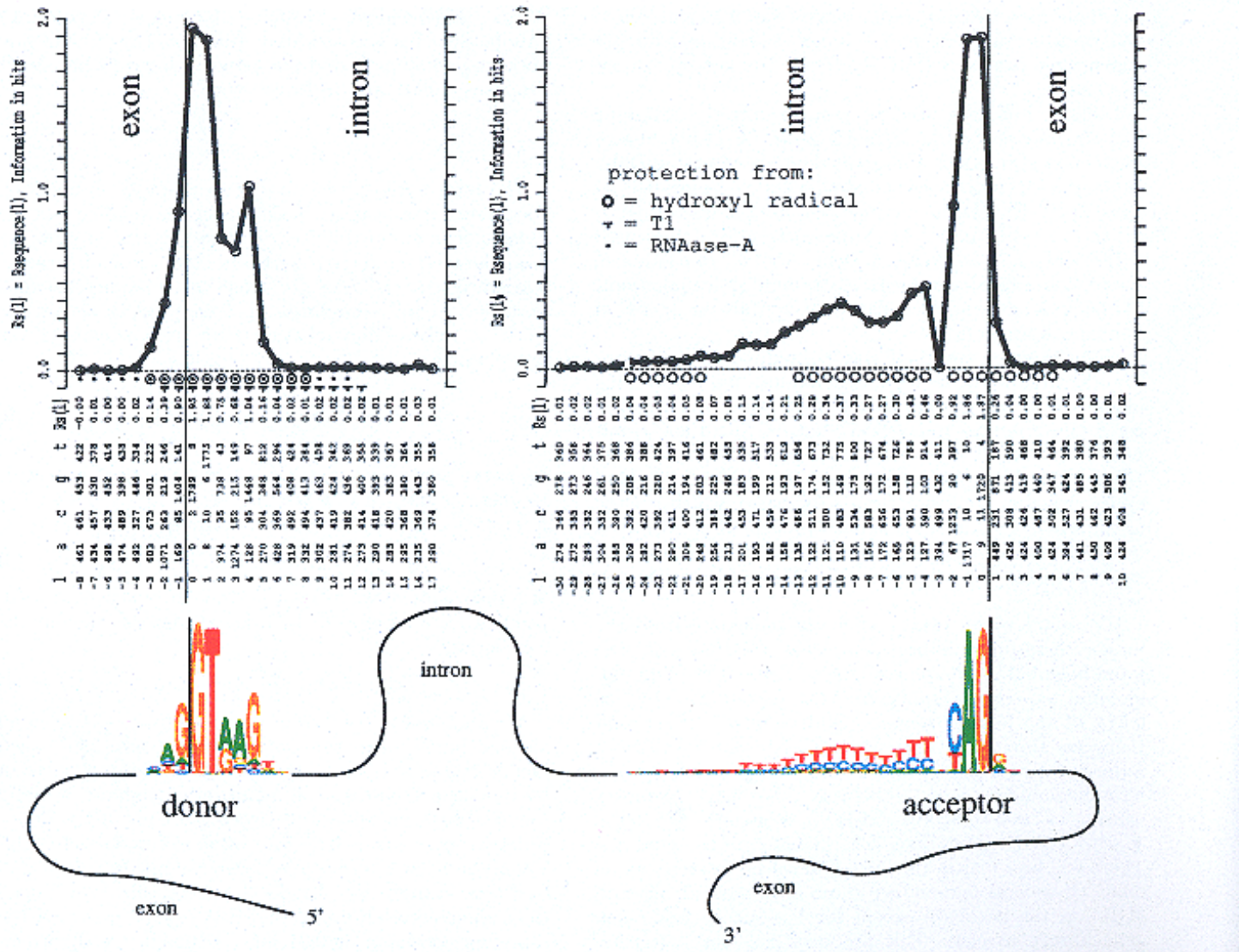

Information curves and sequence logos for human spliceosome binding sites. *J. Mol. Biol*. 1992, **228**: 1124-1136

Features of Spliceosome Evolution and Function Inferred from an Analysis of the Information at Human Splice Sites

R. Michael Stephens[1,2]† and Thomas Dana Schneider[1]‡

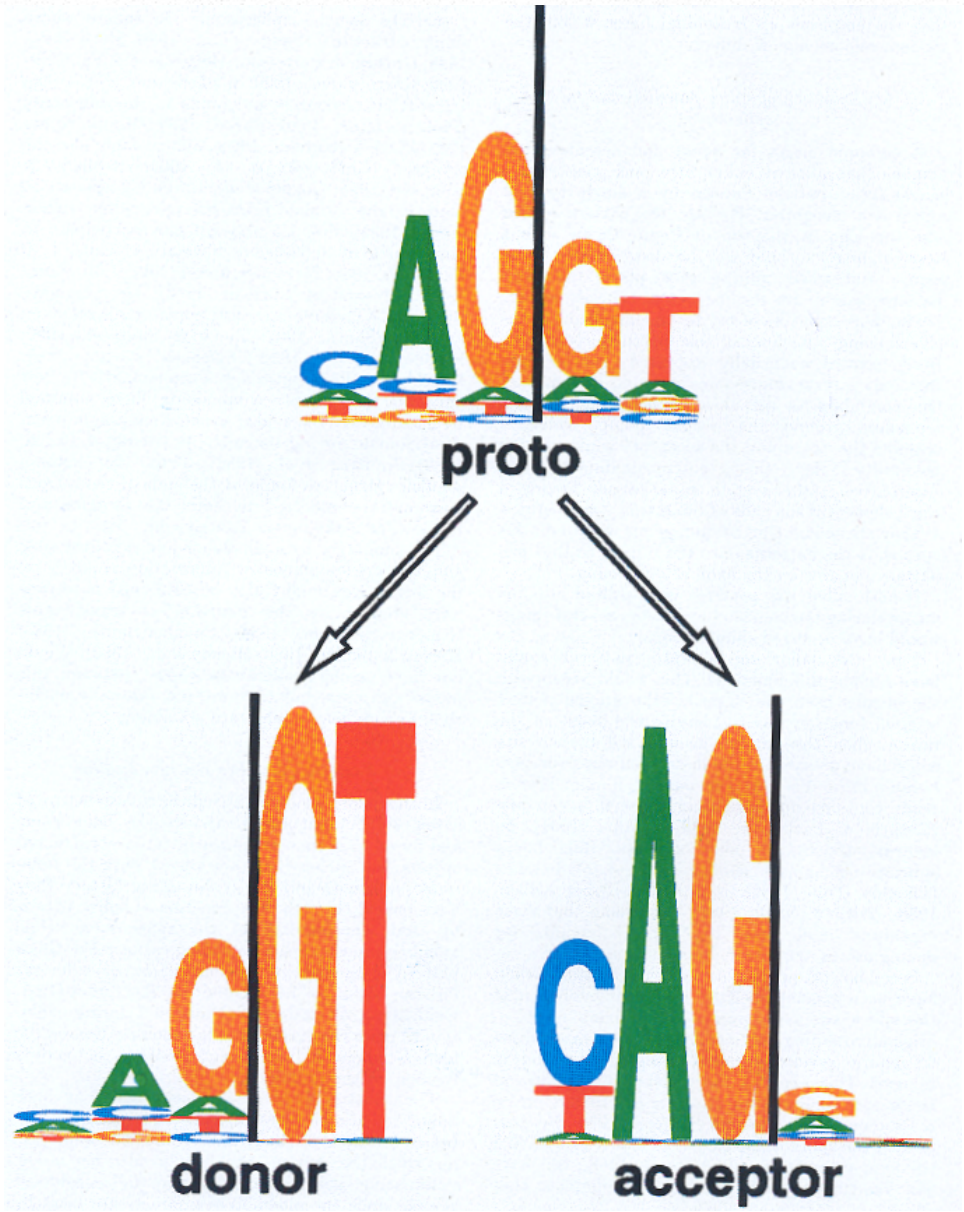

Sequence logos for proto-, donor and acceptor splice sites. *J. Mol. Biol*. 1992, **228**: 1124-1136

Victor Stenger

Something came from nothing because it is more stable than nothing

The Comprehensible Cosmos, Prometheus Books


thank
you

Ion and ENA(Energetic Neutral Atoms) Beam Facility @ IAPS
Rome-Italy

At IAPS (***I**nstitute for **S**pace **A**strophysics and **P**lanetology*) in Rome, a Penning ion source generates a plasma from which the required ions can be extracted with different energies.
-The discharge starts easily and will run very stably for many hours.
-The type of gas used depends on the type of ions required (i.e He, Ar, O, H).
-This facility is mostly used for space ambient simulation and space instrument testing.

→ **Ion beam @ 500÷ 5000 eV**

The ion beam can be used also to obtain **an Energetic Neutral Atoms (ENA)** beam, thanks to charge-exchange processes.

Facility equipment	Description
Vacuum system	Vacuum pumps: scroll, turbopump (or cryopump) reach pressure up to 10–7 mbar. Vacuum chamber: cylindrical calibration chamber of 200 liters capacity
Ion Beam	IQP 10/63 Penning discharge type ion source with energy range of 0-5 keV.
Residual Gas Analyser	Ametek-Dycor quadrupole mass spectrometer with AMU range 1-200.
Rotation, Translation	+/- 45° transverse axis rotation and 0-360° orthogonal axis rotation with 0.01° resolution x-y-z translation (0,5mm increment) and 0-360° rotation (0,1 mrad increment)

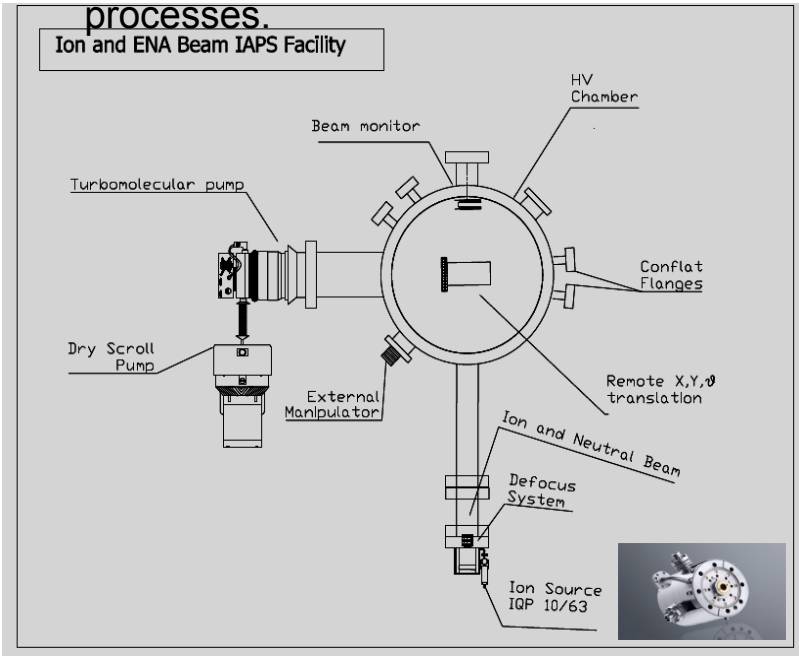

Lab Team @IAPS:
Elisabetta De Angelis, Rosanna Rispoli, Nello Vertolli and Luca Colasanti

Ion and ENA(Energetic Neutral Atoms) Beam Facility @ IAPS, *Rome-Italy*

Sample irradiation test

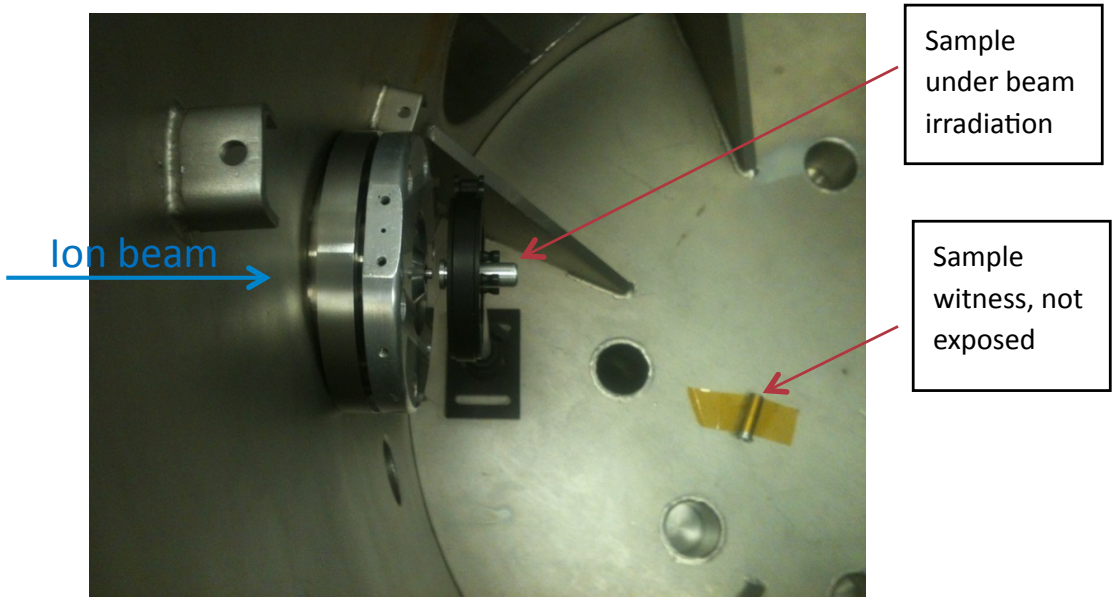

Internal picture of test set-up in vacuum chamber

Irradiation Test condition	
Ion beam specie	*He/He$^+$*
Ion beam energy	*1 keV*
Exposure time	*15h 59min*
Beam intensity	*10^6-10^7 particles/s/ cm^2*
Pressure	*$7*10^{-7}$ mbar*
Temperature	*T amb (~25°C)*

Physical characteristics of the beams

Accelerator	Particle	Energy	Averaged linear energy transfer, keV/μm	Absorbed dose, Gy
Phasotron	protons	170 MeV	0.56	6
Nuclotron	^{12}C ions	500 MeV/ n	11.5	4.58; 3.69
U400M	^{11}B ions	33 MeV/n	57.3 minimum	~ 6

Prof. Raffaele Saladino[1,*],
Dr. Giorgia Botta[1],
Dr. Michela Delfino[1] and
Prof. Ernesto Di Mauro[2]

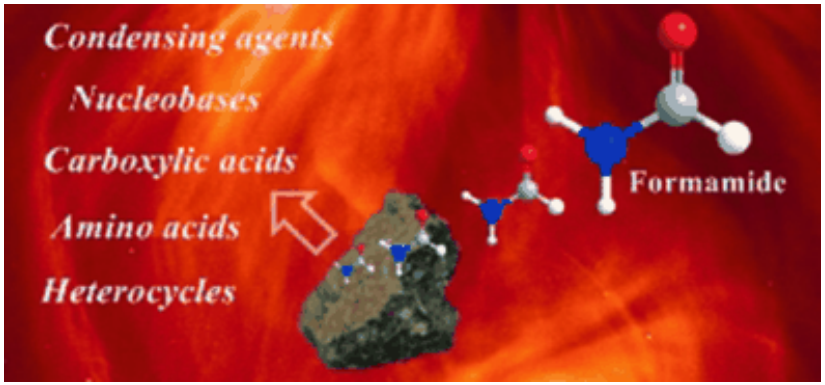

Chemistry - A European Journal
Volume 19, Issue 50,
pages 16916–16922, December 9, 2013

We decided to evaluate the role of meteorites in formamide Prebiotic chemistry under radiation conditions. The choice Of meteorites was due to the fact that these mineral Already showed to be efficient catalysts in the thermal Synthesis (volcanic scenarios) of biomolecule from Formamide.